

Investigation of an Extracorporeal Immobilized Enzyme Device; A Potential Treatment for Blood Deheparinization

by

Guillermo A. Ameer

B.S. Chemical Engineering
University of Texas at Austin
(1993)

Submitted in partial fulfillment of the requirements for the Degree of

**Doctor of Science
in Chemical Engineering**

at the

Massachusetts Institute of Technology

February, 1999

© 1999 Massachusetts Institute of Technology
All rights reserved

Signature of Author _____

Department of Chemical Engineering
December 14, 1998

Certified by _____

Robert Langer
Thesis Supervisor
Kenneth J. Germeshausen Professor of Chemical
and Biomedical Engineering

Accepted by _____

Robert E. Cohen
St. Laurent Professor of Chemical Engineering
Chairman, Committee for Graduate Students

Science



This Doctoral Thesis has been examined by the following Thesis Committee:

Robert S. Langer, Sc.D. _____
Thesis Supervisor
Germeshausen Professor of Chemical and Biomedical Engineering
Department of Chemical Engineering
Massachusetts Institute of Technology

Charles Cooney, Ph.D. _____
Professor of Chemical and Biochemical Engineering
Department of Chemical Engineering
Massachusetts Institute of Technology

William Harmon, M.D. _____
Director of Pediatric Nephrology
Department of Nephrology
The Children's Hospital
Harvard Medical School

Paula T. Hammond, Ph.D. _____
Development Assistant Professor
Department of Chemical Engineering
Massachusetts Institute of Technology

Ram Sasisekharan, Ph.D. _____
Assistant Professor
Division of Bioengineering and Environmental Health
Massachusetts Institute of Technology

Investigation of an Extracorporeal Immobilized Enzyme Device; A Potential Treatment for Blood Deheparinization

by

Guillermo A. Ameer

Submitted to the Department of Chemical Engineering in partial fulfillment of the requirements for the Degree of Doctor of Science in Chemical Engineering

ABSTRACT

Heparin is an anticoagulant used in extracorporeal procedures such as hemodialysis and open heart surgery. Unfortunately, heparin may induce potentially fatal complications in patients at high risk of bleeding. A potential treatment to make heparin anticoagulation therapy safer is the use of an immobilized heparinase I reactor to achieve regional heparinization of a closed circuit. This is a method in which heparin is infused into the extracorporeal circuit pre dialyzer and neutralized post dialyzer. However, a significant problem has been the design of a safe and efficient reactor for medical use.

Taylor-Couette flow was evaluated for potential use in a reactor for blood deheparinization, taking into account clinical specifications and engineering principles. A Taylor-Couette flow device was designed with recirculation ports, strategically placed tangentially to the rotational flow, to allow recirculation of the agarose beads without the use of an external pump. This reactor removed 90% of the heparin's anticoagulant activity from 450 cc of human citrated blood *in vitro* within 3 minutes of operation at a flow rate of 100 ml/min. Even though this device demonstrated to be effective, it was not practical due to the significant decrease in blood cell counts and the large degree of hemolysis that was observed when whole blood was tested (plasma free hemoglobin greater than 800 mg/dL). Therefore, it was shown that the well known beneficial characteristics of Taylor vortices on biological systems are lost when agarose beads are fluidized within whole blood.

These findings motivated a new design which incorporated Taylor-Couette flow, simultaneous separation/reaction, and fluidization of the agarose immobilized heparinase. Fluidization was achieved via membrane induced circumferential flow within the reactive chamber of the device which was separate from the blood cells and the Taylor vortices. Residence time distribution studies were performed and a mathematical model was developed in order to predict and optimize heparin neutralization. The model predicted heparin conversions in saline within a mean of 5% error relative to the experimental results. The new design, referred to as vortex flow plasmapheretic reactor (VFPR), was tested *in vitro* and *ex vivo* in sheep. The VFPR achieved heparin conversions of $44 \pm 0.5\%$ and $34 \pm 2\%$ in saline and human blood, respectively. In addition, there was no hemolysis or cell count decrease. Regional heparinization experiments in sheep resulted in $39 \pm 1.7\%$ mean heparin conversion. The procedure did not effect any clinically significant changes in complete blood counts and total protein concentrations for up to 2 hours. Furthermore, gross necropsy and histopathology reports did not show any negative effects on the brain, kidney, liver, spleen, lungs, and heart.

Thesis Supervisor: Robert Langer

Title: Professor of Chemical and Biomedical Engineering

Acknowledgments

Growing up in Panama, I never imagined that I would contribute to the body of knowledge in the Chemical and Biomedical engineering fields. Also beyond my imagination was the fact that I would do so in the laboratory of Professor Robert Langer at M.I.T., for whom I have the greatest respect. So, needless to say, there are numerous people I have to thank for their contribution (through either direct help or emotional support) to the completion of this thesis. My thesis advisor, Bob Langer, gave me the opportunity to work on this project which has been going on for over two decades. Of course, the problem of safer anticoagulation had been around for much longer and the need for safer heparin therapy among patients with acute renal failure remained unmet. This problem has been the motivation for this research. Bob has been very enthusiastic, supportive, available for the project, and has always given me the freedom to pursue different paths to address the research problem and to develop myself as a scientist. I am also grateful for the opportunity he gave me to go to Japan for two months to broaden my research skills and to make international contacts for future collaborations.

I would like to thank William Harmon, M.D., Paula Hammond, Ph.D., Charlie Cooney, Ph.D., and Ram Sasisekharan, Ph.D. for serving on my thesis committee. Dr. Harmon was a valuable resource for the medical issues that I had to deal with during my research and also for facilitating the contacts that I made at Children's Hospital, Boston MA. John Thompson and the staff of the dialysis unit were very helpful in regards to equipment, the operation of an extracorporeal circuit, and the practical use of heparin. To Paula Hammond and Charlie Cooney I am thankful for the insightful discussions regarding chemistries and the vortex flow reactor, respectively. My thanks to Ram for involving me in the project when he was working with Bob and for his expertise and friendship during my years as a graduate student. His emotional and technical support will always be remembered.

The Langer lab has made my graduate years a fun experience thanks to the many friendly people that have been part of it, both past years and present. Due to the large number of friends that I have made over the years in the lab, it is not feasible for me to mention the highlights of each of their contributions, but in general the discussions that we've had and the interest that they have shown in my project are sincerely appreciated. I am, however, compelled to mention Eric Grovender and Bojana Obradovic for their input on the reactor modeling studies. I also thank my office mates (present and past), Rebecca, Bojana, Nenad, Samir, Mark and Lon, for their ability to make sharing small quarters enjoyable. I could not conceive of a better office experience.

I would like to thank P. Dozois at the M.I.T. Central Machine Shop and Sylvester Szczepanowski at the M.I.T. B.C.S. Machine Shop for machining the reactors. I also thank IBEX Technologies (Montreal Canada) for providing the heparinase I. Recognition is also due to the volunteer blood donors, Srivatsan Raghavan, Dave Ting, and the many other UROPs that I supervised for helping with the experiments. The *in vitro* experiments with human blood were possible thanks to the cooperation of the personnel at the Blood Donor Center of Children's Hospital, Boston, Massachusetts.

To the many friends in Boston that I have met outside of M.I.T., I am also grateful. Specifically, I'd like to thank Tirzah Spencer, who has been an excellent friend, Barbara Brothers for her support and Mihaela Bazalakova for her support and for exposing me to the beauty of Boston and its international crowd. I also appreciate the faith and encouragement that my friends from Texas have shown towards me. In particular Raphaelle Johnson and Gargi Mukherji.

I am also thankful to my family for their support and encouragement. Without their direction I would not have been the first of my family to achieve this degree. I thank my sisters and brother - Sheila, Yvonne, Sharon, and Jorge - for being there when I needed them. Most importantly, I dedicate this thesis to my Mother and Father, for they are the strongest personalities I have ever met, have been available for me regardless of circumstances, and instilled into me the foundation that makes me the person that I am today. Finally, I thank God for he has been with me throughout my life.

Guillermo A. Ameer
December 1998

This work was supported by the National Science Foundation and the National Institutes of Health (GM 25810).

Table of Contents

Title Page.....	1
Committee Page.....	2
Abstract.....	3
Acknowledgments.....	4
Table of Contents.....	6
List of Figures.....	7
List of Tables.....	8
1. Introduction.....	9
1.1 Motivation.....	9
1.2 Specific Aims.....	11
1.3 Immobilized Proteins in Extracorporeal Systems.....	12
1.4 Heparin and its Role in Extracorporeal Blood Circulation.....	16
1.5 Heparinase I.....	18
1.6 Previous Immobilized Heparinase Devices.....	19
1.7 Clinical Model Selection.....	22
1.8 References.....	26
2. The Vortex Flow Fluidized Bed Reactor.....	30
2.1 Introduction.....	30
2.2 Materials and Methods.....	31
2.3 Results and Discussion.....	35
2.4 References.....	44
3. The Vortex Flow Plasmapheretic Reactor.....	46
3.1 Introduction.....	46
3.2 Materials and Methods.....	46
3.3 Results and Discussion.....	49
3.4 References.....	58
4. Reactor Fluid Dynamics and Modeling.....	59
4.1 Introduction.....	59
4.2 Materials and Methods.....	59
4.3 Mathematical Analysis.....	60
4.4 Results and Discussion.....	63
4.5 References.....	70
5. Reactor Performance <i>Ex Vivo</i> in Sheep.....	71
5.1 Introduction.....	71
5.2 Materials and Methods.....	71
5.3 Results and Discussion.....	73
5.4 References.....	90
6. Conclusions and Recommendations for Future Work.....	91
Appendix.....	95

List of Figures

Chapter 1. Introduction

Figure 1.1.	Proposed method for regional heparinization of a patient	12
Figure 1.2.	Illustration of the components of a heparin polysaccharide chain	17
Figure 1.3.	Diagram of the old heparinase I recirculating reactor	21
Figure 1.4.	Diagram of the shaker reactor.....	21

Chapter 2. The Vortex Flow Fluidized Bed Reactor (VFFBR)

Figure 2.1.	Diagram of the vortex flow fluidized bed reactor.....	39
Figure 2.2.	<i>In vitro</i> batch heparin removal by the VFFBR (design I)	40
Figure 2.3.	Safety data for the VFFBR (design I)	40
Figure 2.4.	Release of free hemoglobin into the plasma (design I)	41
Figure 2.5.	Effect of gel volume and rotation rate on hemolysis	41
Figure 2.6.	<i>In vitro</i> batch heparin removal by the VFFBR design II	42
Figure 2.7.	<i>In vitro</i> regional heparinization by the VFFBR design II.....	42
Figure 2.8.	Safety data for the VFFBR (design II)	43
Figure 2.9.	Release of free hemoglobin into the plasma (design II)	43

Chapter 3. The Vortex Flow Plasmapheretic Reactor (VFPR)

Figure 3.1.	Diagram of the vortex flow plasmapheretic reactor	53
Figure 3.2.	Regional heparinization using the packed bed	54
Figure 3.3.	Protein entrapment methods for a Taylor-Couette flow reactor.....	54
Figure 3.4.	Flow dynamics within the VFPR	55
Figure 3.5.	Performance of the immobilized heparinase I packed bed in saline	56
Figure 3.6.	Performance of the VFPR in saline	56
Figure 3.7.	Operation of the VFPR with blood.....	57
Figure 3.8.	Performance of the VFPR with human blood <i>in vitro</i>	57

Chapter 4. Reactor Fluid Dynamics and Modeling

Figure 4.1.	Experimental systems for residence time distribution studies.....	67
Figure 4.2.	Diagram of the reactor sections to be modeled.....	68
Figure 4.3.	Diagram of the compartment model for the VFPR	68
Figure 4.4.	Exit age distribution for compartment 1 and the whole device.....	69

Chapter 5. Reactor Performance *Ex Vivo* in Sheep

Figure 5.1.	Double lumen catheter and <i>ex vivo</i> experimental set up	79
Figure 5.2.	Safety data for control sheep.....	80
Figure 5.3.	Safety data for regionally heparinized sheep 1.....	81
Figure 5.4.	Safety data for regionally heparinized sheep 2.....	82
Figure 5.5.	Safety data for regionally heparinized sheep 3.....	83
Figure 5.6.	Safety data for regionally heparinized sheep 4.....	84
Figure 5.7.	Grouped safety data for regionally heparinized sheep	85
Figure 5.8.	Environmental S.E.M. of the polyester membrane	86
Figure 5.9.a.	Regional heparinization of sheep.....	87
Figure 5.9.b.	Regional heparinization of sheep.....	87
Figure 5.9.c.	Regional heparinization of sheep.....	88
Figure 5.10.	Environmental S.E.M. of plasma exposed bead	89
Figure 5.11.	Environmental S.E.M. of saline exposed bead.....	89

Chapter 6. Conclusions and Recommendations for Future Work

Figure 6.1.	Proposed modification to the VFPR.....	94
-------------	--	----

List of Tables

Chapter 1. Introduction

Table 1.1.	Amino acid composition of heparinase I	19
Table 1.2.	Efficacy of old recirculating reactor	20
Table 1.3.	Current alternatives to systemic heparinization	23

Chapter 2. The Vortex Flow Fluidized Bed Reactor (VFFBR)

Table 2.1.	Dimensions for the VFFBR (designs I and II)	35
Table 2.2.	Minimum rotation rates required in the VFFBR.....	37

Chapter 3. The Vortex Flow Plasmapheretic Reactor (VFPR)

Table 3.1.	Dimensions of the vortex flow plasmapheretic reactor	47
Table 3.2.	Complete blood cell and hemolysis data for the VFPR.....	51
Table 3.3.	Safety data for 1 hour of operation of the VFPR.....	52

Chapter 4. Reactor Fluid Dynamics and Modeling

Table 4.1.	Comparison of mathematical models for E_1 and E_{total} with experiment	63
Table 4.2.	Summary of the model output for four experimental conditions	64
Table 4.3.	Comparison of model predictions with experimental data.....	65
Table 4.4.	Sensitivity analysis on E_{1b}	66

Chapter 5. Reactor Performance *Ex Vivo* in Sheep

Table 5.1.	Total protein and fibrinogen values for sheep experiments	75
------------	---	----

Chapter 1

Introduction

1.1 Motivation

The effective and safe detoxification of blood, toxified either due to high concentration of metabolites or due to drug overdoses, remains a serious problem. Current methods to treat blood toxicity include hemodialysis, hemofiltration or activated charcoal filters. These methods are widely used in the clinic but they lack specificity in metabolite removal and therefore essential metabolites have to be restored continuously (Takao, 1993). Several investigators have proposed the use of immobilized enzymes in extracorporeal bioreactors as a means to specifically carry out a desired reaction without disrupting other blood components (Ambrus *et al.*, 1978; Dumler *et al.*, 1981; Horvath *et al.*, 1973; Langer *et al.*, 1982; Lavin *et al.*, 1985; Olanoff *et al.*, 1975). Even though there is a good understanding of how enzymes can improve or correct pathological conditions or eliminate undesirable metabolites from the blood, immobilized enzyme bioreactors are not widely used in the clinical setting. The main reasons are: the high cost of production of enzymes (specially from animal source), the need to obtain derivatives of the enzymes with unaltered therapeutic activity, but with no toxicity and antigenicity (Klein and Langer, 1986) and the lack of bioreactor designs that are safe and efficient.

Heparin is a very important and widely used drug in modern medicine and surgery. Heparin is used to treat thrombotic disorders and as an anticoagulant to prevent clotting in procedures requiring extracorporeal equipment such as hemodialysis, membrane oxygenation, and cardiopulmonary bypass surgery. However, the use of heparin can lead to complications in patients who are at high risk of bleeding such as those suffering from acute renal failure (Broyer *et al.*, 1986) and those who have undergone open heart surgery (Salzman *et al.*, 1975). Heparin was also found to be the prescribed drug responsible for the most deaths in patients that were otherwise healthy (Porter and Fick, 1977). Currently, the anticoagulant effect of heparin is neutralized with protamine sulfate, a highly basic protein that binds to heparin. However, the use of protamine can cause severe side-effects including hypotension, vasodilation, pulmonary platelet accumulation and bradycardia (Wakefield *et al.*, 1986). This heparin reversal method may benefit patients that require rapid removal of heparin after a surgical procedure but has very limited application in acute renal failure because of the complexity of on line titration and the side effects mentioned earlier.

To address this problem, a novel application of enzymes was introduced by Langer and his co workers in 1982 (Langer *et al.*, 1982). The authors describe the enzymatic degradation of heparin by heparinase I (an alpha eliminase extracted from *Flavobacterium heparinum*) in a dog animal model. An immobilized heparinase blood filter could be used in a regional heparinization system and it is a potential alternative to the current method of neutralizing heparin with protamine. Recently, IBEX Technologies conducted clinical trials with soluble heparinase I to reverse heparinization after cardiovascular surgery and the results are encouraging. In this application heparinase is injected into the patient's bloodstream (Broughton, 1995). However, the repeated use of soluble heparinase towards regional heparinization in acute kidney failure would face similar problems of immunogenicity.

Throughout the last decade, several investigators studied the potential for an enzymatic deheparinization system using an immobilized enzyme fluidized bed system in dog and sheep animal models (Larsen *et al.*, 1984; Freed *et al.*, 1988; Bernstein *et al.*, 1987). Hollow fiber bundles were also explored as a possible heparinase reactor (Comfort *et al.*, 1989). These studies contributed a great deal of knowledge in the area of immobilized enzymes in extracorporeal devices because mathematical models and first principles were developed to aid the design of the device. However, in these reactors, blood flow rates allowed in the fluidized systems were limited to under 200 ml/min. (Freed *et al.*, 1993). This limits the heparinase reactor to only neonates or small children and can not be used on adult patients suffering from acute renal failure and therefore jeopardizes its ability to compete with current heparin reversal methods. In addition to the flow rate limitation, the clinical use of the heparinase reactors was not possible because of significant blood damage (Larsen *et al.*, 1984; Freed, 1988), scarcity and low purity of the native heparinase I, and difficulty of use of the bioreactors in a clinical setting. In summary, the following problems have to be addressed in order for a heparinase reactor to be clinically useful:

1. Bioreactor Design:

- a) particle fluidization at flow rates of 150-400 ml/min.
- b) reactor induced blood damage
- c) efficiency
- d) simplicity

2. Enzyme Immobilization:

- a) high enzyme activity retention
- b) stability in blood
- c) enzyme purity

To address the bioreactor design issues, Taylor vortices are applied to the immobilized heparinase system as will be discussed further. Taylor vortices have been shown to have excellent mixing characteristics in reactors that processed biological systems such as cell cultures, blood plasmapheresis and oxygenation (Gaylor and Smeby, 1976; Mottaghy and Hanse, 1985; Strong and Carlucci, 1976; Jaffrin, 1989). In addition, Cooney and co workers investigated and modeled reaction and mass transfer properties in a particle and membrane vortex flow reactor (Iosilevskii *et al.*, 1993; Moore, 1994). The enzyme immobilization issues are addressed by assessing immobilization chemistries and supports using high purity heparinase I (95%+ by SDS-PAGE) donated by IBEX Technologies. In this research, novel vortex flow reactor designs and their clinical feasibility are investigated. The reactor performance is evaluated for regional heparinization using a sheep animal model. By applying Taylor vortices to immobilized enzyme bioreactors in extracorporeal systems, this research should enhance the knowledge and applications of Taylor vortices in biological and enzymatic systems. The ultimate goal of this research is to allow a safer extracorporeal treatment for the critically ill patient undergoing renal replacement therapy and facing heparin related complications.

1.2 Specific Aims

The general objective of this thesis is to investigate the use of immobilized heparinase I in a reactor that would allow regional heparinization of the extracorporeal circuit for potential use in the treatment of acute renal failure (**Figure 1.1**). The specific objectives of this thesis are:

1. To design, construct, and characterize prototype reactors that utilize porous beads as an enzymatic support
2. To evaluate reactor safety and efficacy through *in vitro* and *ex vivo* experiments in a sheep animal model; specifically,
 - 2.1 To investigate the effect of the device on the blood components
 - 2.2 To assess whether high conversions can be achieved at clinically relevant flow rates for adults (150-400 ml/min.) At the beginning of this research, a high conversion was defined to be 80% per pass through the reactor. After consulting with various nephrologists and clinicians, it was determined that such a high goal for conversion would be necessary only if the circuit were overanticoagulated with heparin. At adequate heparin concentrations, sufficient to prevent clotting in the circuit, 80% conversions could induce clotting at the vascular access of the patient. Therefore, the earlier goal of 80% conversion was reconsidered and replaced with the range of

45-50% conversion. The criteria for this new value are discussed later in the Chapter.

3. To develop a mathematical model that would adequately describe the deheparinization process in the reactor for generalization of the results.

Immobilized heparinase I Reactor

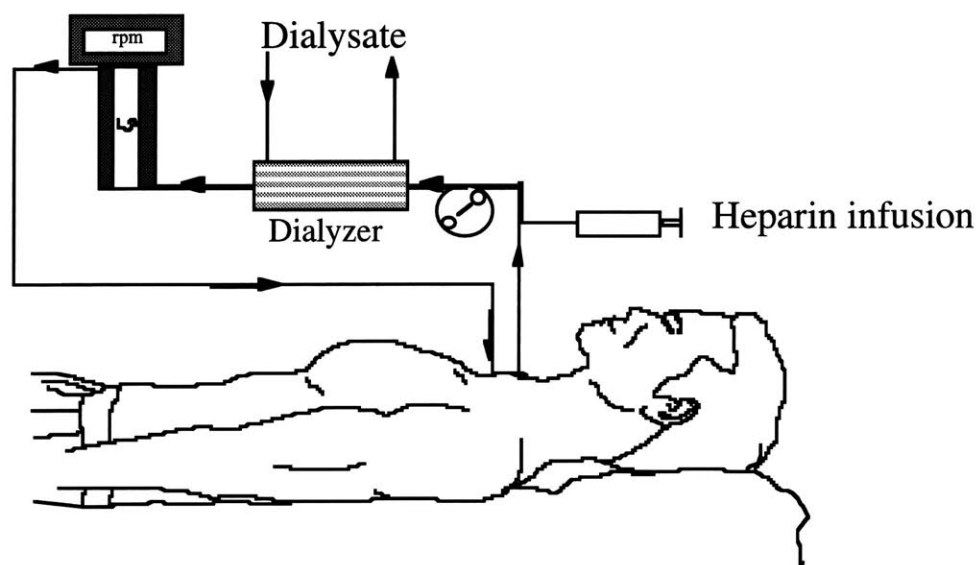


Figure 1.1. Diagram of the proposed method for regional heparinization of a patient. Higher heparin concentrations in the extracorporeal circuit are represented by the thicker lines located between the heparin infusion and the reactor.

1.3 Immobilized Proteins in Extracorporeal Systems

This section reviews studies and applications where immobilized proteins are used to obtain a specific action on a biological fluid that is temporarily pumped through extracorporeal equipment. The immobilized protein may be an enzyme, an antibody or fragment thereof, or protein ligands of high affinities such as protein A in the case of antibody removal. The other applications of immobilized proteins in extracorporeal devices such as dressing and drainage materials, films or ointments, or the passivation of materials to enhance hemocompatibility are reviewed elsewhere (Torchilin, 1991). This section will primarily focus on the medical applications of immobilized enzymes but will also discuss interesting applications for immobilized antibodies or antibody fragments and protein A. Studies of immobilized proteins in extracorporeal devices have dealt primarily with the removal of undesirable metabolites from biological fluids (mainly blood) during

perfusion. The emphasis on detoxification using immobilized enzymes can be attributed to the high specificity and catalytic activity of enzymes. The main areas of interest for immobilized enzymes in extracorporeal devices are: treatment of liver and/or kidney failure, cancer, blood diseases, and more recently, drug overdoses.

Kidney insufficiency can be treated by the removal of excessive urea from the blood in a reactor with immobilized urease. This approach was proven by using a hollow fiber reactor with immobilized urease (Salmona *et al.*, 1974). An important issue that had to be addressed was the elimination of ammonia formed due to the enzymatic hydrolysis of urea. A detoxifying reactor for the removal of urea has also been described (Makarov and Kibardin, 1980). In their arrangement, columns with activated charcoal, immobilized urease, and an inorganic cation exchanger were sequentially arranged. The activated charcoal column achieved complete sorption of creatinine, and partial sorption of urea, the urease column removed most of the urea, and the cation exchanger eliminated the ammonia formed in the urease column.

The accumulation of toxic metabolites like ammonia, mercaptanes, phenols, phenylalanine and free fatty acids in the blood can cause liver insufficiency and coma. In order to treat these conditions a variety of immobilized enzyme reactors have been suggested (Kalghatgi *et al.*, 1980; Pedersen *et al.*, 1979). The current method of blood purification, by passing it through activated charcoal, shows improvement but is usually accompanied with different side reactions because of the non-specific adsorption of many blood proteins and relatively extensive blood damage. Sung and co workers (1986) described the removal of excess bilirubin from the blood for the treatment of endogenous jaundice using an extracorporeal device with immobilized bilirubin oxidase from *Myrothecium verrucaria*. The enzyme was immobilized on CNBr-activated Sepharose. Its thermostability was 5 times higher than that of the soluble enzyme. The column reactor contained 15 ml of the immobilized enzyme gel and oxidized 60% of the elevated bilirubin.

Immobilized enzyme devices have also been investigated as a potential treatment of amino acid-dependent tumors. L-asparaginase was immobilized by incorporation into cellulose triacetate fibers or dacron (Salmona *et al.*, 1974) and covalently bound on the inner surface of nylon tubing (Horvath *et al.*, 1973) or collagen films (Olanoff *et al.*, 1975). L-asparaginase can reduce the plasma L-asparagine concentration significantly, thereby depriving the tumor cells of this amino acid. Normal cells synthesize asparagine while certain lymphomas depend on circulating asparagine to grow. Systems have been developed that resulted in almost quantitative removal of asparagine from the blood in dogs, monkeys (Olanoff *et al.*, 1975) and man (Sampson *et al.*, 1974). The first results from clinical trials with immobilized asparaginase were described by

Dumler and co workers in 1981. L-asparaginase was immobilized in a regenerated cellulose hollow fiber reactor via trichloro-s-triazine. Blood asparagine levels decreased by 30% at flow rates of 200 ml/min. in a hollow fiber reactor with immobilized L-asparaginase when compared to traditional dialysis. The use of the L-asparaginase reactor led to noticeable temporary improvement in two out of three patients with tumors. The L-asparaginase reactor did not provoke any immunological reactions even though some of the patients demonstrated anaphylaxis after parenteral administration of the native enzyme. Arginine-dependent tumors can be treated with extracorporeal reactors with immobilized arginase. Arginase, immobilized in a hollow fiber reactor, was used to treat familial hyperargininemia in model experiments performed with rabbit blood (Rossi, 1981; Kanalas *et al.*, 1982). Within the reactor, arginine was separated from blood by means of a semipermeable membrane to low molecular weight substances.

The absence of the enzyme phenylalanine hydroxylase, which degrades the amino acid phenylalanine, results in the genetic disorder Phenylketonuria. Patients suffering from this disease have a very elevated plasma level of phenylalanine which results in neuropsychiatric disorders. A promising treatment of this disorder may be the enzyme phenylalanine ammonia lyase which converts phenylalanine into non-toxic transcinannamic acid. Ambrus and co workers (1978) proved the possibility of using devices with immobilized phenylalanine ammonia lyase when they quantitatively removed phenylalanine rapidly from a sample of citrated blood. Incorporating a multi-tubular device containing phenylalanine ammonia lyase immobilized on the inner surface of nylon tubings lead to a 2-fold decrease in blood phenylalanine. Low levels of phenylalanine could be maintained for at least two days (Pedersen *et al.*, 1979). In similar experiments, the use of a hollow fiber enzyme reactor shunted between the femoral artery and femoral vein of a dog for two hours decreased blood phenylalanine levels from 15 to 2 mg/100 ml. The number of red blood cells, leukocytes and platelets remained constant throughout the treatment (Ambrus *et al.*, 1983).

Another application of immobilized enzymes to cancer therapy involves carboxypeptidase, which cleaves folate and methotrexate. Folate is required for cancerous cells and the effect of the enzyme is a severe folate deficiency. Methotrexate is a folate antagonist which is administered to cancer patients during chemotherapy. By using an immobilized carboxypeptidase reactor, higher drug doses of methotrexate can be administered for shorter time periods and the excess drug can be eliminated on demand. This approach was investigated by Bertino and co workers (1979), who constructed an immobilized carboxypeptidase reactor to remove methotrexate in canine blood *in vivo*. The enzyme was linked via glutaraldehyde to nylon tubing and anisotropic hollow fibers. The *in vivo* experiments were conducted at blood flow rates of 500 ml/min. for a 2 hour period. Neither reactor was able to lower methotrexate blood levels significantly.

Plotz and co workers (1974) described the use of agarose immobilized albumin, packed into a column, for the removal of protein-bound metabolites and toxins. Thyroxine, tauro lithocholate, chenodeoxycholate, and digitoxin bound tightly. Digoxin, as expected, was not removed. The authors reported the *in vitro* removal of bilirubin from 10 ml of anticoagulated whole blood with slight decreases in calcium and magnesium. There were no significant changes in blood cells, platelets, electrolytes or clotting factors. However, the apparent hemocompatibility of the column was demonstrated for very low flow rates (0.5-2.5 ml/min.). The beads could be repeatedly reused without loss of efficiency after ethanol elution.

The use of immunoadsorption methods may take place in the clinical setting when an enzyme is not feasible or readily available to remove an undesirable substance from blood. Immunoadsorption relies on the specificity and high affinity of antibodies to deplete antigen plasma concentrations. A potential application for immunoadsorption is in the treatment of dialysis related amyloidosis (DRA), a debilitating and potentially fatal disease that could benefit from the specific and significant removal of the protein beta-2-microglobulin (β_2m) from blood. This protein is implicated in the amyloid fibrils that deposit in the joints and create cystic bone lesions, destructive arthropathy, and soft tissue damage (Schaeffer *et al.*, 1995). DRA is a consequence of the longer survival times that are now associated with patients with end-stage renal disease (ESRD). Currently, the incidence of ESRD in the United States exceeds 250,000 patients and is rising by approximately 8% per year. Hemodialysis is the principal therapy for these patients, all of which are expected to develop DRA after long-term treatment. Immunoadsorbent approaches to extracorporeal removal of β_2m have previously been investigated. These studies consisted of immobilizing murine derived, anti-human β_2m , monoclonal antibodies onto either regenerated cellulose hollow fibers or Sepharose beads (Vallar *et al.*, 1994; Vallar *et al.*, 1995). The studies with the hollow fiber device determined that the membrane-antibody coupling capacity was insufficient to remove the necessary quantities of β_2m to effectively treat or prevent β_2m . The Sepharose based device was used as an immunoadsorbent column to remove β_2m from plasma *in vitro*. The drawbacks of this system were the required separation of the blood cells from plasma and the low β_2m binding capacity of the device.

Another use of immobilized proteins for the specific removal of substances from blood is the use of the protein A column (Arbiser *et al.*, 1995). Protein A immunoadsorption is a therapy for the treatment of diseases that are caused by pathogenic autoantibodies. The method works because protein A binds to the Fc portion of IgG. Therefore, this antibody class can be removed from the blood of the patient. However, the procedure also relies on plasma separation prior to

circulation, significantly increasing the cost of the therapy. Currently, the protein A column is predominantly used in the treatment of idiopathic thrombocytopenic purpura but other applications that rely on the removal of autoantibodies are under investigation.

An important problem in extracorporeal blood circulation therapy is the fast and specific removal of heparin from the blood after completion of the treatment or as a means to control heparin levels. A desirable treatment modality for patients who are at high risk of bleeding such as in acute hemodialysis is regional heparinization to minimize the patient's exposure to heparin. To solve this problem, an extracorporeal reactor with immobilized heparinase I was proposed (Langer *et al.*, 1982). Heparinase I, an enzyme that specifically degrades heparin, was immobilized on Sepharose 4B and fluidized in a blood filter modified with an external recirculation line and a peristaltic pump. The extracorporeal shunt containing the immobilized enzyme was tested *in vitro* in human blood and incorporated into the circulation of a dog. Human blood was anticoagulated with 90 U of heparin /ml and passed through the reactor at a flow rate of 50 ml/min. After one pass (2 min.), 60 % of the heparin's anticoagulant activity was destroyed and almost all the activity was gone after 6 minutes according to activated partial thromboplastin time (apTT) measurements. For the *in vivo* experiments in dogs, nearly all of the heparin's anticoagulant activity measured by apTT, whole blood recalcification time (WBRT), and azure assays was gone within 2 minutes. In the experiments, blood continued to flow unrestricted through the filter even after six passes. Products of the enzymatically degraded heparin were tested for cytotoxic and mutagenic effects and none of these effects were observed. Blood taken from the dogs showed no decrease in hematocrit, a 30% decrease in white blood cells, and a 70% decrease in platelet count. These values were in accordance to those obtained for tests of extracorporeal circuits in dogs. Further studies aiming to improve the safety and efficacy of the heparinase reactor introduced an oscillating mechanism to help suspend the particles and eliminate the recirculation line and peristaltic pump that was used in the original reactor (Freed, 1988). In these studies, the reactor effected an 83% deheparinization over 2 hours in human blood and 79% deheparinization over 40 minutes in systematically heparinized lambs at flow rates of 100 ml/min.

1.4 Heparin and its Role in Extracorporeal Blood Circulation

Heparin is a polysaccharide composed of alternating units (and variously sulfated residues) of alpha-D-glucosamine monosaccharides and uronic acids joined together by 1-4 glycosidic linkages. The uronic acid residues are either L-iduronic acid or D-glucuronic acid. The D-glucosamine residues are either N-sulfated or N-acetylated. A more complete description of heparin is found in **Figure 1.2**. Commercial heparin is extracted predominantly from bovine lung or from porcine intestinal mucosa. Heparin has been widely used by the medical community

throughout the world as the anticoagulant of choice to prevent blood from clotting within an extracorporeal circuit. It is also used to treat and prevent thrombosis. It is now believed that the anticoagulant activity of heparin comes mainly from its ability to bind antithrombin III and accelerate the inhibition of thrombin and inhibit the activation of prothrombin. The biological activity of heparin is expressed in U.S. Pharmacopoeial (USP) units. The USP unit of heparin is the quantity that will prevent 1.0 ml of citrated sheep plasma from clotting for 1 hour after the addition of 1:100 CaCl₂ solution.

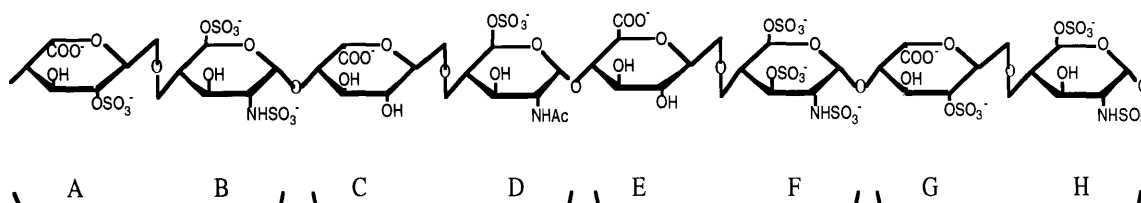


Figure 1.2. Illustration of the components of a heparin polysaccharide chain showing N-sulpho-6-O-sulpho-alpha-D-glucosamine (B,H), N-sulpho-3,6-di-O-sulpho-alpha-D-glucosamine (F), N-acetyl-O-sulpho-alpha-D-glucosamine (D), alpha-L-iduronic acid (C), 2-O-sulpho-alpha-L-iduronic acid (A,G), and beta-D-glucuronic acid (E). The pentasaccharide sequence DEFGH is involved in the binding to antithrombin. Braces indicate the repetition of disaccharide units comprising a uronic acid residue linked to a glucosamine (AB,CD,EF,GH). Ac=acetyl (Petitou, 1989)

Heparin is used during hemodialysis and hemofiltration. These are forms of renal replacement therapy for patients with uremia caused by chronic and acute renal failure. These techniques employ semi-permeable membranes that allow clearance of uremic toxins from the circulation by diffusion or filtration. Even though new membranes are continuously being developed to enhance the hemocompatibility of the membranes and tubing used in the extracorporeal circuit, none have been able to displace the use of anticoagulants. The addition of heparin can be a complicating factor especially in patients with uremia who already have predisposition to both bleeding and atheroma. This tendency of bleeding can be life threatening in patients who are acutely ill, or have complications such as thrombocytopenia or disseminated intravascular coagulation (Ireland *et al.*, 1989). Bleeding accounts for 3.7% of deaths in patients with renal failure and therefore still poses a major clinical problem (Broyer *et al.*, 1986). Swartz and Port (1979) found that bleeding complications occurred 10-19% of the time using either low dose heparin or regional heparin regimens in patients with increased risk of bleeding. They also estimated that 25% of all patients suffering from acute renal failure have an elevated risk of

bleeding. Heparin free dialysis has been used occasionally but it is generally unsuccessful due to the high frequency of systemic clotting (Deary *et al.*, 1991). Typical heparin level in hemodialysis treatment is approximately 0.5 USP units/ml blood.

It is well recognized that major activation of the coagulation cascade takes place during cardiopulmonary bypass surgery (CPB) and higher doses of heparin than those used for hemodialysis are necessitated (Jobes *et al.*, 1981). This type of surgery is an every day occurrence in many hospitals. CPB equipment has a much greater surface area and employs much higher flow rates (5 l/min. compared to 300 ml/min.). A heparin level of 3.6 USP units/ml was recommended as the minimum safe level for avoidance of micro-coagulation and its sequelae (Senning, 1959). A clear correlation was observed between excess circulating heparin and blood loss (Wright *et al.*, 1964). High risk patients include those with recent myocardial infarction, post-operative patients, patients with ulcers and diabetics (Basu *et al.*, 1984).

1.5 Heparinase I

Heparinase I is an eliminase originally extracted from *Flavobacterium heparinum* that cleaves heparin at alpha-glycosidic linkages in heparin's repeating unit. The elimination reaction results in a site of unsaturation in the terminal uronic acid, but the glucosamine reducing end remains an unaltered residue (Linker and Hovingh, 1972). The molecular weight of the enzyme is approximately 43,000 Daltons and its Km for heparin is around 4 μ M (0.11 mg/cc) (Yang *et al.*, 1985; Bernstein *et al.*, 1987). The amino acid composition is shown in **Table 1.1**. Out of twelve polysaccharides tested, heparinase I was found to specifically act only on heparin and heparan monosulphate (Yang *et al.*, 1985). The activity of heparinase I on heparan monosulphate was only 28% of that on heparin. The activity towards heparan monosulphate can be attributed to the various heparin-like regions on the polysaccharide. The activity maximum of purified heparinase I occurs at pH 6.5 and 0.1 M NaCl and the stability maximum occurs at pH 7 and 0.15 M NaCl.

Heparinase I cleaves heparin to produce di-, tetra-, hexa- and octasaccharides which have greatly reduced anticoagulant activity (Linhardt *et al.*, 1982). The degradation products are neither mutagenic or cytotoxic at doses that were 100 times the doses expected in the application of a heparinase reactor (Linhardt *et al.*, 1982; Larsen *et al.*, 1984; Langer *et al.*, 1982). Studies showed that the heparin fragments were excreted five times more rapidly than heparin in both normal and nephrectomized animals. No acute toxicity was observed in rats injected with heparin fragments. However, upon autopsy, the investigators found hemorrhages in the lungs of rats injected with heparin (Larsen *et al.*, 1986).

Table 1.1 Amino acid composition of heparinase (Sasisekharan, 1991).

Amino acid	number
Ala	29
Val	19
Leu	21
Ile	23
Pro	18
Met	6
Phe	18
Trp	6
Gly	25
Ser	25
Thr	24
Cys	3
Tyr	29
Asn	22
Gln	18
Asp	21
Glu	18
Lys	43
Arg	12
His	4

1.6 Previous Immobilized Heparinase I Devices

The original immobilized heparinase device used a Bentley 250 ml infusion filter (model PFT-100) adapted with a silicon rubber U-tube and a peristaltic pump to recirculate the immobilized heparinase agarose beads at a flow rate of 300 ml/min. The flow rate of the blood through the reactor was 50 ml/min. When the heparinase filter was tested *in vitro* using human blood, 60 % of the heparin's anticoagulant activity, as measured by activated partial thromboplastin time (apTT), was gone in 2 minutes, and almost all the activity was gone after 6 minutes (3 passes). In dogs (at the same flow rate) there was an 80% 1st pass heparin activity loss and after 2 passes there was a 90% loss. After the experiments, blood samples showed no decrease in hematocrit, a 30% decrease in white blood cell count, and a 70% decrease in platelet count (Langer *et al.*, 1982). Plasma hemoglobin levels were not reported.

Bernstein modified a 250 ml blood filter (Model AF-10 American Hospital Supplies) to increase the flow rate and improve the hemocompatibility of the original heparinase reactor. He added six pairs of holes (2.5 mm diameter) to each segment of the recirculation line within the reactor. **Figure 1.3** shows a diagram of the reactor. The particles which have a minimum diameter of 150 microns, are retained in the reactor by a 40 micron cut-off mesh. This reactor was loaded with 85 cc of agarose immobilized heparinase (activity 100-150 units/cc gel) and used to treat sheep. **Table 1.2** shows the efficiency of the recirculating reactor for two flow rates. Over 1 hour of *ex vivo* use, the reactor induced: 1) no change in hematocrit (Hct), 2) a decrease in WBC count to 47 % of initial by 20 minutes and rebounding to 72% of initial over 60 minutes, 3) a decrease in Plt count to 55% of initial, and 4) an increase in plasma hemoglobin (HbP) to 89 ± 33 mg% (Bernstein *et al.*, 1987). Control reactor studies showed that the recirculation line and peristaltic pump were the major source of blood damage for this type of reactor (Freed, 1988; Larsen, 1984).

The efficacy of the recirculating reactor decreased to 65% of initial over 1 hour of *ex vivo* use at 200 ml/min. This was attributed to the aggregation of particles within the reactor, therefore decreasing the amount of accessible enzyme (Bernstein *et al.*, 1987). However these experiments demonstrated the concept of regional heparinization because the heparin levels in the extracorporeal circuit were maintained at 2.64-2.77 times the level in the animal.

Table 1.2. Efficacy of recirculating reactor with external peristaltic pump. Values at the start and the end of the experiment are shown (Bernstein *et al.*, 1987).

Flow rate (ml/min.)	Clearance (ml/min.)		Fractional Clearance (%)	
	Initial	Final	Initial	Final
120	56	36	47	27
200	70	50	35	25

Another heparinase reactor design used a shaker mechanism to oscillate the vessel and fluidized the beads through secondary flows (Freed, 1988). Four prototype reactors were built and systematically analyzed through flow visualization studies and *in vitro* experiments with human blood. An illustration of the two reactor types selected, "tapered" and "blue-top" is given in **Figure 1.4**. The reactor was designed for use in pediatric patients who are at especially high risk for hemorrhagic complications following systemic heparinization (Cilley *et al.*, 1986).

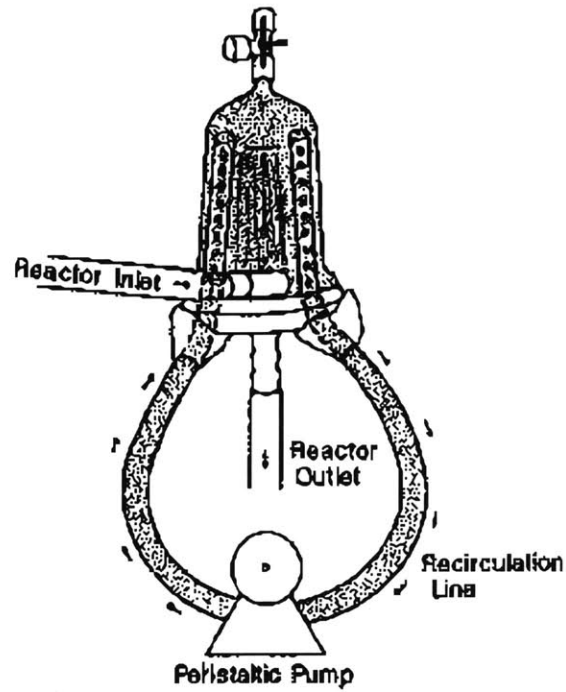
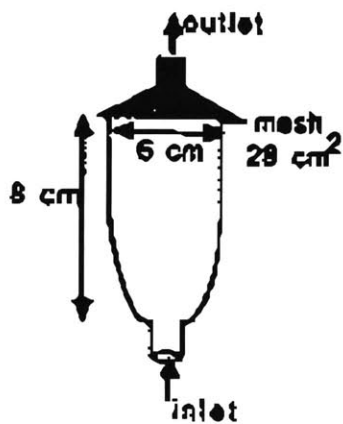


Figure 1.3. Diagram of the heparinase reactor that was modified to include a recirculation line that was connected to a peristaltic pump (Bernstein *et al.*, 1987).

"Blue Top"



"Tapered"

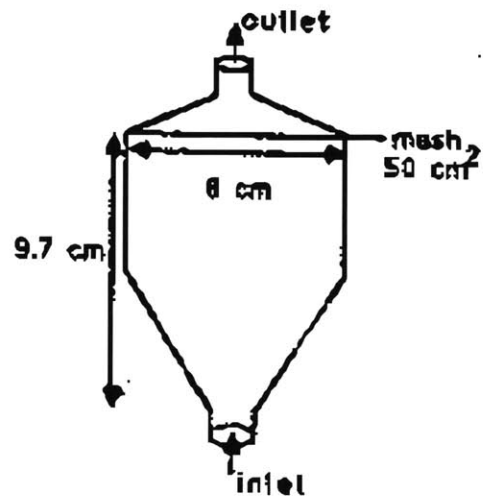


Figure 1.4. Diagram of the reactors that employed the shaker mechanism to fluidize the agarose beads (Freed, 1988).

Efficacy was assessed via the profiles of blood heparin levels derived from whole blood recalcification time (WBRT) measurements done on samples drawn from the reactor outlet. The blue-top vessel containing 20 cc (3,000 units) of agarose-immobilized heparinase effected a 60% deheparinization over 1 hour with little associated blood damage (HbP < 15 mg%). A protocol was developed to "decontaminate" the agarose immobilized heparinase to further reduce reactor damage and therefore increase the enzyme loading. The tapered vessel was tested with 40 cc (2800 units) of the "decontaminated" immobilized enzyme and effected a 74% deheparinization over 1 hour with minimal hemolysis (HbP < 15 mg%). In *ex vivo* studies in lambs, a $79 \pm 2\%$ deheparinization required 27-33 min. vs. 63 min. in untreated lambs. The 1 hour HbP levels were approximately 94 mg%.

In conclusion, the heparinase reactors that have been developed to date have the following limitations:

Recirculating Reactor:

1. Blood flow rates were limited to under 200 ml/min.
2. Induced significant blood damage with or without the beads (perhaps due to the fluidization mechanism)
3. Reactor efficiency *ex vivo* decreased to 65% of initial over 1 hour (perhaps due to particle aggregation)

Oscillating Reactor:

1. Blood flow rates were limited to under 100 ml/min.
2. Application is limited to batch deheparinization of small children
3. The reactor design was too complex to be implemented in clinical practice

1.7 Clinical Model Selection

Applications of the Immobilized Heparinase I Reactor

There are two potential modes of operation of the immobilized heparinase device: 1) regional heparinization where the extracorporeal circuit is heparinized with minimal exposure to the patient and 2) rapid batch heparin removal after the patient is exposed to high levels of heparin. After a survey of the different extracorporeal therapies that use heparin (e.g. hemodialysis, extracorporeal membrane oxygenation (ECMO), or open heart surgery) hemodialysis was selected as the model system to introduce the immobilized heparinase reactor into the clinic. Hemodialysis was selected because it involves less complications than open heart surgery or ECMO. The goals for this model are: 1) to assess whether 50 % reduction in heparin levels in one pass can be achieved at a blood flow rate of 150-400 ml/min., 2) to assess whether the reactor performance can

be maintained for 4 hours at 37°C, and 3) to minimize blood damage to an amount below or comparable to that of the hemodialyzer.

An immobilized heparinase reactor would have its greatest impact in the treatment of acute renal insufficiency. Anticoagulation is one of the most important components of renal replacement therapy and heparin is the oldest and most frequently used anticoagulant. In patients suffering from acute renal failure, the risk of bleeding is greatly increased and excessive anticoagulation may result in bleeding complications reported to occur in 5-26% of treatments (Zusman *et al.*, 1981). Current alternatives to systemic heparinization include variable heparin dosing, low molecular weight heparin, regional heparinization and neutralization with protamine, regional citrate anticoagulation with trisodium citrate, nafamostat mesilate, and prostaglandin analogue infusion. Despite these alternatives, acute kidney failure is a serious problem with an unmet need for effective deheparinization. The relative advantages and disadvantages of the alternate techniques are shown in **Table 1.3**.

Table 1.3. Advantages and disadvantages of current alternatives to systemic heparinization (Mehta, 1994).

Method	Advantages	Disadvantages
Saline flush	No anticoagulant employed	Poor filter operation
Low-Dose Heparin	Standard method, easy to use, inexpensive	Bleeding risk, thrombocytopenia, average filter patency
Regional Heparin with Protamine	Reduced hemorrhage	Complex, protamine effects, hypotension
LMW heparin	Decreased risk of bleeding	Expensive, special monitoring, availability, some filter clotting
Regional citrate	No bleeding, no thrombocytopenia, improved filter life	Complex, requires calcium monitoring, occasional alkalosis
Nafamostat mesilate	No heparin needed, less systemic effects	some filter clotting, Japan only, not compatible with PAN membranes
Prostacyclin	Less bleeding, improved filter patency	needs some heparin, hypotension, expensive

An immobilized heparinase reactor could be used in a regional heparinization regime in either of the two currently accepted methods to treat acute kidney failure: continuous renal

replacement therapy (CRRT) and intermittent hemodialysis (IHD). Continuous arteriovenous hemofiltration (CAVH) and continuous venovenous hemofiltration (CVVH) are forms of CRRT which differ in vascular access and the treatment may last for several days. A stated advantage of CRRT is that it is particularly suitable for patients in intensive care units who have multiple organ failure and are generally hemodynamically unstable. It is also easier to administer the large daily volumes of parenteral nutrition than in the case of IHD (Mehta, 1994). CAVH relies on the natural pressure difference between the vein and the artery for circulation through the extracorporeal circuit; therefore, flow rates range from 50-100 ml/min. in adults. CVVH uses a pump to circulate the blood at a flow rate of 200 ml/min. Acute renal failure treatment with IHD typically may last from 2-4 hours and flow rates range from 200-400 ml/min. in adults. The immobilized heparinase reactor issues that need to be addressed for CRRT are:

- 1) prolongation of the stability of the immobilized heparinase in blood, and
- 2) a replacement method of the enzymatic support that would not disrupt the operation of the dialyzer or filter.

Criteria for Reactor Design

The Taylor vortex flow reactor (VFR), was selected to evaluate the application of immobilized heparinase I for regional heparinization. A vortex flow reactor consist of two concentric cylinder in which the inner cylinder is able to rotate and the outer is stationary. At a critical rotation rate, secondary flow instabilities termed Taylor vortices appear in the annulus and their morphology can vary depending on the magnitude of the axial flow rate and the rotation rate. Therefore, the VFR induced secondary flows without the physical hazards of external momentum. The design criteria for a clinically feasible immobilized heparinase reactor for use in regional heparinization involves the following:

- 1) Efficacy: reactor inlet blood activated clotting time (ACT) of 220-240 sec and reactor outlet ACT of 170-180 sec (45-50% average steady state single pass conversion),
- 2) Safety: no significant effect on whole blood cells such as hemolysis (less than 150 mg plasma free hemoglobin /dL), rapid cell and platelet count reduction, or excessive white cell or platelet activation,
- 3) Stability: Stable operation at flow rates of up to 300 ml/min., and
- 4) Simplicity: Simple operation and low cost.

There are two conventional forms of operation for the VFR:

- 1) a fluidized bed VFR in which the immobilized heparinase beads are suspended within the whole blood, annular path, and

2) a membrane VFR in which heparinase is immobilized onto a membrane placed on the inner and outer cylinders.

During this research a third form of operation for the VFR was developed which combines a microporous membrane and fluidization of agarose beads. A modular design was implemented so that the reactor would be separate from the motor and control panel. This would allow for a disposable unit and ease of use.

The Fluidized Bed VFR. The fluidized bed configuration would allow the highest contact surface area for reaction with minimal external mass transfer limitations as demonstrated by Freed and co workers (1993). But clogging of the agarose beads against a retaining mesh was still a problem for flow rates above 100 ml/min. Therefore a recirculating loop that did not require an external pump was designed to shunt the top and bottom of the device and allow recirculation of the agarose via the natural rotational flow dynamics.

The Membrane VFR. The conventional method of immobilizing heparinase onto a membrane and placing the membrane on the inner and outer cylinders of the VFR was not pursued because the retention of heparinase activity after immobilization to several porous membranes was minimal (< 5%) and the surface to volume ratio required was not feasible (Appendix). Therefore, a modified membrane design was adopted using agarose beads as the support for the immobilized heparinase and a porous membrane for cell separation. In this novel configuration, the membrane was placed in the inner surface of the outer cylinder and the immobilized heparinase was injected into the compartments created by the membrane and the cylinder (reactive compartment).

Criteria for Enzyme Immobilization

Several important issues must be taken into account when designing an immobilized enzyme device for blood contact. First, the chemistry used for the immobilization process should result in a stable covalent bond between the enzyme and the support and should not introduce toxic substances in the support that could be difficult to eliminate. Secondly, the support for the immobilization should be mechanically and chemically stable, non toxic (before and after immobilization), and readily available. Supports in the shape of beads and membranes are examined. The former allows a high reactive surface area but at the same time has reduced hemocompatibility and potential limitations for high flow rate applications. In addition, the beads require a mechanism to prevent their escape from the reactor. If a retaining mesh is used, the possibility of clogging at the outlet becomes an important issue. Membranes have better mechanical advantages but typically have the disadvantage of reduced reactive surface area if the process is mass transfer limited. In either case, immobilization typically reduces the activity of the enzyme and may even destroy it.

References

- Ambrus, C., Ambrus, J.L., Horvath, C., Pedersen, H., Sharma, S., Kant, C., Mirand, E., Guthrie, R., and Paul, T. 1978. Phenylalanine depletion for the management of phenylketonuria: Use of enzyme reactor with immobilized enzymes. *Science* **201**: 837-839.
- Ambrus, J. J., Codey, C., and Virand, E.A. 1983. *In vivo* safety of hollow-fiber enzyme-reactors with immobilized phenylalanine ammonia lyase in a large animal model for phenylketonuria. *J. Pharmacol. Exp. Ther.* **224**: 598.
- Arbiser, J.L., Dzieczkowski, J.S., Harmon, J.V., and Duncan, L.M. 1995. Leukocytoclastic vasculitis following staphylococcal protein A column immunoadsorption therapy. *Arch Dermatol.* **131**:707-709.
- Basu, D., Gallus, A. J., Hirsh, and Cade, J. 1984. *New Eng. J. Med.* **100**: 358.
- Bernstein, H., Yang, V., Lund, D., Randhawa, M., Harmon, W., and Langer, R. 1987. Extracorporeal enzymatic heparin removal: Use in a sheep dialysis model. *Kidney Int.* **32**: 452-463.
- Bertino, J., Condos, S., Horvath, C., Khaltagi, K., and Pedersen, H. 1979. *Cancer Research* **38**: 1936,1978.
- Broughton, R. 1995. Personal Communication. IBEX Technologies, Montreal, Canada.
- Broyer, M., Brunner, F.P., Brynger, H., Fassbinder, W., Guillou, P.J., and Oules, R. 1986. Demography of dialysis and transplantation in Europe. *Nephrology, Dialysis and Transplantation* **1**: 1.
- Cilley, R. E., Zwischenberger, J.B., Andrews, A.F., Bowerman, R.A., Rodolff, D.W., and Barlett, R.H. 1986. Intracranial hemorrhage during extracorporeal membrane oxygenation in neonates. *Pediatrics* **78**: 69-74.
- Comfort, A. R., Albert, E.C., and Langer, R. 1989. Immobilized enzyme cellulose hollow fibers: I. Immobilization of Heparinase. *Biotech. Bioeng.* **34**: 1366-1373.
- Deary, D.F., Gajaria, M., Fryer-Keene, S., and Willumsen, J. 1991. *Pediatric Nephrology* **5**: 220-224.
- Dumler, F., Singh, P., Jackson, C.E., Kini, K.R., Samhour, A.M., Halvorson, H.R., and Shore, J.D. 1981. Extracorporeal enzyme therapy. Use of an L-asparaginase reactor-dialyser in a clinical setting. *ASAIO J.* **4**: 70.
- Freed, L.E. 1988. An enzymatic fluidized bed reactor for blood deheparinization; Development and testing in lambs on extracorporeal circulation. Ph.D. dissertation, M.I.T.
- Freed, L.E., Vuniak, G.V., Drinker, P.A., and Langer, R. 1988. A novel bioreactor based on suspended particles of agarose-immobilized species. *Trans. Am. Intern. Organs* **34**: 732-738.
- Freed, L.E., Vunjak-Novakovic, G.V., Bernstein, H., Cooney, C. L., and Langer, R. 1993. Kinetics of immobilized heparinase in human blood. *Ann. Biomed. Engng.* **21**: 67-76.

- Freed, L.E., Vunjak-Novakovic, G.V., Drinker, P.A., and Langer, R. 1993. Bioreactor based on suspended particles of immobilized enzyme. *Ann. Biomed. Engng.* **21**: 57-65.
- Gaylor, J.D.S., and Smeby, L.C. In: *Physiological and Clinical Aspects of Oxygenator Design*; Dawids, S.G., and Engell, H.C. 1976. Eds., Elsevier: North-Holland, Amsterdam; pp. 65-79.
- Horvath, C., Sardi, A., and Woods, F.S. 1973. L-asparaginase tubes: Kinetic behavior and application in physiological studies. *J. Appl. Physiol.* **34**: 181.
- Iosilevskii, G., Brenner, H., Moore, C.M.V., and Cooney, C.L. 1993. Mass transport and chemical reaction in Taylor-vortex flows with entrained catalytic particles: applications to a novel class of immobilized enzyme biochemical reactors. *Phil. Trans. R. Soc. Lond.* **345**: 259-294.
- Ireland, H., Rylance, P.B. and Kesteven, P. 1989. In: *Heparin: Chemical and biological properties, clinical applications*; Lane, D.A., and U. Lindahl, Eds., CRC Press: Boca Raton, pp. 549.
- Jaffrin, M.Y., 1989. Innovative processes for membrane plasma separation. *J. Membrane Sci.* **44**: 115-129.
- Jobes, D.R., Schwartz, A.J., Ellison, N., Andrews, R., Ruffini, R.A., and Ruffini, J.J. 1981. Monitoring heparin anticoagulation and its neutralization. *Annals of Thoracic Surgery* **31**: 161.
- Kalghatgi, K.K., Horvath, C. and Ambrus, C.M. 1980. Multi-tubular reactors with immobilized-phenylalanine ammonia lyase for use in extracorporeal shunts. *Res. Commun. Chem. Pathol. Pharmacol.* **27**: 551.
- Kanalas, J.J., Spector, E.B. and Cederbaum, S.D. 1982. Hollow-fiber reactors containing mammalian arginase: An approach to enzyme replacement therapy. *Biochem. Med.* **27**: 46.
- Klein, M.D., and Langer, R. 1986. Immobilized enzymes in clinical medicine: An emerging approach to new drug therapies. *Trends in Biotech.* **14**: 179-186.
- Langer, R., Linhardt, R.J. Hoffberg, S., Larsen, A.K., Cooney, C.L., Tapper, D. and Klein, M. 1982. An enzymatic system for removing heparin in extracorporeal therapy. *Science* **217**: 261-263.
- Larsen, A.K., Newberne, P.M., and Langer, R. 1986. Comparative studies of heparin and heparin fragments: Distribution and toxicity in the rat. *Fundamental and Applied Toxicology*, **7**: 86-93.
- Larsen, A.K., Linhardt, R.J., Tapper, D., Klein, M. and Langer, R. 1984. Effect of extracorporeal deheparinization on formed blood components. *Artif. Organs.* **8**: 198-203.
- Lavin, A., Sung, C., Klibanov, A.M. and Langer, R. 1985. Enzymatic removal of bilirubin from blood; A potential treatment for neonatal jaundice. *Science*, **230**: 543-545.
- Linhardt, R.J., Grant, A., Cooney, C.L. and Langer, R. 1982. Differential anticoagulant activity of heparin fragments prepared using microbial heparinase. *J. Biol. Chem.* **257**: 7310-7313.
- Linker, A., and Hovingh, P. 1972. Heparinase and heparitinase from *Flavobacteria*. *Meth. Enzymol.* **28**: 902-911.
- Makarov, K.A., and Kibardin, S.A. 1980 'Immobilized biopreparations in medicine' , Moscow.

- Mehta, R.L., 1994. Anticoagulation during continuous renal replacement. *ASAIO J.* **40**: 931-935.
- Moore, C.M.V., 1994. Characterization of a Taylor-Couette vortex flow reactor. Ph.D. dissertation, M.I.T.
- Mottaghy, K., and Hanse, H.J. 1985. Effect of combined shear, secondary and axial flow of blood on oxygen uptake. *Chem. Engng. Commun.* **36**: 269-279.
- Olanoff, L.S., Bernath, F.R. and Venkatasubramanian, K. 1975. Perfusion trials with collagen immobilized enzyme in an extracorporeal reactor. *Amer. Chem. Soc. Polym. Prepr.* **16**: 203.
- Pedersen, H., Horvath, C., and Ambrus, C.M. 1979. Preparation of immobilized L-phenylalanine ammonia lyase in tubular forms for depletion of L-phenylalanine. *Res. Commun. Chem. Pathol. Pharmacol.* **20**: 559.
- Petitou, M. 1989. In: Heparin: Chemical and biological properties, clinical applications; Lane, D.A., and U. Lindahl, Eds., CRC Press Inc.: Boca Raton, pp. 65-79.
- Plottz, P.H., Berk, P.D., Scharschmidt, B.F., Gordon, J.K. and Vergalla, J. 1974. Removing substances from blood by affinity chromatography. I. Removing bilirubin and other albumin-bound substances from plasma and blood with albumin conjugated agarose-beads. *J. Clin. invest.* **5**: 778-785.
- Porter, J., and Fick, H. 1977. Drug related deaths among medical inpatients. *J. Amer. Med. Assoc.* **237**: 879-881.
- Rossi, V., 1981. Immobilization of arginase on hollow-fiber hemodialyzer. *Int. J. Artif. Organs* **4**: 102.
- Salmona, M., Saronio, C.I., Bartosek, J., Vecchi, A. and Mussini, E. 1974. In: Insolubilized enzymes; M. Salmona, C.S., Garattini, S. Eds., Raven Press: New York, pp. 189.
- Salzman, E.W., Deykin, D. and Shapiro, R.M. 1975. Management of heparin therapy, controlled prospective trial. *New Eng. J. Med.*, **292**: 1046.
- Sampson, D., Han, T., Hersh, L.S. and Murphy, G.P. 1974. Extracorporeal chemotherapy with L-asparaginase in man. *J Surg Oncol.*, **6**: 39.
- Sasisekharan, R., 1991. Cloning and biochemical characterization of heparinase from *Flavobacterium heparinum*. Ph.D. dissertation, Harvard University.
- Senning, A., 1959. Plasma heparin concentrations in extracorporeal circulation. *Acta. Chirurgica. Scandinavica* **117**: 55.
- Schaeffer, J., Floege, J., Ehlerding, G. and Koch., K.M. 1995. Pathogenetic and diagnostic aspects of dialysis-related amyloidosis. *Nephrol Dial Transplant.* **10(3)**: 4-8.
- Strong, A. B., and Carlucci, L. 1976. An experimental study of mass transfer in rotating Couette flow with low axial Reynolds number. *Can. J. Chem. Engng.* **54**: 295-298.
- Sung, C., Lavin, A., Klibanov, A.M. and Langer, R. 1986. An immobilized enzyme reactor for the detoxification of bilirubin. *Biotech. Bioeng.* **28**: 1531.
- Swartz, R.D., and Port, F.K. 1979. Preventing hemorrhage in high risk hemodialysis. Regional versus low dose heparin. *Kidney Int.* **16**: 513-518.

Takao, N. 1993. In: Biomedical applications of polymeric materials; Tsuruta, T., Hayashi, T., Kataoka, K., Ishihara, K., Kimura, Y. Eds., CRC Press: Boca Raton; pp. 192-208.

Torchilin, V. P. 1991. In: Immobilized enzymes in medicine; Springer-Verlag: Berlin; pp. 135-145.

Vallar, L., and Rivat, C. 1994. Regenerated cellulose-based hemodialyzers with immobilized proteins as potential devices for extracorporeal immunoadsorption procedures: An assessment of protein coupling capacity and *in vitro* dialysis performances. *Artif. Organs* **20**:8-16.

Vallar, L., Costa, P.M.P., Teixeira, A., Pfister, M., Barrois, R., Costa, P.P. and Rivat, C. 1995. Immunoadsorption procedure as a potential Method for the specific β_2 m removal from plasma of patients with chronic renal failure. *J. of Chromatography B: Biomed. App.* **664**: 97-106.

Wakefield, T.W., Lindblad, B., Whitehouse, W., Hantler, C., and Stanley, J.C. 1986. Attenuation of hemodynamic and hematologic effects of heparin protamine sulfate interaction after aortic reconstruction in a canine model. *Surgery* **100**: 45-51.

Wright, J. S., Osborn, J.J., Perkins, H.A. and Gerbode, F. 1964. Heparin levels during and after hypothermic perfusion. *Journal of Cardiovascular Surgery* **5**: 244.

Yang, V. C., Linhardt, R.J. Bernstein, H. Cooney, C.L. and Langer, R. 1985. Purification and characterization of heparinase from flavobacterium heparinum. *J. Biol. Chem.* **260**: 1849-1857.

Zusman, R. M., Rubin, R.H., Cato, A.E., Cocchetto, B.S., Crow, J.W., Tolkoff-Rubin, N. 1981. Hemodialysis using prostacyclin instead of heparin as the sole antithrombotic agent. *New Eng. J. Med.* **304**: 934-939.

Chapter 2

The Vortex Flow Fluidized Bed Reactor

2.1 Introduction

The optimum management of heparin therapy in the critically ill patient is an important problem that continues to affect the medical community. The use of heparin and its antagonist protamine has been associated with potentially fatal complications in high risk patients such as those suffering from acute renal failure and those who have undergone open heart surgery (Broyer *et al.*, 1986; Salzman *et al.*, 1975). The immobilized heparinase I approach could be an alternative therapy to protamine reversal and also a way to achieve regional heparinization in extracorporeal circuits for hemodialysis and hemoperfusion. However, an important issue that needs to be addressed for the successful application of extracorporeal therapies that involve immobilized enzymes or antibodies is the development of bioreactors that are safe, efficient, easy to use, and cost effective.

Current bioreactor designs can be divided into two categories: membrane based devices such as hollow fiber cartridges, and porous particle devices in the form of packed columns or fluidized beds. Several investigators have bound the protein of interest to the walls of a hollow fiber dialyzer to enhance the whole blood compatibility of the system but in many cases the surface area requirements for the efficacy of such devices remain impractical (Comfort, 1988a; Vallar, *et al.*, 1996). Others have suggested the use of porous particles, such as agarose or cellulose beads, in either the packed bed or fluidized bed mode as a way to optimize the protein or adsorbent loading per volume of device (Gejyo *et al.*, 1993; Langer *et al.*, 1982). Vunjak-Novakovic and co workers (1988) have demonstrated the importance of secondary flows in an oscillating bioreactor for the even fluidization of agarose. Nevertheless, despite the presence of secondary flows, the oscillating bioreactor was limited to flow rates of up to 100 ml blood/min due to the packing of the beads at the reactor outlet (Freed *et al.*, 1988).

In this chapter, secondary flows (Taylor vortices) and “flow-induced” agarose recirculation was combined to facilitate the use of agarose immobilized heparinase I in the clinical setting. Taylor vortices are flow instabilities that occur within the annular gap of concentric cylinders when the inner cylinder is rotated above a critical rotation rate. Taylor vortices have been shown to have excellent mixing characteristics in reactors that processed biological systems such as cell cultures, blood plasmapheresis, and oxygenation (Beaudoin *et al.*, 1987). However, no one has

investigated the use of Taylor vortices with immobilized enzyme fluidized systems for medical applications.

The studies in this chapter examined whether the advantages of Taylor vortices could be incorporated into an immobilized heparinase I fluidized bed reactor that would meet the following criteria: 1) high whole blood flow rates of 150 - 400 ml/min, 2) efficient conversions, and 3) minimal blood damage as determined by blood cell counts, platelet counts, and hemolysis.

2.2 Materials and Methods

The reactor vessel is made from concentric polycarbonate cylinders (6.38 cm OD and 5.10 cm OD with 0.32 cm wall thickness) and sheets purchased from Commercial Plastics (Somerville, MA) with polycarbonate inlet and outlet ports (0.96 cm ID) purchased from Avecor Cardiovascular Inc. (Plymouth, MN). The inner cylinder rotates on 0.32 cm OD stainless steel pins from Small Parts Inc. (Miami Lakes, FL). Silicone O-rings were purchased from Marco Rubber Inc. (Andover, MA). The reactor components were machined according to specifications at the MIT Central Machine Shop.

The inner cylinder rotated via a custom made magnetic coupling drive system which consisted of eight neodymium iron boron disc magnets (Dia = 1.28 cm Length = 0.64 cm Cat# 27DNE3216) from Magnet Sales & Manufacturing Inc. (Culver City, CA) and an external Bodine PM electric motor and controller (Bodine Type FPM) from Bodine Electric Company (Chicago, IL). Four neodymium iron boron disc magnets were placed in the top end of the inner cylinder with the north/south magnet pair perpendicular and in opposite polarity to the east/west pair. A similar magnet set up was placed at the end of the motor. Magnetic coupling was achieved when the magnets on the motor and the inner cylinder aligned themselves according to magnetic polarity. The magnetic force between the inner cylinder and the motor driver was strong enough to rotate the inner cylinder, eliminating direct contact of the blood path with the motor shaft. Rotation rate was detected through an optical sensor and displayed on a digital panel meter from Cole Parmer Instruments Co. (Niles, IL). Temperature measurements were made by T-type thermocouples connected to a digital panel meter from Cole Parmer Instruments Co. (Niles, IL). Medical grade photoreactive adhesive ELC type 4M12 was from Electro-Lite Corporation (Danbury, CT).

Drip chambers (12 ml, polyvinylchloride) were from Lifemed (Compton, CA) and Qosina Corporation (Edgewood, NY). Tygon medical grade tubing (0.64 cm ID and 0.96 cm ID) was from VWR Scientific (Boston, MA). The peristaltic blood pump (model Draker Willock 7401) was donated by Children's Hospital (Boston, MA). Ethylene oxide was from Andersen (Oyster Bay, NY). Medical grade heparin solution for blood studies (porcine, 1,000 units/ml) was from

Elkin-Sinn (Cherry Hill, NJ). Powdered heparin for enzyme activity determination (porcine, 166 units/mg) was from Hepar Industries (Franklin, OH). Normal saline (0.9% NaCl) was from Abbott (Chicago, IL) and PBS (0.154 M NaCl and 0.01M sodium phosphate, pH = 7.4) was from Life Technologies (Grand Island, NY). Heparin levels in blood were monitored with model 801 Hemochron coagulation timers and P214 glass activated test tubes from Cardio Medical Products (Rockaway, NJ).

Agarose particles (8%, 50-100 mesh, 200 μm average diameter) were from BioRad (Rockville, NY); Cyanogen Bromide and Lysine Hydrochloride were from Sigma Chemical Company (St. Louis, MO); Heparinase I, produced from *Flavobacterium heparinum*, was generously donated by IBEX Technologies (Quebec, Canada). The enzyme preparation was 95% pure heparinase I as determined by RP-HPLC (company documentation) with a specific activity of 242 IU/ml and protein concentration of 2.6 mg/ml. One IU (international unit) is defined as the amount of enzyme required to produce 1 μmol of product per minute. Human blood was obtained from healthy male and female volunteers. The blood was collected by a professional staff at the Blood Donor Center of Children's Hospital (Boston, MA). Plasma hemoglobin levels were determined with an assay kit from Sigma Chemical Company (St. Louis, MO).

Protein concentration in saline

The coomassie blue dye method of Bradford was used to measure the concentration of heparinase in buffered saline. A volume of 800 μl of sample was mixed with 200 μl of dye solution and incubated at room temperature for 5 minutes. The absorbance at 595 nm was measured and compared to a standard curve prepared with known bovine albumin concentrations ranging from 1 to 20 $\mu\text{g/ml}$. The standard curve was linear in the above range.

Activity of soluble heparinase I

The activity of heparinase I was defined using the international unit (IU). One IU is the amount of heparinase that would produce 1 μmol of double bonds/min. The appearance of heparin degradation products was monitored at 232 nm in a quartz cuvette. Briefly, 20 μl of heparinase solution was added to 3 ml of heparin solution (2 mg/ml) in 100 mM MOPS 5 mM calcium acetate pH 7.4 at 30 $^{\circ}\text{C}$. The initial rate was calculated from the slope of the curve and converted to IU using 3800 M^{-1} molar absorptivity.

Cyanogen bromide activation of agarose

1 volume of agarose gel (200 μm average bead diameter) was washed with 10 volumes of deionized (DI) water to remove any preservatives. After resuspending the gel in 1 volume of DI

water and 2 volumes of 2 M sodium carbonate the solution was chilled in an ice bath. Next, 0.2 volume of a solution of cyanogen bromide in acetonitrile (1g/ml) was added to the gel solution and the mixture was stirred vigorously in the fume hood for 5 minutes. Using a sintered glass funnel, the activated gel was isolated and washed with the following: 10 volumes of DI water, 5 volumes of 1 mM hydrochloric acid, and 5 volumes of 0.1 M sodium bicarbonate 0.5 M NaCl pH 8.3 buffer.

Immobilization of heparinase I

After extensive washing of the activated gel, the heparinase solution (18 mg in 100 ml 0.1 M sodium bicarbonate 0.5M NaCl pH 8.3) was incubated with the beads (100 ml) at 4°C for 5 hrs to allow binding. Following heparinase binding, the immobilized heparinase was incubated overnight at 4°C in a lysine solution (0.2 M lysine hydrochloride 0.1M sodium bicarbonate 0.5M NaCl) to cap any unreacted sites. The immobilized heparinase was then washed with 5 volumes of cold pH 8.3 buffer and 30 volumes of phosphate buffered saline (PBS) pH 7.4, and 10 volumes of distilled water. The amount of bound protein was determined by a mass balance between the original enzyme solution and the washes. The immobilized heparinase I was resuspended in an equal volume of PBS, pH 7.4, and stored at 4 °C.

Activity of the immobilized heparinase I

The activity of the heparinase bound to the beads was measured using a modified UV 232 activity assay. A known volume of beads, approximately 0.1 ml, was added to 4 ml of a heparin solution (25 mg/ml). Under vigorous swirling at 37 °C, 0.1 ml samples were taken at 1 minute intervals for 4 minutes and quenched in 0.9 ml of 30 mM HCl. The samples were centrifuged and the absorbance of the supernatant was measured at 232 nm. The activity was then calculated from the slope between the data points using 5000 M⁻¹ as the molar absorptivity.

Measurement of heparin activity in blood

Whole blood recalcification times (WBRT) were used to indirectly determine the amount of heparin present in blood. Briefly, 200 µl of citrated blood (3.8% 1:10 dilution) was added to Hemochron p214 test tubes containing glass particles. At t=0, 200 µl of CaCl₂ was added to the test tube and the Hemochron 801 clot timer machine was immediately started. The test tube was gently mixed for 10 seconds and inserted into the test well of the Hemochron 801. The time required for a clot to form was recorded. The unknown samples were compared to a standard curve which was linear in the range of 0 - 4 USP units heparin/ml blood.

Measurement of free hemoglobin in plasma

A hemoglobin detection kit from Sigma was used to monitor the release of hemoglobin into the plasma. The kit is based on the catalytic effect of hemoglobin on the oxidation of 3,3',5,5'-tetramethylbenzidine (TMB) by hydrogen peroxide. Briefly, 10 μ l of sample is added to 4 ml of reagent and measured at 600 nm at 25°C. The color formation in the reaction is proportional to the hemoglobin concentration in the sample. Any measurements above 2.6 mg hemoglobin/dL-pass were considered to be unsafe. The criteria for significant hemolysis was derived from interviews with physicians and hemolysis data from currently used medical devices.

Measurement of complete blood counts

Blood samples were taken to the M.I.T. Medical Laboratory for automated analysis of the red cell, white cell, and platelet populations.

***In vitro* batch removal of heparin from blood**

The assembled reactor was incorporated into a closed circuit primed with normal saline which consisted of a blood warmer, blood pump, and a drip chamber and pressure monitor. The circuit was then connected to a 450 cc reservoir of citrated human blood which was spiked with heparin to achieve a final concentration of approximately 2 USP units Heparin /cc blood. The blood flow and rotation rate of the reactor were adjusted to either 100 ml/min or 200 ml/min and 500 or 200 rpm, respectively. The temperature of the system was monitored directly with a T type thermocouple probe. At time = 0, a 50% slurry of agarose immobilized heparinase was injected via the drip chamber into the blood circuit and allowed to enter the annular space of the reactor where Taylor vortices were present. Samples were constantly taken from the outlet port during the experiment and analyzed for efficacy and safety of the device.

Design and construction of the vortex flow fluidized bed reactor (VFFBR)

The reactor was machined from polycarbonate tubing and had an outside diameter of 6.38 cm. Two versions were tested: a narrow gap ($r_{\text{outer}} - r_{\text{inner}} = 0.32$ cm), 24.00 cm length device (design I) and a wide gap ($r_{\text{outer}} - r_{\text{inner}} = 0.64$ cm), 14.00 cm length device (design II). In addition to the inlet and outlet ports, the reactor was fitted with two tangential ports (0.96 cm Dia.) to accommodate a recirculation line. The dimensions and the diagram for the device are shown in **Table 2.1** and **Figure 2.1**, respectively. A 1 inch length retaining mesh with a mesh opening of 44 μ m was placed along the circumference of the outer cylinder proximal to the outlet port to prevent the beads from escaping the device. The maximum volume of the device was limited to 150 ml. This volume was a clinical specification to minimize hemodilution of the patient.

Table 2.1. Dimensions for designs I and II.

	Design I	Design II
Total volume	150 cc	150 cc
Length	24 cm	14 cm
Recirculation port I.D.	0.96 cm	0.96 cm
r_i	2.55 cm	2.23 cm
r_o	2.87 cm	2.87 cm
Gap width	0.32 cm	0.64 cm

Determination of agarose fluidization conditions

The reactor was operated at various rotation rates and flow rates in a closed circuit with either water or 42% glycerol. The criteria for adequate fluidization of the agarose was: 1) the absence of dead zones as judged by visible agarose accumulation at any point in the reactor and 2) constant pressure drop across the reactor as judged by a pressure gauge at the reactor outlet. Visual assessment of the agarose beads and flow conditions in the reactor were used to determine adequacy of fluidization. At a fixed flow rate, the rotation rate of the inner cylinder was increased and decreased until the fluidization conditions were met.

2.3 Results and Discussion

In this study, for the first time, it has been shown that Taylor-Couette flow together with “flow-induced” recirculation can be used as a reactor system to fluidize agarose immobilized species. The characteristics of Taylor-Couette flow have been studied extensively since their discovery by G.I. Taylor (1923). To date, the most common application of Taylor vortices in industry is filtration, which was developed within the last fifteen years (Kroner and Nissinen, 1988; Vigo *et al.*, 1985). Taylor vortices were selected as a means for fluidizing the agarose beads because the beneficial mixing effects of the vortices on biological cells have been demonstrated (Beaudoin *et al.*, 1987). In addition, models and correlations for the high mass transfer rates observed for fluidized particles within Taylor vortices have been developed (Iosilevskii *et al.*, 1993; Moore, 1994). However, the sole presence of Taylor vortices is not sufficient to fluidize agarose beads at high flow rates. This is due to the fact that most porous particle support materials such as agarose have a density that is very similar to the fluid in which they are suspended, making the fluidization process difficult at clinically relevant flow rates (150-400 ml/min) (Moore, 1994).

The use of fluidized bed reactors in whole blood in vitro as well as ex vivo has previously been described (Freed *et al.*, 1988; Langer *et al.*, 1982). In one configuration, a recirculation line

and a peristaltic pump were used to help fluidize the beads to prevent bead packing at the reactor outlet. Further studies determined that using a peristaltic pump to recirculate an agarose-blood slurry significantly contributed to the observed blood damage (Larsen *et al.*, 1984). Therefore, elimination of a recirculating pump was a design objective.

The immobilization procedure used for the present study bound 95% of the soluble enzyme with an activity retention of 30-40%. The average activity of the agarose immobilized heparinase I was 12-16 IU/ml packed wet gel. Another important issue for the use of immobilized enzymes is detachment or leaching of the enzyme from the support. Over a period of 4 days, no detectable leaching of heparinase I occurred from the agarose beads in buffer as judged by protein concentration and soluble enzyme activity assays (the UV 232 nm activity assay is sensitive to 0.5 µg/ml of pure heparinase). A previous analysis of the immobilization of heparinase on solid supports also showed no significant leaching using cyanogen bromide activation chemistry vs. other covalent methods, as long as thorough post immobilization washes with high salt buffer were performed (Comfort *et al.*, 1988b; Leckband and Langer, 1991). In regards to toxicity issues, animal experiments demonstrated that the heparin degradation products were non toxic for doses of up to 100 times the expected clinical exposure concentration (Larsen *et al.*, 1986). Furthermore, healthy volunteers from a phase 1 clinical trial did not elicit any acute reaction to soluble heparinase I (Broughton, 1995).

In the present study, a Taylor-Couette flow device was constructed and modified with a recirculation line in order to allow even fluidization of agarose beads at high flow rates (**Figure 2.1**). The selected tangential location of the recirculation ports allowed continuous flow and fluidization of the beads without the aid of an external pump. Design I (narrow gap) was able to remove 90% of the heparin's anticoagulant activity from 450 cc of human citrated blood *in vitro* within 3 minutes of operation at a flow rate of 100 ml/min (**Figure 2.2**). However, for the operating conditions used, fluidization of the agarose beads within the Taylor vortices caused extensive damage to the red cells, white cells, and platelets (**Figure 2.3**). **Figure 2.4** shows hemolysis during the experiment, an effect of the fluidization of agarose beads within the Taylor vortices on the red cell membrane. The red cells were ruptured and hemoglobin was released into the plasma (HbP). The hemolysis that resulted was above the safety criteria of 2.6 mg hemoglobin/dL-pass (1 pass = 4.5 min). Further experiments demonstrated that the degree of hemolysis was directly proportional to the volume fraction of agarose and to the rotation rate of the inner cylinder (**Figure 2.5**).

In order for the fluidization to occur at relatively high flow rates, the rotation rate had to be maintained above a minimum predetermined value in order to continuously recirculate the agarose

beads. **Table 2.2** shows the rotation rates necessary to achieve adequate fluidization of the beads for various flow rates in water and in a 42% glycerol/water solution of similar viscosity to blood. The viscosity of the solution had a significant effect on the critical rotation rate for fluidization at specific flow rates. At the optimum rotation rate for each flow rate, up to 50% agarose volume fraction could be evenly fluidized within the 150 ml volume device.

Table 2.2. Minimum rotation rates required in the VFFBR for even fluidization of 50 cc of agarose beads. At lower rotation rates, the beads either accumulated at the reactor outlet or in the recirculation line.

Flow rate (ml/min)	Minimum rotation rate for fluidization (rpm)	
	Water	42% Glycerol
100	200	200
200	250	300
300	350	400
400	450	500

Two steps were taken (design II) to reduce the blood damage that resulted from design I: 1) the gap width was increased while maintaining the annular volume constant and 2) the rotation rate was reduced to 200 rpm. The results for the efficacy and safety of design II are shown in **Figures 2.6 - 2.9**. The reactor was able to remove 80% of the initial heparin effect within 3 minutes of recirculation at 100 ml/min (**Figure 2.6**). This deheparinization efficacy was comparable to that of design I. However, the blood cell count, platelet count, and hemolysis data for design II (**Figures 2.8 and 2.9**) were a significant improvement over the results from design I. The cell and platelet counts remained within 95% of the initial value for design II. The rate of hemolysis (5.4 mg/dL-pass), while above our safety criteria of 2.6 mg/dL-pass, represented a 14 fold reduction in hemolysis rate compared to design I. After the initial heparin removal by design II, a constant infusion of heparin (pre reactor but post blood reservoir) was initiated to simulate regional heparinization. The advantage of regional heparinization is that a patient at risk of bleeding would be exposed to significantly lower heparin levels without jeopardizing the optimal anticoagulation status and functionality of the extracorporeal circuit. At 100 ml/min, the average inlet and outlet WBRT were 269±10 and 235±6 seconds, respectively (**Figure 2.7**). These values corresponded to an average single pass heparin removal of 23%. For regional heparinization to be clinically significant, the reactor should effect an average single pass heparin removal of at least 45%. Nevertheless, these results demonstrated the feasibility of regional heparinization with the

VFFBR. An increase in conversion could be achieved by increasing the specific activity of the immobilized enzyme. Even though heparin was continuously removed, the potential formation of clots around the agarose beads can not be determined in the current system because the blood was also citrated.

As mentioned above, the dimensions and rotation rate (200 rpm) used for design II reduced the red cell hemolysis rate by 14 fold for the same agarose volume fraction used in design I. However, the rotation rate required to maintain good fluidization at blood flow rates higher than 150 ml/min was higher than 200 rpm. For 50 cc of gel, 200 rpm was the maximum rotation rate that could be used without significant hemolysis (data not shown). Because it was found that the rate of hemolysis is proportional to the gel volume used, it should be possible to increase the flow rate capacity by reducing the gel volume and increasing the rotation rate accordingly.

In summary, the concept of using Taylor-Couette flow as a potential way to fluidize agarose immobilized heparinase in whole blood was introduced. A modified Taylor-Couette flow device evenly fluidized high gel volume fractions at high flow rates (100 - 400 ml/min) when tested in water and in a blood substitute. However, when the device was tested in blood, some damage to blood cells and platelets was noticed. Even though the mixing properties of Taylor vortices have been shown to be gentle on blood cells, the effects of suspending solid particles within the vortices and in whole blood have not been examined. The results in this chapter suggest that when Taylor-Couette flow is combined with macroscopic solid particles such as agarose beads, lysis of the red cells becomes an important issue. Chapter 4 investigates a novel method, based on Taylor-Couette flow and the principle of simultaneous separation/reaction, to eliminate the hemolysis problem reported in this chapter. Nevertheless, design and operational criteria that can be used to minimize hemolysis in a whole blood fluidized particle system were established, especially if blood flow rates higher than 150 ml/min are desired.

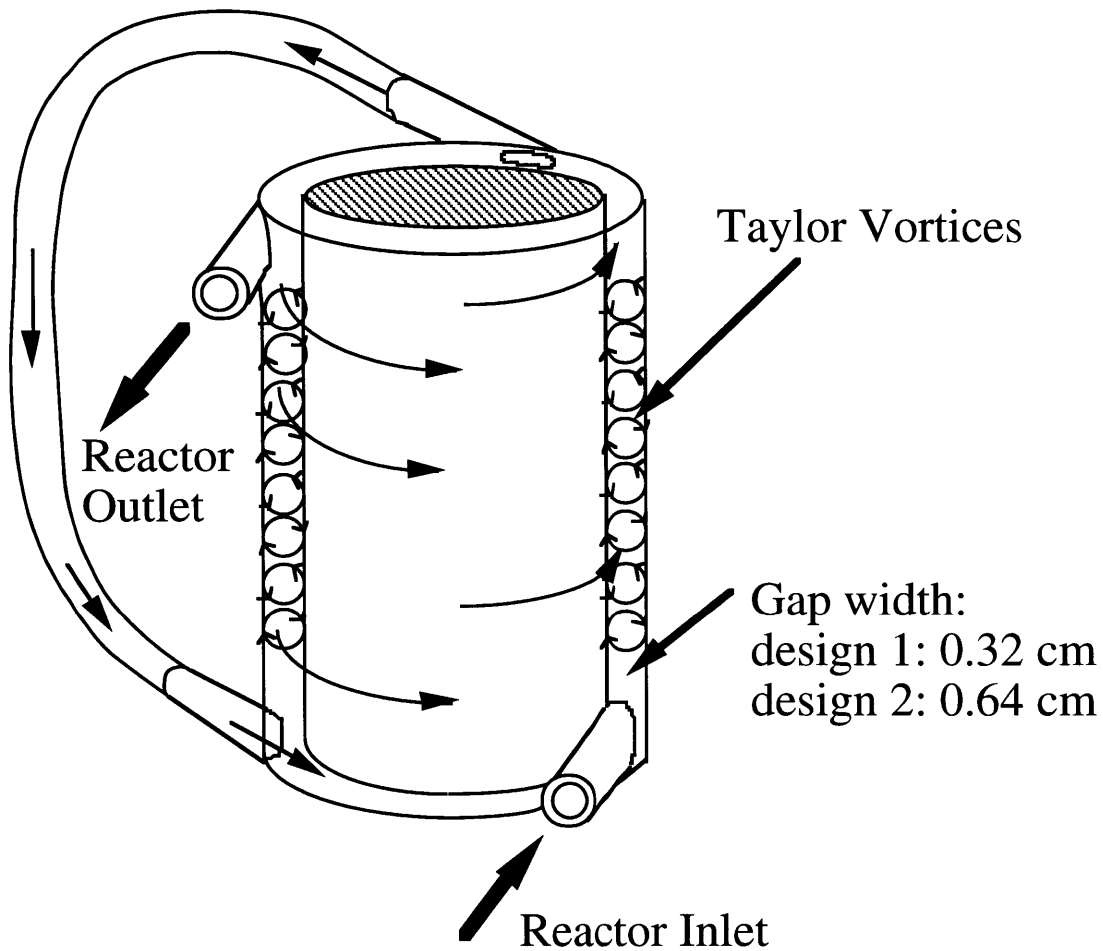


Figure 2.1. Diagram of the vortex flow fluidized bed reactor (VFFBR). The design tested incorporated a recirculation loop whose entrance and exit ports were tangent to the flow direction within the annulus. This modification allowed even fluidization of high gel volume fractions at high flow rates (400 ml/min.) as long as a predetermined rotation rate was maintained. Whole blood entered and exited the device while the agarose was continuously recirculated via the recirculation line.

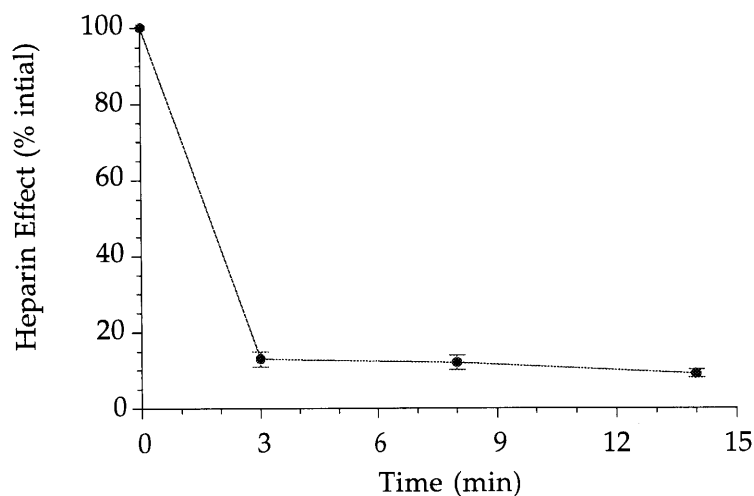


Figure 2.2. In vitro batch heparin removal by the VFFBR (design I) from 450 cc of citrated human blood. Blood flow rate was 100 ml/min, rotation rate was 500 rpm, and the temperature was 32°C. Enzyme loading was 800 IU (50 cc of gel). Whole blood recalcification times (WBRT) were measured. WBRT dropped from 392 ± 13 sec to 157 ± 8 sec within 3 minutes. This represented a decrease from 3.2 to 1.3 times the baseline value (121 ± 8 sec) before addition of the heparin (mean \pm SD of 4 measurements).

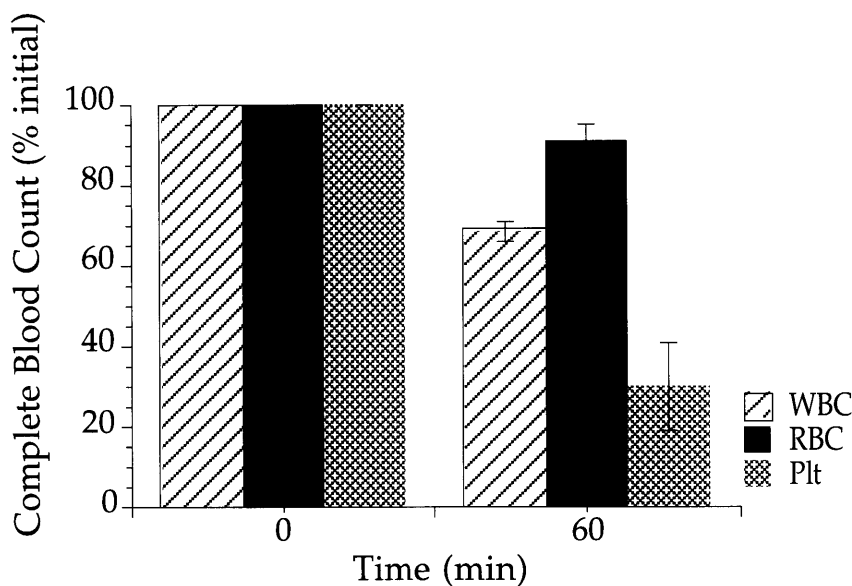


Figure 2.3. Safety data for the VFFBR (design I). At the end of the experiment there was a significant decrease in the white blood cells, red blood cells, and platelets count (mean \pm SD of 2 experiments).

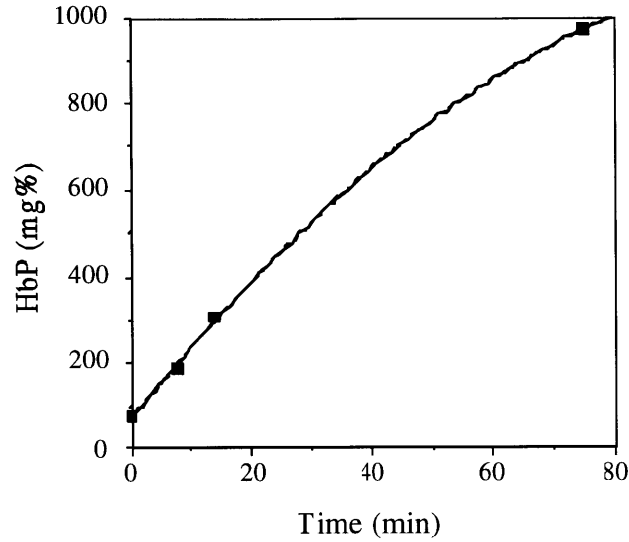


Figure 2.4. Release of free hemoglobin into the plasma (design I). At a rotation rate of 500 rpm and a gel volume of 50 cc, hemolysis was significant (76 mg/dL-pass) in the VFFBR and attributed to the high shear within the agarose beads and Taylor vortices (mean \pm S.D. of 2 experiments, bars are the size of the data points).

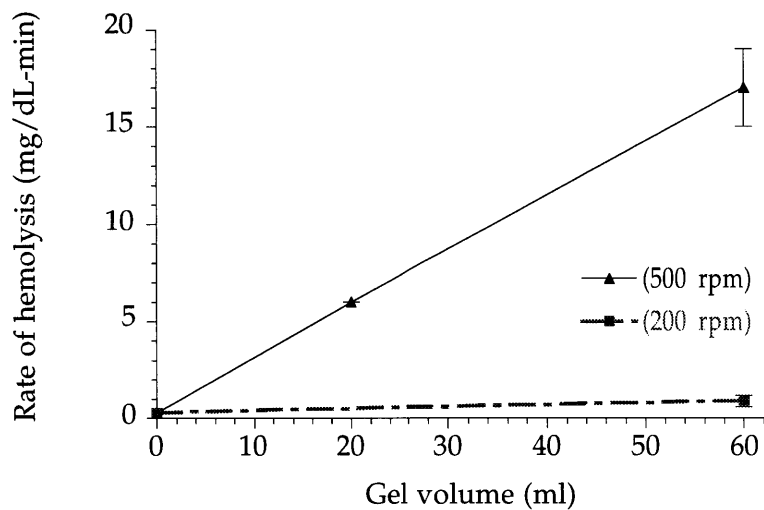


Figure 2.5. Effect of gel volume and rotation rate on hemolysis (mean \pm SD of 2 experiments). The rate of hemolysis was directly proportional to the rotation rate of the inner cylinder. At 500 rpm, an increase in gel volume effected an increased rate of hemolysis relative to a rotation rate of 200 rpm.

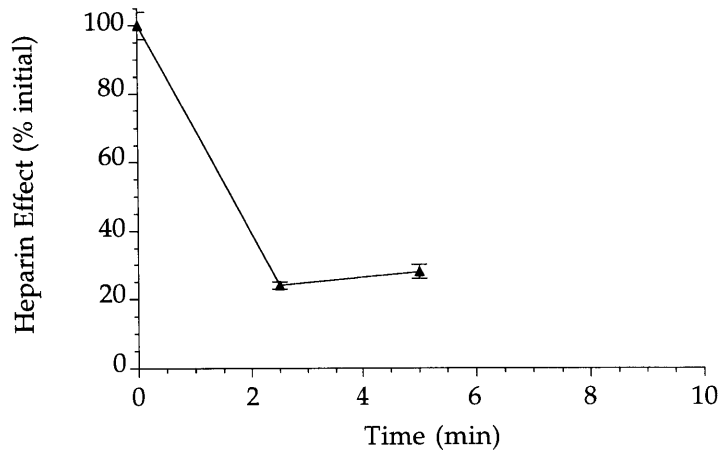


Figure 2.6. In vitro batch heparin removal by the VFFBR (design II) from 450 cc of citrated human blood. Blood flow rate was 100 ml/min, rotation rate was 200 rpm, and the temperature was 32°C. Enzyme loading was 675 IU (50 cc of gel). Whole blood recalcification times (WBRT) were measured. WBRT dropped from 403 ± 20 sec to 190 ± 1 sec within 3 minutes. This represented a decrease from 3.3 to 1.5 times the baseline value (123 ± 5 sec) before addition of the heparin (mean \pm SD of 4 measurements).

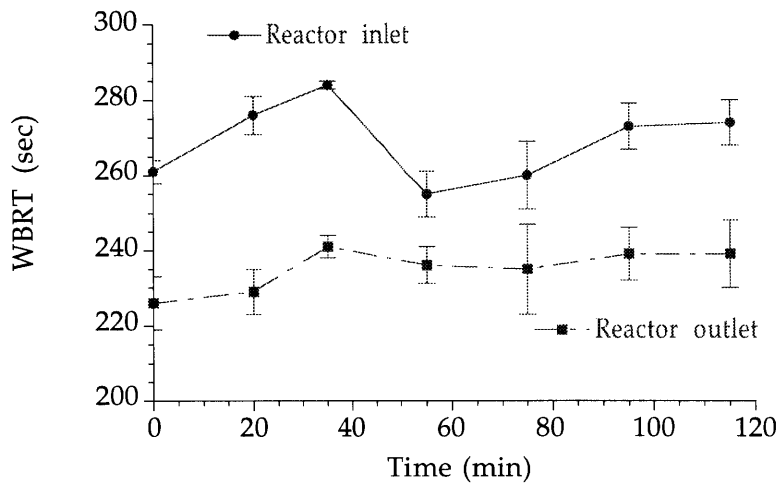


Figure 2.7. In vitro regional heparinization with design II using 450 cc of citrated human blood. Blood flow rate was 100 ml/min, rotation rate was 200 rpm, and the temperature was 32°C. Enzyme loading was 675 IU (50 cc of gel). The mean inlet and outlet WBRT were 269 ± 10 and 235 ± 6 seconds, respectively (mean \pm SD of 4 measurements).

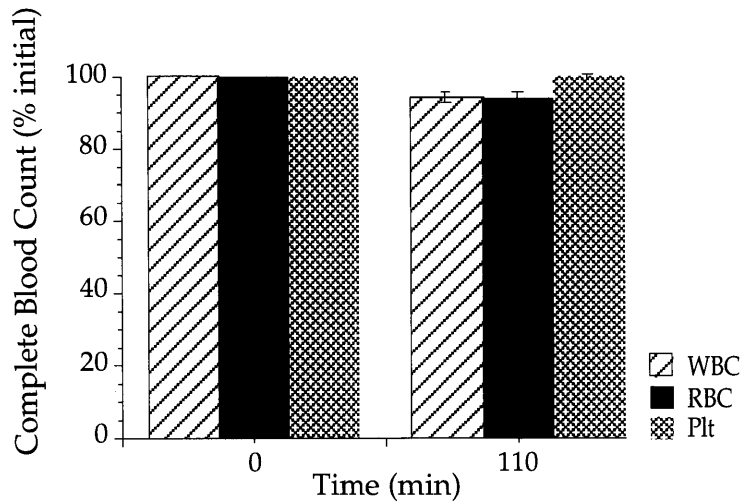


Figure 2.8. Safety data for the VFFBR (design II). After approximately two hours of operation, there was no clinically significant decrease in the blood cells, suggesting a more gentle mixing process in the device. Blood flow rate was 100 ml/min, rotation rate was 200 rpm, and the temperature was 32°C. Enzyme loading was 675 IU (50 cc of gel) (mean \pm SD of 2 experiments).

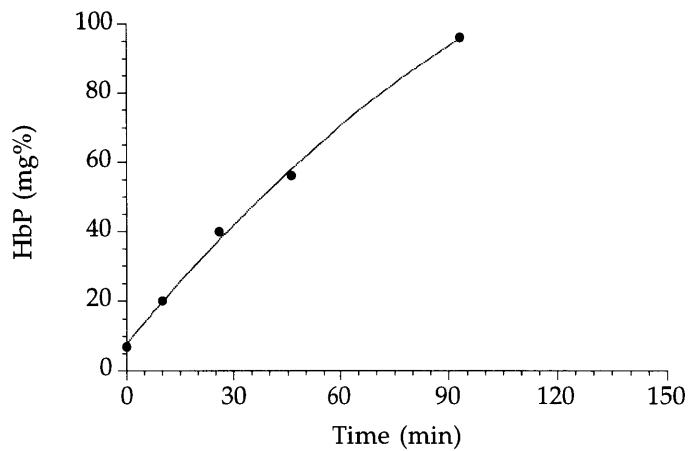


Figure 2.9. Release of free hemoglobin into the plasma (design II). At a rotation rate of 200 rpm the rate of release of hemoglobin was 5.4 mg/dL-pass (mean \pm S.D. of 2 experiments, bars are the size of the data points).

References

- Beaudoin, G. and Jaffrin, M.Y. 1987. High efficiency plasmapheresis using rotating membrane device. *Life Support Syst.* **5**: 273-278.
- Broughton, R. 1995. Personal Communication. IBEX Technologies, Montreal, Canada.
- Broyer, M., Brunner, F.P., Brynner, H., Fassbinder, W., Guillou, P.J., and Oules, R. 1986. Demography of dialysis and transplantation in Europe. *Nephrology, Dialysis and Transplantation* **1**: 1-3.
- Comfort, A.R. 1988a. Immobilization chemistry, cellulose support, and kinetic evaluation of a heparinase device for the removal of heparin from the bloodstream. Ph.D. thesis, Massachusetts Institute of Technology, MA
- Comfort, A.R., Mullon, C.J.P., Koh, J., Albert, E., Tosone, C.P., Hall, J., and Langer, R. 1988b. Stability and immunologic activity of immobilized heparinase and bilirubin oxidase. *ASAIO Trans.* **34 (3)**: 538-542.
- Freed, L.E., Vunjak, G.V. Drinker, P.A. and Langer, R. 1988. A novel bioreactor based on suspended particles of agarose-immobilized species. *ASAIO Trans.* **34 (3)**: 732-738.
- Gejyo, F., Homma, N. Hasegawa, S., and Arakawa, M. 1993. A new therapeutic approach to dialysis amyloidosis: Intensive removal of beta-2-microglobulin with adsorbent column. *Artif. Organs*, **17 (4)**: 240-243.
- Iosilevskii, G., Brenner, H., Moore, C.M.V., and Cooney, C.L. 1993, Mass transport and chemical reaction in Taylor-vortex flows with entrained catalytic particles: Application to a novel class of immobilized enzyme biochemical reactors. *Phil. Trans. R. Soc. A* **345**: 259-294.
- Kroner, K.H., and Nissinen, V. 1988. Dynamic filtration of microbial suspensions using an axially rotating filter. *J. Membrane Sci.* **36**: 85-100.
- Langer, R., Linhardt, R.J., Hoffberg, S., Larsen, A.K., Cooney, C.L., Tapper, D., and Klein, M. 1982. An enzymatic system for removing heparin in extracorporeal therapy. *Science* **217**: 261-263.
- Larsen, A.K., Linhardt, R.J., Tapper, D., Klein, M., and Langer, R. 1984. Effect of extracorporeal enzymatic deheparinization on formed blood components. *Artif. Organs* **8(2)**: 198-203.
- Larsen, A.K., Newberne, P.M., and Langer, R. 1986. Comparative studies of heparin and heparin fragments: Distribution and toxicity in the rat. *Fundam. Appl. Toxicol.* **7**: 86-93.
- Leckband, D. and Langer, R. 1991. An approach for the stable immobilization of proteins. *Biotechnol. Bioeng.* **37**: 227-237.
- Moore, C.M.V. 1994 Characterization of a Taylor-Couette vortex flow reactor. Ph.D. thesis Massachusetts Institute of Technology, MA
- Salzman, E.W., Deykin, D., and Shapiro, R.M. 1975. Management of heparin therapy, Controlled prospective trial. *New Eng. J. Med.* **292**: 1046-1050.

Taylor, G.I. 1923. Stability of a viscous liquid contained between two rotating cylinder. Phil. Trans. R. Soc. A **223**: 289-343.

Vallar L, and Rivat, C. 1996. Regenerated cellulose-based hemodialyzers with immobilized proteins as potential devices for extracorporeal immunoadsorption procedures: Assessment of protein coupling capacity and *in vitro* dialysis performances. Artif. Organs **20 (1)**: 8-11.

Vigo, F., Uliana, C., and Lupino, P. 1985. The performance of a rotating module in oily emulsions ultrafiltration. Sep. Sci. Technol. **20**: 213-230.

Vunjak-Novakovic, G., Shiva, V.A., Freed, L.E., Cooney, C.L. and Langer, R. 1988. Computer-aided visualization and analysis of fluid and particle motion in multiphase systems. Biochem. Eng. Quarterly **2**: 249-252.

Chapter 3

The Vortex Flow Plasmapheretic Reactor (VFPR)

3.1 Introduction

The results from Chapter 2 showed that agarose immobilized heparinase I fluidized within high blood flow rates and turbulent vortices resulted in blood damage and hemolysis (Ameer *et al.*, 1999). To minimize blood damage, a device that simultaneously effected plasma separation and the enzymatic reaction with the capacity to treat high whole blood flow rates was designed and constructed. The new reactor design uses Taylor-Couette flow (also known as Taylor vortex flow) as a means to achieve good mixing and to minimize cell concentration polarization on the membrane (Beaudoin and Jaffrin, 1987). Taylor-Couette flow is established when the inner cylinder of an annulus is rotated beyond a critical rotation rate determined by the critical Taylor number (Taylor, 1923). The flow instabilities generated within the annulus create a secondary flow pattern in the form of periodic vortices termed Taylor vortices. Taylor-Couette flow devices have primarily been used in filtration applications (Holeschovsky and Cooney, 1991; Kroner and Nissinen, 1988). During filtration, the Taylor vortices effectively reduce concentration polarization at the membrane surface. Reported filtrate fluxes are significantly higher than those observed in conventional hollow fiber devices (Ohashi *et al.*, 1988). Membrane induced circumferential flow was observed in the immobilized enzyme compartment and was able to fluidize the agarose beads. The objective of this study was to evaluate the feasibility and efficacy of this novel device for regional heparinization *in vitro* using buffered saline and human blood.

3.2 Materials and Methods

The materials used to build and operate the VFPR were the same as those described in Chapter 2. The agarose particles (6%, 100-200 mesh, 100 μm average diameter) were from BioRad (Rockville, NY). Blue dextran (2,000 kD) was from Sigma Chemical Company (St. Louis, MO). Polyester membranes (1 μm pore size) were from Whatman Inc. (Clifton, NJ).

Heparin Concentration in Saline

An assay using Azure II dye was used to monitor heparin concentrations during the experiments. (Lam *et al.*, 1976). A 4.5 ml volume of the Azure II dye solution (0.01 mg/ml) was added to 0.5 ml of the heparin solution to be tested. The sample was mixed and incubated at room temperature for 1 minute before measuring the absorbance at 500 nm. A standard curve for this assay was prepared by using solutions of known heparin concentrations ranging from 0 to 3 USP units/ml heparin (~ 0 - 19 $\mu\text{g/ml}$). The standard curve was linear in the above range.

Reactor Design

The reactor consisted of two concentric cylinders and a microporous membrane to separate the blood cells from the agarose immobilized heparinase. The outer stationary cylinder was counter bored to accommodate an unsupported microporous polyester membrane along the circumference of its inner surface. This set up created a separate annular compartment (reactive chamber) for the agarose immobilized enzyme. A second, smaller compartment (plasma collection chamber) was counter bored into the outer cylinder to accommodate a cylindrical 15 μm polyester mesh to prevent the agarose beads from escaping the device and to minimize the pressure drop across agarose beads in the reactive chamber. To improve heparin mass transfer from the main annulus into the reactive chamber, a plasma pump was used to force convective flow of heparin through the membrane. The reacted solution was recombined into the main annulus of the device. Agarose beads, dyed with blue dextran, were used as tracer beads (2 v/v% tracer agarose: plain agarose) to visually assess fluidization in the reactive chamber when the inner cylinder was rotated. The chamber was considered to be fluidized as long as there were no stagnant tracer beads in the chamber. This device is referred to as vortex flow plasmapheretic reactor (VFPR) and is shown in **Figure 3.1**. The dimensions of the VFPR are summarized in **Table 3.1**.

Table 3.1. Dimensions of the Vortex Flow Plasmapheretic Reactor (VFPR).

Total reactor volume	125 cm ³
Reactor length	15 cm
Reaction chamber vol.	70 cm ³
r_i (inner cylinder)	2.70 cm
r_o (membrane)	2.87 cm
Gap width (r_o - r_i)	0.17 cm
Membrane length	11.0 cm

Regional Heparinization Studies in Saline

Packed Bed Study

Figure 3.2 shows the experimental system. A packed bed configuration was used to test the heparin removal capacity of the agarose immobilized heparinase. Approximately 35 ml (packed wet volume) of the active beads were loaded into the column ($r = 1.3$ cm, $h = 7$ cm) to give a total activity of 495 IU. The feed solution consisted of 100 mM MOPS and 5 mM CaCl₂ in isotonic saline adjusted to pH 7.4. A constant infusion of heparin was used pre-column but post-reservoir

to simulate regional heparinization. The heparin concentrations entering and exiting the packed bed were measured using the Azure II assay described above. A peristaltic pump was used to control the flowrate of solution through the packed bed which was maintained at 60 ml/min. The system was maintained at 37 °C with a water bath.

VFPR Study

Regional heparinization studies, similar to the packed bed experiments described above, were performed with the VFPR. A 500 ml volume of the feed solution, heated to 33 °C, was recirculated through the circuit at 120 ml/min with the plasma pump adjusted to 60 ml/min. The rotation rate of the inner cylinder was set to 1,200 rpm, which corresponds to a shear rate of 9,200 s⁻¹. This shear rate is below the hemolysis limit of 20,000 s⁻¹ reported in the literature (Fischel *et al.* 1988; Heuser and Opitz, 1980). Approximately 20 ml of immobilized heparinase (Specific activity 10-15 IU/ml wet gel) was injected into the reactive chamber of the VFPR and was fluidized by the flow dynamics in that chamber. The infusion of heparin pre-reactor was adjusted to achieve clinically relevant heparin plasma concentrations which are in the range of 5 - 12 µg heparin/ml plasma. Heparin concentrations were measured at the inlet and outlet of the reactor using the Azure II assay.

***In Vitro* Regional Heparinization Studies with Human Blood**

The assembled reactor was incorporated into a closed circuit primed with normal saline. The circuit consisted of a blood warmer, blood pump, drip chamber and pressure monitor. The experimental set up was similar to the VFPR saline studies. A 450 cc volume of human donor blood was collected in heparin at the Blood Donor Center of Children's Hospital of Boston. Approval was obtained from the M.I.T. Committee for the use of Humans as Experimental Subjects and the required consent forms and protocols were implemented. The hematocrit (v/v% of blood cells) of the bag was adjusted to 30-35 % by dilution with saline to match the values normally encountered in the clinical setting. The blood was pumped at a flow rate of 160 ml/min. The VFPR rotation rate was set at 1,200 rpm and the plasma pump was set at 60 ml/min. Cell leakage into the reactive chamber was prevented by placing a strip of medical grade adhesive tape (type 7759 from Adhesive Research, Inc., Glen Rock, PA) within the reactor's outer cylinder and adhering the polyester membrane onto the tape with photoreactive adhesive. The temperature of the blood circuit was constant at 33 °C. A pressure gauge was placed between the reactive chamber outlet and the plasma pump to monitor clogging of the microporous membrane. Blood samples were taken at the inlet and outlet of the device and heparin levels were indirectly assayed by WBRT's, as described in the Materials and Methods section of Chapter 2. Blood samples also were drawn at the reactor outlet for further hemocompatibility tests.

Reactor Hemocompatibility

Human blood samples were taken to the M.I.T. Medical Laboratory for automated analysis of the red cell, white cell, and platelet populations. In addition, fibrinogen, antithrombin III, and total protein levels were assayed at Quest Laboratories. Hemolysis was measured through the release of free hemoglobin into the plasma. A hemoglobin detection kit from Sigma was used. The kit is based on the catalytic effect of hemoglobin on the oxidation of 3,3',5,5'-tetramethylbenzidine (TMB) by hydrogen peroxide. In this assay, a 10 μ l sample is added to 4 ml of reagent and measured at 600 nm at 25°C. The color formation in the reaction is proportional to the hemoglobin concentration in the sample.

3.3 Results and Discussion

Figure 3.3 shows the schematic of a Taylor-Couette flow device and three possible approaches, including the proposed design, to include a surface immobilized species. Suspension of the agarose immobilized species within Taylor vortices in whole blood, as shown in **Figure 3.3-A**, resulted in significant lysis of the red cells (Ameer *et al.*, 1999). **Figure 3.3-B** illustrates the use of a membrane as an immobilization support. A concern with a membrane Taylor-Couette flow device was the lower surface area to volume ratio that could be attained for a reasonable size device. In addition, the membrane mass transfer coefficient has been reported to be orders of magnitude smaller than the mass transfer coefficient to a fluidized bead (Moore, 1994). The reactor configuration in **Figure 3.3-C** was designed so that the blood cells and platelets would not come into contact with the agarose beads and therefore minimize hemolysis. The unsupported polyester microporous membrane used for cell separation undulated as a result of the rotation rate of the inner cylinder. These undulations generated a secondary circumferential flow in the reactive chamber. The author hypothesizes that the mechanism for the generation of the flow in the reactive chamber is similar to that of peristalsis. The flow was determined to be circumferential after monitoring the trajectory of tracer beads and small bubbles that were formed in the reactive chamber. This flow fluidized the agarose beads throughout the reactive chamber as judged visually by the distribution of tracer beads. The fluidization of the beads within the plasma is illustrated in **Figure 3.4**. An additional advantage to this design is the fact that the immobilized species is only exposed to blood plasma and the device can handle blood flow rates of up to 400 ml/min. Such high flow rates are possible because there are no “bead retaining” meshes in the main blood path that could clog or clot.

***In vitro* Regional Heparinization Studies in Saline**

Packed Bed Study

The results for the regional heparinization experiments, using the packed bed, are shown in **Figure 3.5**. The steady state heparin conversions (diamonds) were between 80 and 99 % at 37°C and a flow rate of 60 ml/min. The activity of the beads was checked at the end of the experiment and they lost only 10% of initial. Therefore, the observed decline in conversion towards the end of the run may have been due to fluid channeling through the bed. Nevertheless, these results, though obtained in saline, demonstrate the feasibility and efficacy of regional heparinization using immobilized heparinase. However, the use of an immobilized heparinase packed bed with blood is not feasible due to hemocompatibility issues. In addition, the high pressure drop generated across the column is not desirable when working with a patient's blood. Therefore, alternative approaches had to be pursued to achieve similar conversions in a "blood compatible" reactor system.

VFPR Study

As discussed earlier, the VFPR design was intended to overcome the "blood compatibility" and throughput issues associated with agarose immobilized heparinase. The results of the VFPR experiments in saline are shown in **Figure 3.6**. The reactor maintained mean inlet and outlet heparin concentrations of 11 ± 0.5 and 6.0 ± 0.2 $\mu\text{g/ml}$ (\pm S.E.M.), respectively. These values corresponded to a mean heparin conversion of $44 \pm 0.5\%$ (\pm S.E.M.) for an inlet flow rate into the reactor of 120 ml/min and a plasma pump flow rate of 60 ml/min. This heparin conversion, if achieved in a patient, would meet the minimum efficacy design criteria for an immobilized heparinase reactor as stated in the Introduction. It is expected that the overall heparin conversion through the device would depend on the amount of immobilized enzyme, the fluidization conditions, and the flow split through the microporous membrane.

VFPR Regional Heparinization Studies *In Vitro* with Human Blood

Reactor Efficacy

Even though good heparin neutralization results were obtained in the above saline experiments, the important measure for an immobilized heparinase reactor is its performance in blood. **Figure 3.7** shows a picture of the reactor during operation with blood. The results for regional blood heparinization using 10 ml of agarose immobilized heparinase (specific activity 16 IU/ml gel) are shown in **Figure 3.8**. The reactor maintained a mean WBRT difference of 67 seconds between the inlet and outlet. This difference corresponded to a mean heparin conversion

of $34 \pm 2\%$ (\pm S.E.M.) at a blood flow rate of 160 ml/min and a plasma pump flow rate of 60 ml/min. This mean conversion, obtained with half the volume of immobilized enzyme that was used in the saline studies, does not fall within the target range of 45-50%, however, the data demonstrates the feasibility of using the VFPR design to achieve regional heparinization with negligible blood damage. Bead volumes of up to 30 ml (42% of the reactive chamber volume) have been fluidized within the reactive chamber. Therefore, an increase in the volume of the immobilized enzyme injected into the reactive chamber (up to 30 ml) should improve the observed heparin conversion as long as adequate agarose fluidization is present. Further use of the enzyme with the VFPR was reserved for the reactor modeling studies in saline and the *ex vivo* evaluation of the reactor in sheep, as discussed in Chapters 4 and 5, respectively.

Reactor Safety

The results for the hemocompatibility of the VFPR are summarized in **Tables 3.2** and **3.3**. The white and red cell counts changed by less than 3% of their initial values. The platelet count had an 8% reduction relative to the concentrations at the beginning of the run. The concentrations of free hemoglobin released into the plasma were well below the safety criteria of 150 mg/dL. Therefore, eliminating contact between the cells and the agarose beads was an efficient way to significantly reduce hemolysis. These results are favorable when compared to those of previous immobilized heparinase reactors in which fluidized agarose beads within whole blood negatively affected the cell counts (Larsen *et al.*, 1984). In the *in vitro* studies with human blood performed by Larsen, white cell and platelet counts decreased to 10% of their initial values when tested in a recirculating reactor. This blood damage was attributed to mixing conditions in the reactor. As discussed in Chapter 2, the fluidization of agarose beads within Taylor vortices in whole blood resulted in white cell and platelet counts of 70% and 30% of their initial values, respectively.

Table 3.2. Complete blood cell and hemolysis data for the VFPR.

Time (min)	WBC (% initial)	RBC (% initial)	Plt (% initial)	HbP (mg/dL)
0	100	100	100	11
30	97	98	103	18
60	100	99	92	15

Table 3.3. Safety data for 1 hour of operation of the VFPR.

Time (min)	Total Protein (% initial)	Fibrinogen (% initial)	Antithrombin III (% initial)
0	100	100	100
60	103	87	100

It is important to know whether an extracorporeal device is nonspecifically depleting proteins in blood. This is especially important for an immobilized heparinase reactor because the anticoagulant activity of heparin in blood depends on the presence of many other proteins in the “clotting cascade”, specifically antithrombin III. **Table 3.3** summarizes the relative changes in total serum protein, antithrombin III, and fibrinogen for a reactor run. Total protein (primarily albumin and immunoglobulins) and antithrombin values were unchanged during the experimental run. A decrease in the concentration of fibrinogen, a precursor protein to fibrin clots, was a measure of the degree of fibrin generation within the system. Even though there was a 13% drop in this protein there were no fibrin clots visible to the naked eye upon inspection of the device after the experimental run. This observation does not rule out the fact that microclots may be forming on the surface of the beads. Nevertheless, the VFPR fulfilled the safety design criteria regarding device effect on blood cells and platelet count.

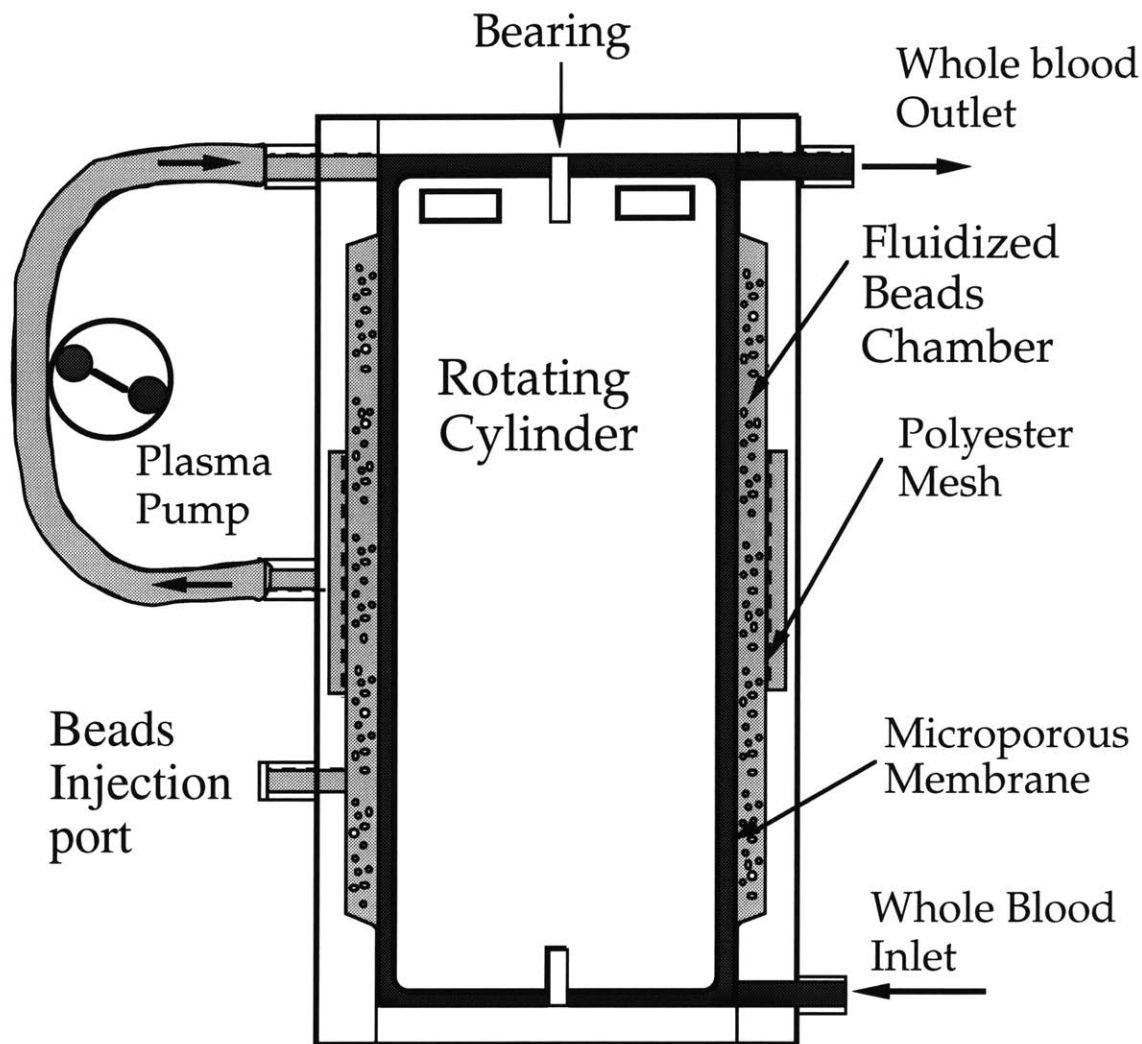
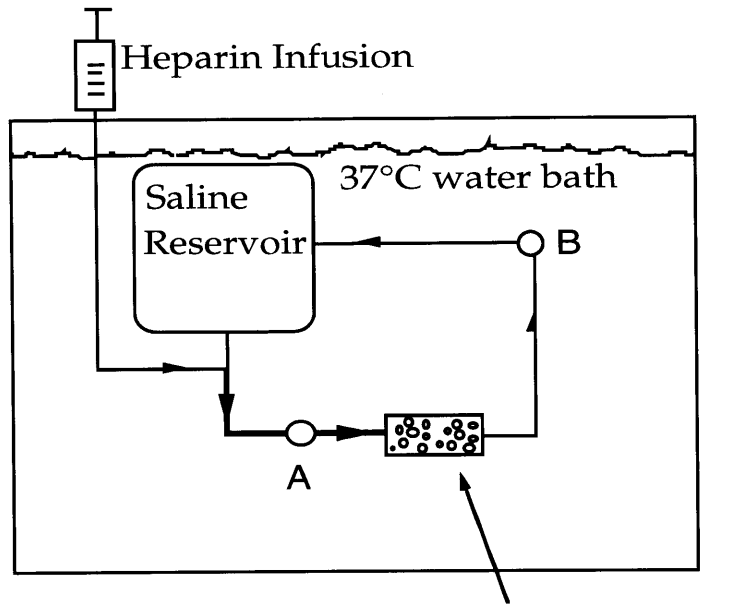


Figure 3.1. Diagram of the vortex flow plasmapheretic reactor (VFPR). Flow is split between the whole blood path and the reactive chamber via a microporous membrane. Undulations of the microporous polyester membrane fluidize the agarose immobilized heparinase I in the reactive chamber. The membrane undulations are a result of the flow dynamics induced by the rotation rate of the inner cylinder. The treated plasma is returned to the whole blood path where it is remixed with the cell components.



Immobilized Heparinase I

Figure 3.2. Experimental set up for regional heparinization using the immobilized heparinase I packed bed. The thick lines going into the packed bed represent the heparinized portion of the circuit.

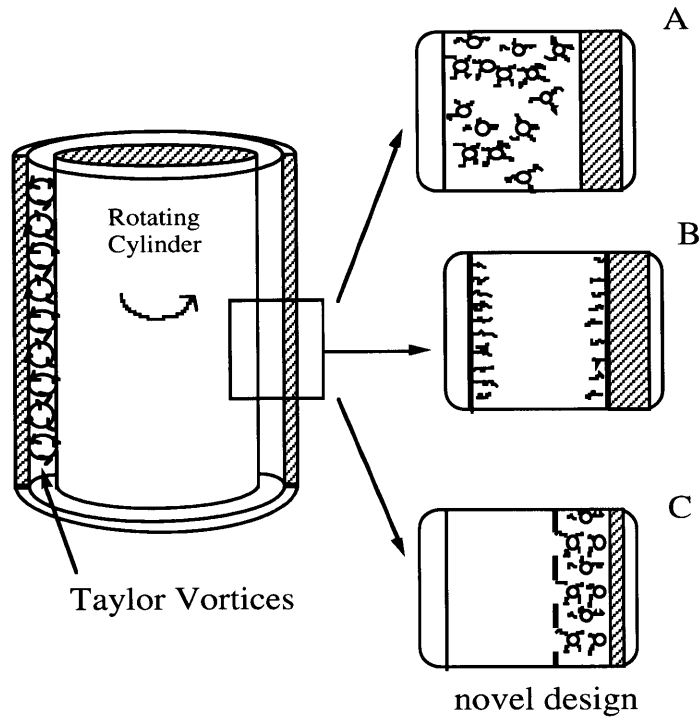


Figure 3.3. Protein entrapment methods for a Taylor-Couette flow reactor. **A:** Fluidization of the agarose immobilized species within Taylor vortices in the whole blood path. **B:** Immobilization of the species onto walls of the reactor. **C:** Entrapment of the agarose immobilized species within a microporous membrane and the outer cylinder.

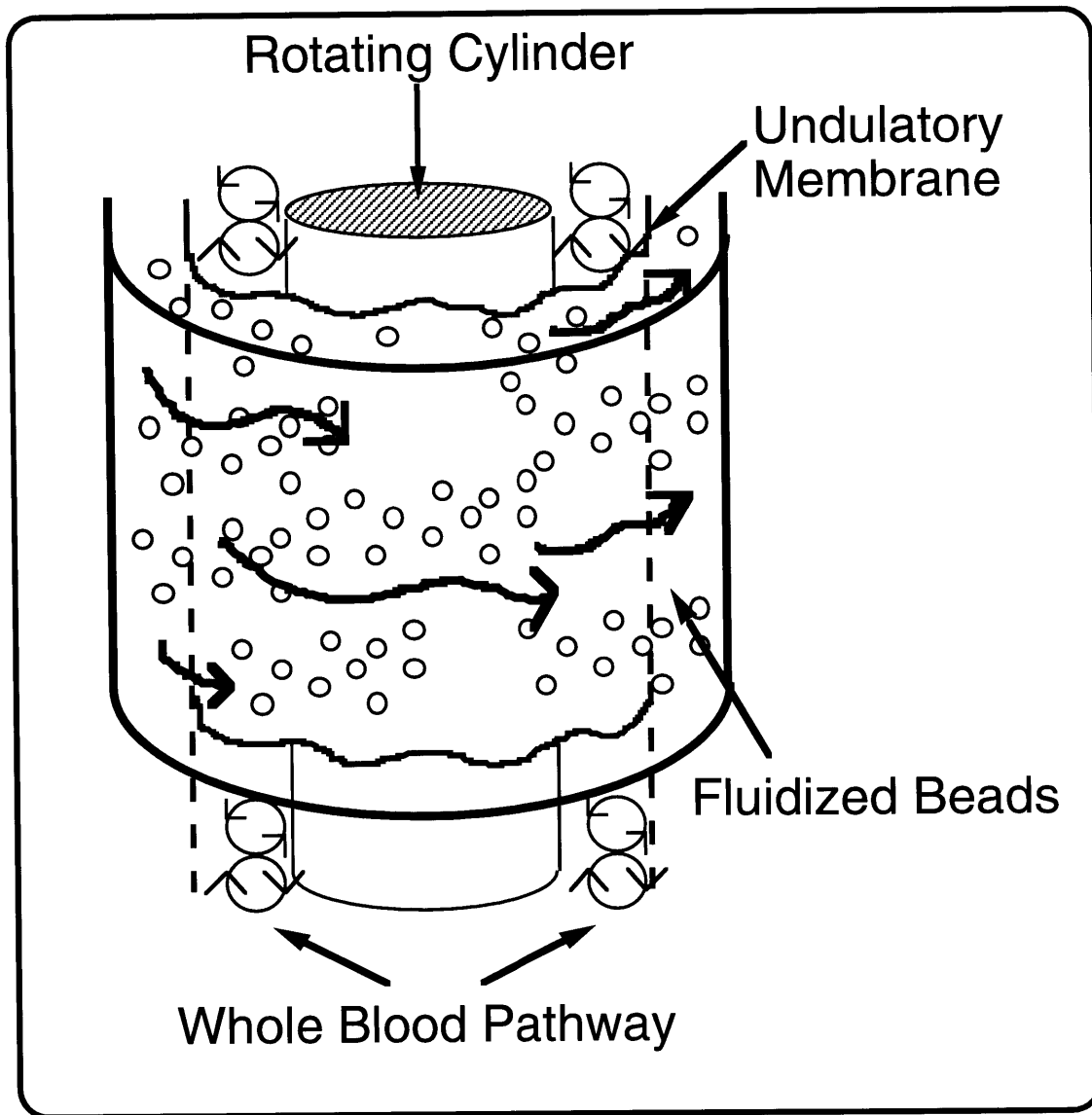


Figure 3.4. Flow dynamics within the VFPR. Membrane undulations induce a secondary circumferential flow within the reactive chamber. This flow is able to fluidize the agarose immobilized heparinase I and minimize external mass transfer limitations.

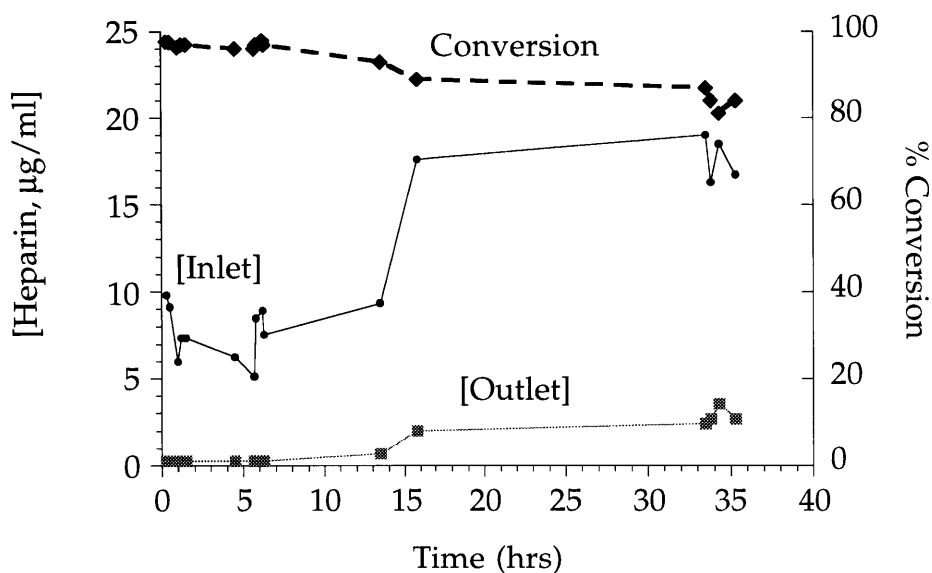


Figure 3.5. Performance of the immobilized heparinase I packed bed reactor in saline. Inlet flow rate was 60 ml/min at 37°C. Heparin concentrations into the packed bed were similar to the clinical concentrations of heparin that would be used for regional heparinization. Results for 1 experiment involving 3 sample measurements. (S.E.M. is the size of the data points)

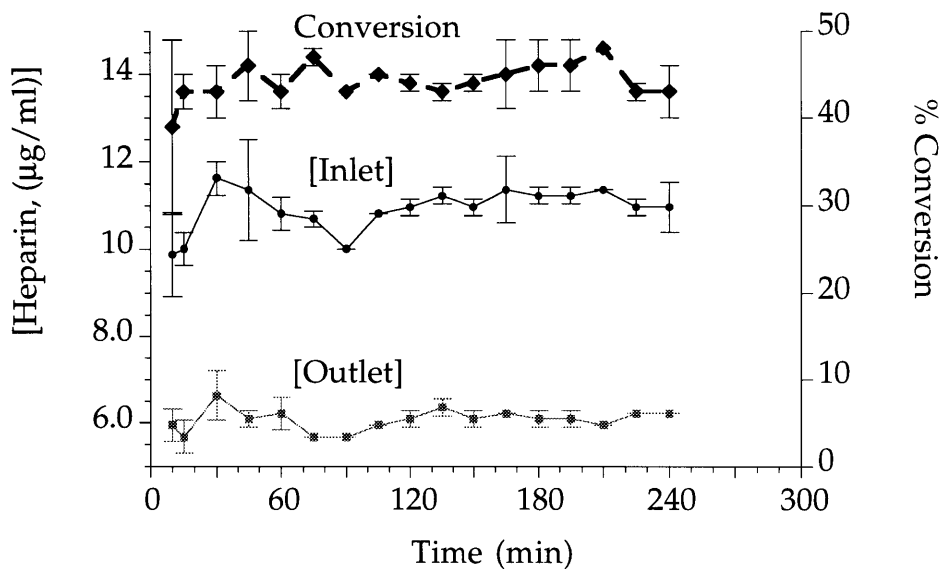


Figure 3.6. Performance of the VFPR in saline. Reactor inlet flow rate was 120 ml/min at 33°C. The flow split was adjusted so that 50% of the inlet flow would go through the reactive chamber. Rotation rate was 1,200 rpm. Results for two experiments involving 3 sample measurements. (mean ± S.E.M.)

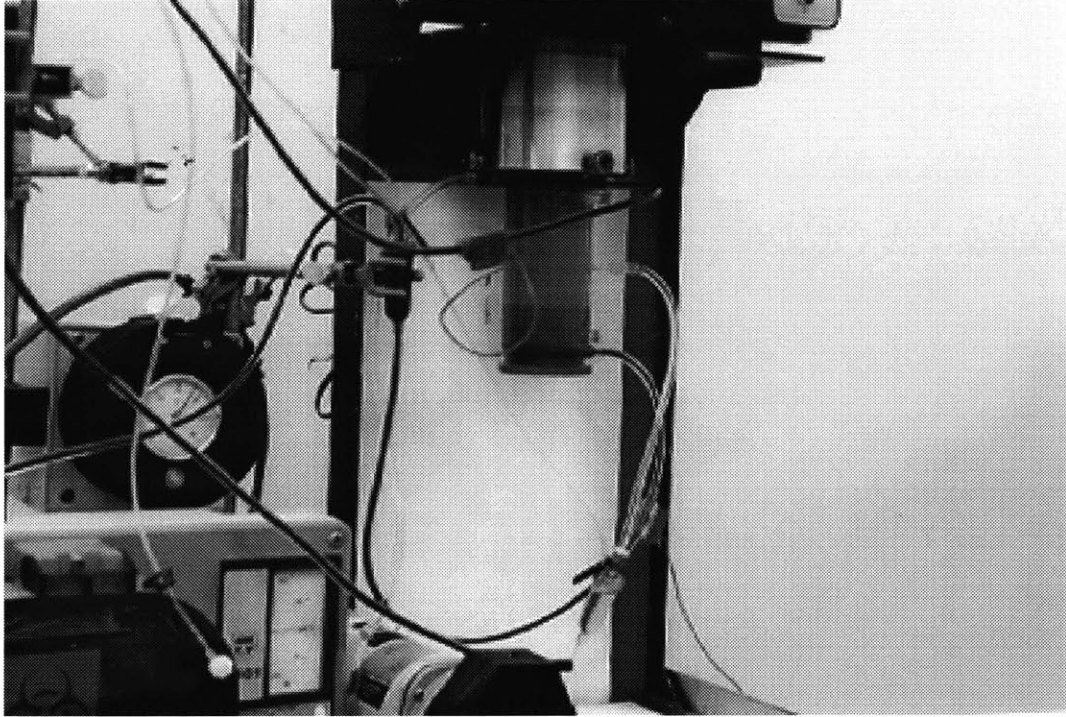


Figure 3.7. Photo of the VFPR during operation with blood. Blood plasma was pumped through the yellow side port in the center of the device and returned into the blue port located at the top and rear of the device.

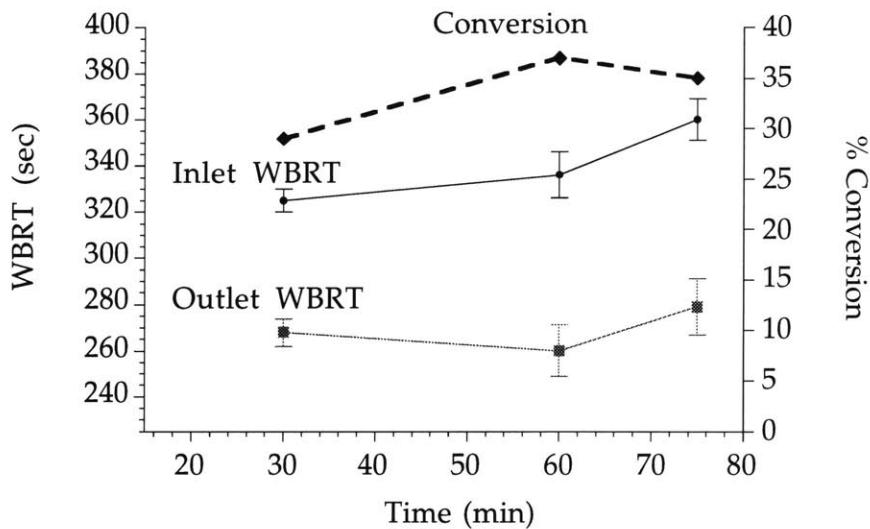


Figure 3.8. Performance of the VFPR with human blood *in vitro*. Reactor inlet flow rate was 160 ml/min at 33°C. Plasma pump flow rate was 60 ml/min. Hematocrit was adjusted to 30% to simulate that of a patient suffering from renal failure. The mean conversion during the experiment was 34 ± 2%. Results for 1 experiment involving 4 sample measurements. (mean ± S.E.M.)

References

- Ameer, G.A., Harmon, W., Sasisekharan, R., and Langer, R. 1999. Investigation of a whole blood fluidized bed Taylor-Couette flow device for enzymatic heparin neutralization. *Biotechnol. Bioeng.* In Press.
- Beaudoin, G. and Jaffrin, M.Y. 1987. High efficiency plasmapheresis using rotating membrane device. *Life Support Syst.* **5**: 273-278.
- Fischel, R.J., Fischer, H., Shatzel, A., Langer, W.P., Cahill, D., Gervail, D., and Ascher, N.L. 1988. Couette membrane filtration with constant shear stress. *Trans. Am. Soc. Artif. Intern. Organs* **34**: 375-385.
- Heuser, G. and Opitz, R., 1980. A couette viscometer for short time shearing of blood. *Rheology* **17**: 17-24.
- Holeschovsky, U.B. and Cooney, C.L., 1991. Quantitative description of ultrafiltration in a rotating filtration device, *AIChE J.*, **37(8)**:1219-1226.
- Kroner, K.H., and Nissinen, V., 1988. Dynamic filtration of microbial suspensions using an axially rotating filter. *J. Membrane Sci.* **36**: 85-100.
- Lam, L.H., Silbert, J.E., and Rosenberg, R.D., 1976. The separation of active and inactive forms of heparin. *Biochem. Biophys. Res. Commun.* **69**: 570-577.
- Larsen, A.K., Linhardt, R.J., Tapper, D., Klein, M., and Langer, R. 1984. Effect of extracorporeal enzymatic deheparinization on formed blood components. *Artif. Organs* **8(2)**: 198-203.
- Moore, C.V.L. 1994 Characterization of a Taylor-Couette vortex flow reactor. Ph.D. thesis Massachusetts Institute of Technology, Cambridge MA
- Ohashi, K., Tashiro, K., Kushiya, F., et. al 1988. Rotation-induced Taylor vortex enhances filtrate flux in plasma separation. *Trans. Am. Soc. Artif. Intern. Organs* **34**: 300-307.
- Taylor, G.I., 1923. Stability of a viscous liquid contained between two rotating cylinders. *Phil. Trans. Roy. Soc.* **A223**: 289-343.

Chapter 4

Residence Time Distribution Analysis and Modeling of the Vortex Flow Plasmapheretic Reactor

4.1 Introduction

The VFPR separates the blood cell components via a microporous membrane and enzymatically degrades plasma heparin. The degradation takes place in a separate, fluidized, agarose immobilized heparinase I, compartment. The reactor also can accommodate high inlet flow rates (150-400 ml/min). This novel design eliminates contact between the blood cells and the agarose beads. Also, it has shown to be effective and “biocompatible” *in vitro* (Chapter 3) and *ex vivo* in sheep (Chapter 5).

The goal of the study presented herein was to characterize the flow dynamics within the novel bioreactor on a macroscopic scale and to predict heparin conversion or neutralization. Understanding the flow dynamics also would allow optimization of the design. The residence time distribution of a conventional Taylor-Couette flow device has been reported (Pudjiono *et al.*, 1992). However, the proposed bioreactor design, which relies on simultaneous separation and reaction, is a novel configuration that has not been previously characterized. In the present study, residence time distribution experiments were performed at various operating conditions using the inert tracer/pulse injection method. A mathematical compartment model was developed to describe the residence time distributions and was tested against experimental results for kinetics of heparin conversions.

4.2 Materials and Methods

Residence Time Distribution Studies

Residence time distribution (RTD) studies were performed through the pulse injection of an inert dye (1 ml, 50 mg/ml Blue Dextran MW 2,000,000 from Sigma Chemical Company, St. Louis, MO) into the reactor inlet and the measurement of the exit dye concentration over time. RTD studies were performed on the whole device, as shown in **Figure 4.1.a**, to obtain the total exit age distribution function, E_{total} . Additional RTD studies were performed with the plasma line draining into a separate container, as shown in **Figure 4.1.b**. These studies measured the exit age distribution function of the annular compartment, E_1 . The total device inlet flow rate was set at either 120 or 150 ml water/min with the plasma pump set at 55, 60, and 75 ml/min. These flow

rates were comparable to the flow conditions used in previous *ex vivo* experiments. An additional plasma pump setting of 95 ml/min was tested as an extreme operating condition of the VFPR. The inner cylinder rotation rate was 1,200 rpm. Samples were collected at the outlet every 5 seconds for up to 3.5 minutes and read at 620 nm on a Shimadzu 1201S UV-Visible spectrophotometer (VWR Scientific Products, Boston MA).

Steady State Heparin Conversion Studies

These studies were performed as described in section 3.2.

4.3 Mathematical Analysis

To characterize flow, it is necessary to know the residence time distribution, earliness of mixing, and state of aggregation of the fluid (Levenspiel 1972). If the latter two factors can be ignored, the output concentration, C_{out} , of a compartment can be determined from the input concentration, C_{in} , and the exit age distribution function, E , as the convolution integral (Levenspiel, 1972):

$$C_{out}(t) = \int_0^t C_{in}(t')E(t-t')dt' \quad (1)$$

The short notation for Equation 1 is $C_{out} = C_{in} * E$.

The vortex flow plasmaphoretic reactor (VFPR) consists of two sections, A and B, separated by a microporous membrane as shown in **Figure 4.2**. Section A represents the non reactive annular region where the blood cells and Taylor vortices are present. This section is modeled as compartment 1. Section B is the cell-free chamber that contains the agarose immobilized heparinase. We decided that section B should incorporate a bypass flow, Q_{by} , and the reactive zone which is modeled as compartment 2. The fluid flow rates within compartments 1 and 2 are labeled Q_1 and Q_2 , respectively. The total transmembrane flow rate through section B is the plasma flow rate, $Q_{pl} = Q_2 + Q_{by}$.

The flow into the device, Q_{bl} , is separated such that a fraction of fluid, $z = Q_1/Q_{bl}$, flows through section A and leaves the reactor. The remaining fraction, $(1 - z) = Q_{pl}/Q_{bl}$, is forced from section A, through the cylindrical microporous membrane, into section B via a plasma pump. The processed fluid is returned to the top of section A where it is mixed with Q_1 and exits the device. A macroscopic flow schematic of the model for the VFPR is shown in **Figure 4.3**. Here E_{1a} is the exit age distribution function in compartment 1 when the output flow is measured at the reactor outlet. The exit age distribution function of compartment 1 at the microporous membrane is E_{1b} . The exit age distribution function of compartment 2 is E_2 .

Direct data acquisition for E_{1b} is difficult to obtain experimentally. Therefore, it was assumed that the exit age distribution function of the fluid exiting through the membrane was equal to the exit age distribution function of the fluid exiting the reactor outlet ($E_{1b} = E_{1a} = E_1$). This assumption minimized the number of parameters and calculations for the model and was checked via a sensitivity analysis on E_{1b} . Back flow from compartment 2 to compartment 1 was also neglected. The exit age distribution function, E_{total} , for the whole device is obtained from:

$$E_{total} = E_1 (z + x_b(1 - z)) + (1 - (z + x_b(1 - z))) E_1 * E_2 \quad (2)$$

where:

z = experimental fraction of total flow going through compartment 1,

x_b = fraction of flow through compartment 2 that bypasses the enzyme media (fitted parameter),

E_1 = exit age distribution for compartment 1, and

E_2 = exit age distribution for compartment 2.

The E_1 was initially obtained experimentally (**Fig. 4.1.b**) and then calculated with a tanks in series model (Levenspiel, 1972) by fitting the number of tanks (N_1) and the residence time (τ_1) to the data in the time domain. The exit age distribution function of compartment 2 (the reactive compartment), E_2 , was difficult to obtain directly by experiment. Therefore, E_2 was determined by assuming a tanks in series model and varying the number of tanks, N_2 , and the bypass fraction, x_b , to fit the experimental RTD curve for E_{total} . Heparin conversions in compartment 2 were predicted from (Levenspiel, 1972)

$$X_2 = 1 - \left(\frac{1}{\left(1 + \left(\frac{\tau_2}{N_2} \right) k_{het} \left(\frac{V_p}{V_{liq}} \right) \right)^{N_2}} \right) \quad (3)$$

where:

τ_2 = fluid residence time in compartment 2,

N_2 = number of equal sized tanks in series that model flow in compartment 2,

k_{het} = observed 1st order heterogeneous kinetic constant for the heparin degradation reaction in saline,

V_p = wet gel volume of agarose immobilized heparinase, and

V_{liq} = void volume of liquid in the reactor.

A series of saline kinetic experiments were performed to determine k_{het} in Equation 3. These experiments were performed in well mixed, small scale batch reactors at 37°C. Heparin degradation by heparinase I was shown to follow Michaelis-Menten kinetics (Ernst *et al.*, 1996). At the heparin concentrations of interest (6 - 12 µg/ml), the Michaelis-Menten rate expression can be reduced conveniently to a first order reaction. The observed rate constant, k_{het} , was calculated from the data by linear regression of the reaction rate expression for a first order reaction in a batch reactor (Equation 4).

$$C(t) = C_0 e^{-\left(k_{het} \frac{V_p}{V_{liq}}\right)t} \quad (4.a)$$

or

$$\ln[C(t)] = \ln[C_0] - k_{het} \frac{V_p}{V_{liq}} * t \quad (4.b)$$

where:

t = time, and

C_0 = initial concentration

The regressions were performed for $V_p/V_{liq} = 0.02$ and 0.01 for a fixed specific enzyme loading of 16 IU/cc of gel. One IU is defined as the amount of enzyme that would produce 1 µmol of double bonds/min. The ratio V_p/V_{liq} in Equation 3 represents the volume fraction of beads in compartment 2 that was used for a given reactor run.

Overall heparin conversions for the VFPR were calculated from:

$$X_{total} = (1 - (z + x_b(1 - z)))X_2 \quad (5)$$

4.4 Results and Discussion

Whole blood is a complex multiphase particulate system consisting of cells, platelets, and plasma. The VFPR separates blood cells and platelets from the immobilized enzyme via a microporous membrane. The target patient population for the clinical application of an immobilized heparinase I reactor has a hematocrit (% volume blood cells) range between 25 and 30. Heparin, the substrate to be degraded, is only present in the plasma. For this reason, the flow rates used in the residence time distribution studies represent blood plasma flow. Hence, for an experimental inlet flow rate (Q_{bl}) of 120 ml/min, the equivalent whole blood inlet flow rate to the reactor would be in the range of 160 - 172 ml/min during clinical application.

The complex flow dynamics in the VFPR are manifested in the exit age distribution of the pulse injection of an inert dye. A representative experimental residence time distribution, together with the model predictions, is shown in **Figure 4.4**. The experimental E_1 is well described with the tanks in series model. The bypass fraction, x_b , and the exit age distribution function for compartment 2, E_2 , are optimized to obtain the best model prediction for the E_{total} of the device using Equation 2. The correlation coefficients for the model prediction of E_1 and E_{total} for the operating conditions tested are summarized in **Table 4.1**.

Table 4.1. Agreement between mathematical models for E_1 and E_{total} with experimental RTD curves. E_1 was modeled with the tank in series model and E_{total} was modeled by Equation 2.

Q_{bl} (ml/min)	Q_{pl} (ml/min)	z	r^2 (E_1)	r^2 (E_{total})
120	60	0.500	0.9869	0.9723
150	55	0.633	0.9840	0.9849
150	75	0.500	0.9907	0.9350
150	95	0.367	0.9843	0.8954

As demonstrated by the plots in **Figure 4.4** and the correlation coefficients, the mathematical model is able to closely describe the experimental residence time distribution curves. **Table 4.2** summarizes the model predictions for four different experimental set points for Q_{bl} and Q_{pl} . The reactor model has shown that for the ranges tested, the compartments can be described with 4-5 equal sized, ideal CSTRs in series in the case of compartment 1 and 2-4 CSTRs in series for compartment 2, the reactive zone. Mixing in compartment 2 decreased with higher plasma flow rates, Q_{pl} , while the percent bypass flow increased. The bypass flow through compartment 2 ranged from 11.7 % for $Q_{pl} = 55$ ml/min to 37 % for $Q_{pl} = 95$ ml/min.

Table 4.2. Summary of the model output for four experimental conditions.

Q_{bl} (ml/min)	Q_{pl} (ml/min)	z	x_b	N_1	τ_1 (min)	N_2	τ_2 (min)	Q_2 (ml/min)
120	60	0.500	0.132	4	0.44	2	1.40	52
150	55	0.633	0.117	5	0.30	2	1.24	49
150	75	0.500	0.240	4	0.35	3	1.16	57
150	95	0.367	0.370	4	0.44	4	1.04	60

The model results for mixing were used to predict heparin conversions in the VFPR. **Tables 4.3.a** and **4.3.b** show the predicted and experimental heparin conversions for two gel loadings, 10 and 20 cc (16 IU/cc gel). The rate constant, k_{het} , used to calculate heparin conversion, was found to be $15.7 \text{ min}^{-1} * \text{ml saline/ml gel}$. The model predicts experimental heparin conversions to within a mean relative error of 5.5%. The maximum single pass experimental conversion attained was $42.1 \pm 0.7\%$ for $Q_{bl} = 120$ and $Q_{pl} = 60$ ml/min. This observed experimental maximum was in agreement with the maximum conversion predicted by the model for the various operating conditions. For clinical application of the VFPR, heparin conversions in the range of 45-50% are desirable.

Table 4.3.a Comparison of model predictions with experimental data for a 10 cc gel volume of agarose immobilized heparinase I. Specific activity was 16 IU/cc gel. n = 6, average \pm S.E.M.

Gel vol. = 10 cc	Plasma Pump Flow Rate, Q_{pl} (ml/min)			
	55	60	75	95
X_2 (%)	81.1	84.0	83.2	82.5
Predicted X_{total} (%)	26.3	36.4	31.6	32.8
Experimental X_{total} (%)	26.2 \pm 1.7	34.8 \pm 1.9	31.5 \pm 0.3	29 \pm 1.1
% error	0.4	4.6	0.3	13.0

Table 4.3.b Comparison of the model with experimental data for a 20 cc gel volume of agarose immobilized heparinase I. Specific activity was 16 IU/cc gel. n = 6, average \pm S.E.M.

Gel vol. = 20 cc	Plasma Pump Flow Rate, Q_{pl} (ml/min)			
	55	60	75	95
X_2 (%)	92.6	94.0	94.7	95.0
Predicted X_{total} (%)	30.0	40.8	36.0	37.8
Experimental X_{total} (%)	31.7 \pm 1.8	42.1 \pm 0.7	40.2 \pm 0.4	35.2 \pm 1.3
% error	5.4	3.0	10.0	7.4

The model assumption of $E_{1b} = E_{1a}$ was tested for $Q_{b1} = 120$ and $Q_{pl} = 60$, and the results are shown in **Table 4.4**. There was only a maximum relative difference of 4 % among the predicted conversions (relative to $N_{1a} = N_{1b} = 4$) after varying N_{1b} from 1 to 50. These results suggest that the simplifying assumption about the exit age distribution function for compartment 1 was reasonable ($E_{1b} = E_{1a}$). Therefore, the simpler model is sufficient.

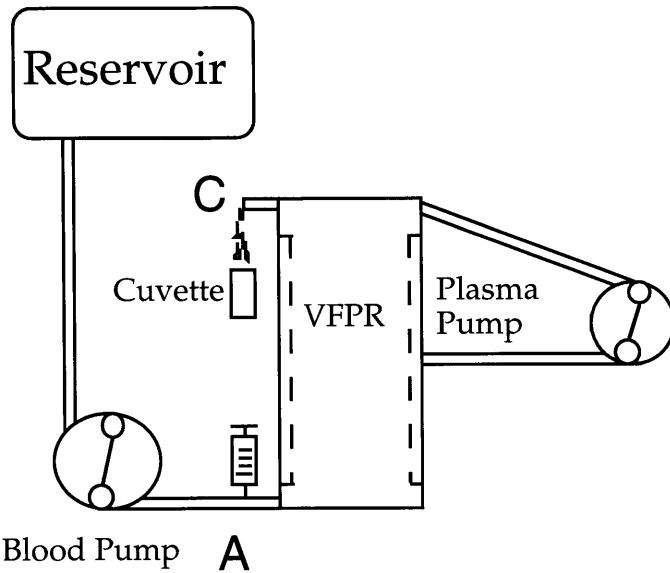
Table 4.4. Sensitivity analysis on E_{1b} for $Q_{bi} = 120$ ml/min and $Q_{pi} = 60$ ml/min. The number of equal sized tanks in series for compartment E_{1a} and E_2 were kept constant at $N_{1a} = 4$, $N_2 = 2$, respectively.

N_{1b}	x_b	r^2	Conversion, X_{total} , (%)
1	0.094	.9702	42.6
4	0.132	.9723	40.8
15	0.142	.9739	40.3
50	0.146	.9746	40.1

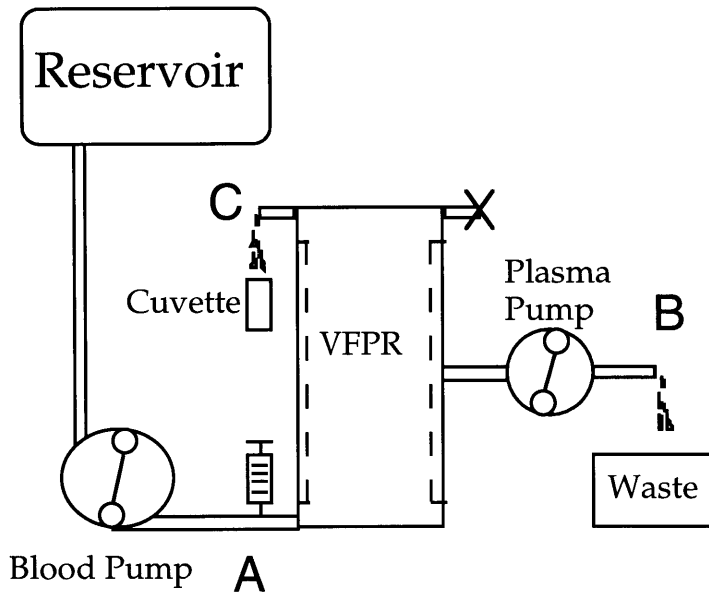
A physical reason for the bypass predicted by the model may lay with the permeability of the membrane. The membranes used to construct the reactor had water fluxes of up to 150 ml/min - cm^2 at 0.7 bar, according to the manufacturer. The reactor membrane surface area was approximately 200 cm^2 . This surface area will allow up to 30 liters/min to be filtered. Therefore, an uneven flux distribution across the membrane may be occurring and could be causing filtrate bypass through the immobilized enzyme in section B. One way to test this hypothesis is to replace the high flux membrane (150 ml/min- cm^2) with a lower flux membrane (e.g. 1.0 ml/min- cm^2). This substitution should reduce the amount of fluid bypassing the immobilized enzyme beads by evening out the filtrate flux distribution across the membrane.

In summary, a simplified two compartment model was developed to simulate the flow in a novel and physically complex device that relies on simultaneous separation and reaction to function. The mathematical model employed linear combination and the convolution integral to adequately fit the RTD curves of the reactor. To fully determine the accuracy of the compartment model for the VFPR, a second order reaction could be tested. Further testing of the model with a second order reaction was not performed in the current study since the reaction of interest, heparin degradation by heparinase I, is adequately described by first order reaction kinetics for the operating conditions of interest. In addition, due to the immediate need to develop a practical reactor for clinical application in humans, most of the research effort was placed on testing the reactor *ex vivo* in sheep. Nevertheless, each compartment was described well with the tanks in series model and kinetic performance in saline was correctly predicted. The difference between the physical flow split and the model split was accounted for via a bypass fraction parameter, which is believed to represent the physics of the process. By incorporating the bypass zone parameter into the model, the author could account for the suboptimal conversions observed in the VFPR. For

the VFPR tested, the model predicted that an approximate maximum flow rate of 60 ml/min (63% of $Q_{pl} = 95 \text{ ml/min}$) will get exposed to the immobilized enzyme.



a.



b.

Figure 4.1. Experimental systems for the residence time distribution studies using the inert tracer/pulse injection method. **a.** Total residence time distribution of the reactor. **b.** Residence time distribution in compartment 1.

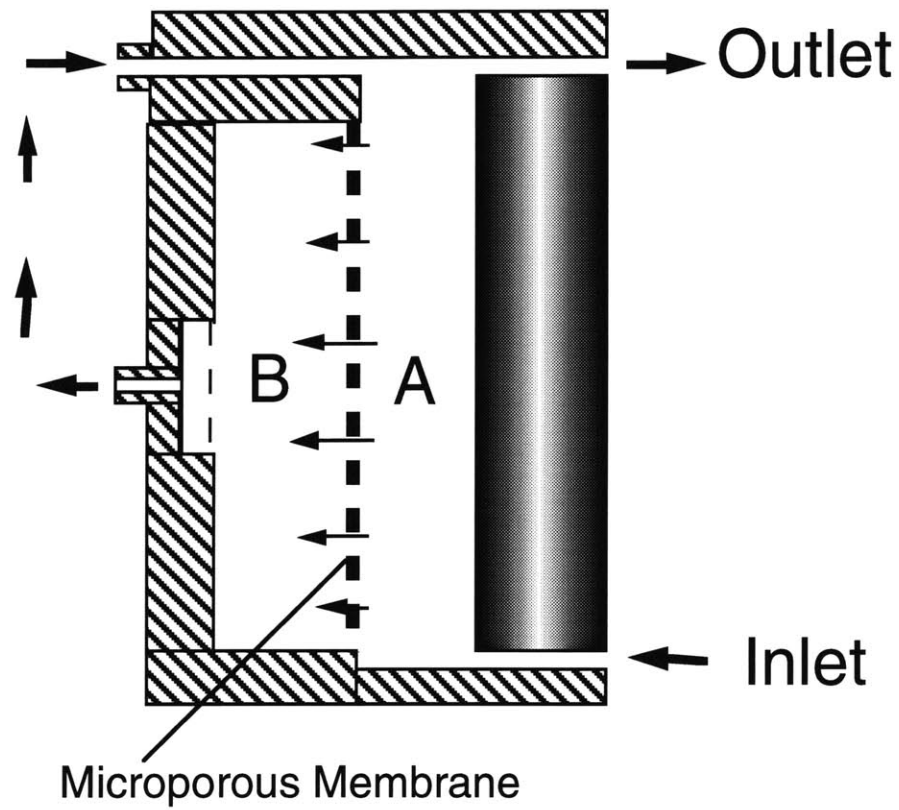


Figure 4.2. Diagram of the reactor sections to be modeled.

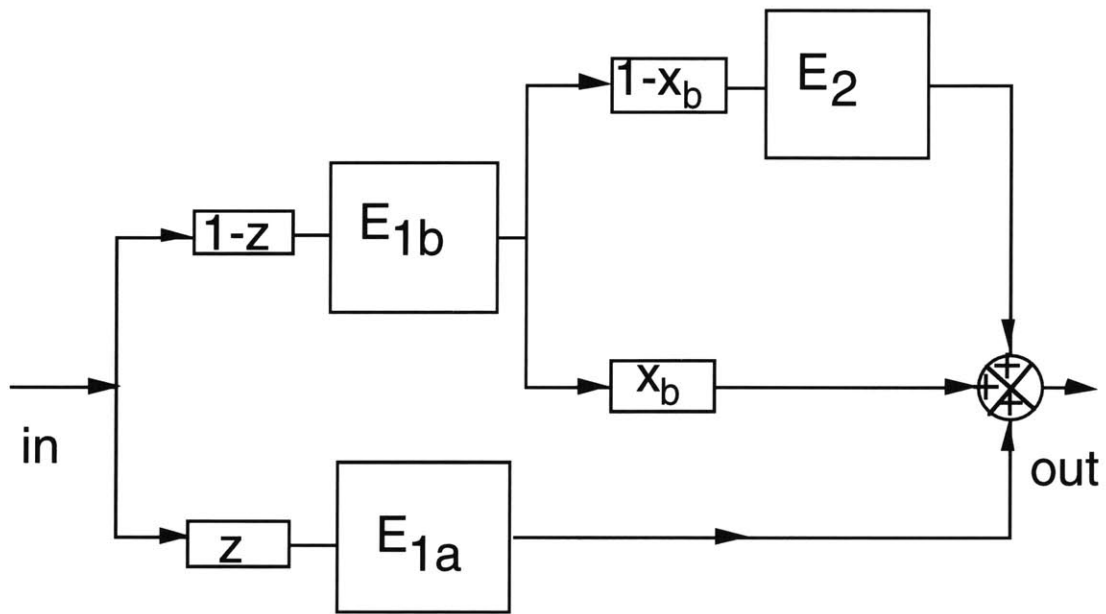


Figure 4.3. Diagram of the compartment model for the VFPR.

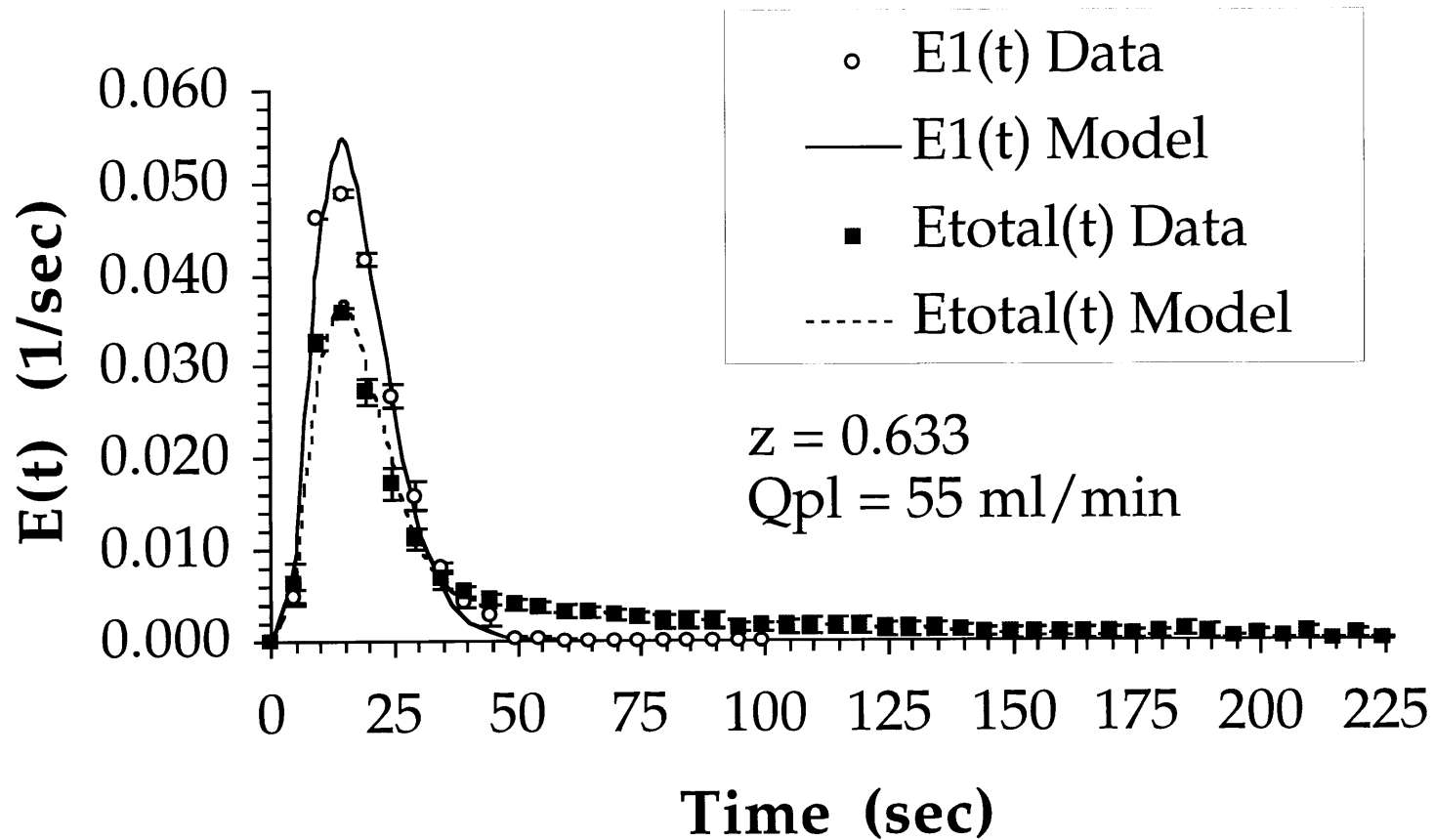


Figure 4.4. Exit age distribution for compartment 1 and the whole device operated at $Q_{bl} = 150 \text{ ml/min}$ and $Q_{pl} = 55 \text{ ml/min}$. The experimental data for E_1 was modeled with the tanks in series model. The experimental data for the whole device was modeled by Equation 2. $n = 3$ experiments, Mean \pm S.E.M.

References

Ernst, S., Venkataraman, G., Winkler, S., Godavarti, R., Langer, R., Cooney, C.L., and Sasisekharan, R. 1996. Expression in *Escherichia coli*, purification and characterization of heparinase I from *Flavobacterium heparinum*. *Biochem. J.* **315**: 589-597.

Levenspiel, O., 1972. *Chemical Reaction Engineering*, John Wiley & Sons, New York.

Pudjiono, P.I., Tavaré, N.S., Garside, J., and Nigam, D.P., 1992. Residence time distribution from a continuous Couette flow device. *Chem. Eng. J.* **48**: 101-110.

Chapter 5

Reactor Performance *Ex Vivo* in Sheep

5.1 Introduction

The previous studies using the VFPR demonstrated that regional heparinization could be effected in saline as well as in human blood *in vitro*. The positive safety results from *in vitro* experiments with human blood supported further testing *ex vivo*. In addition, data from animal studies are a prerequisite to clinical trials in humans. The objective of the studies in this chapter was to investigate the efficacy and safety of the novel reactor when used for regional heparinization in a sheep animal model. The sheep was the animal model of choice because of its comparable size to humans (no need for scale up), its similar hemodynamic characteristics to that of humans (Burhop *et al.*, 1991), and feasibility to compare the current data with that of previous research in this model (Bernstein *et al.*, 1987). Clotting times were monitored pre and post reactor to indirectly measure heparin neutralization. Reactor safety was assessed by white blood cell and platelet counts, degree of hemolysis, and specific protein concentrations.

5.2 Materials and Methods

Animal Preparation and Regional Heparinization of the Circuit

The experimental protocol for the use of animals was approved by the M.I.T. Committee on Animal Care and followed throughout the experiments. A total of 5 animals were used for the feasibility studies of the reactor. One animal was exposed to the reactor without agarose beads to assess whether the reactor materials and the complex fluid flow within the device would negatively affect the blood cells or the animal. The other four sheep were exposed to the agarose immobilized heparinase I to simulate regional heparinization. A double lumen catheter (Medcomp Inc., Harleysville, PA) was used to gain vascular access to the blood circulation of healthy male sheep (35-45 Kg). The catheter was inserted through the left internal jugular vein and guided into the right atrium of the heart (**Figure 5.1.a**). Blood flows of up to 200 ml/min were attained with no visible adverse effects to the animal. An extracorporeal procedure was performed up to 4 times on each animal depending on the patency of the catheter.

A diagram of the experimental set up is shown in **Figure 5.1.b**. The extracorporeal circuit consisted of a closed loop which included: the animal, a blood pump, a plasma pump, a bubble trap, a thrombus trap, and the reactor. The bubble and thrombus traps help prevent bubbles and emboli, which may form during operation of the reactor, from entering into animal. To

incorporate and test the reactor in an extracorporeal circuit, a standard pediatric dialysis tubing, generously donated by Children's Hospital (Boston MA), was adapted with Tygon S-50 HL medical grade tubing and O.E.M. fittings obtained from VWR (Boston, MA) and Qosina Corporation (Edgewood, NY), respectively. The animal was awake for the duration of the procedure which ranged from one to two hours. A special sling was used to prevent the animal from moving and injuring itself. The total volume of the extracorporeal circuit was kept to a minimum to reduce hemodilution (under 150 ml).

The circuit was initially primed with normal saline obtained from Abbott Laboratories (North Chicago, IL). After all the air was purged, the immobilized enzyme (1:1 slurry in normal saline) was injected into the reactive chamber. During enzyme infusion, the plasma pump flow rate and the inner cylinder rotation rate were set to 60 ml/min and 1,200 rpm, respectively. Before commencing extracorporeal circulation, an intravenous injection of heparin (5,000 USP units) was administered to systemically heparinize the animal. The arterial and venous lines from the circuit were connected to their respective ports on the double lumen catheter. The saline used to prime the circuit was pumped back into the animal to compensate for the blood volume in the circuit. This procedure was tolerated well by the animal.

Regional heparinization of the circuit was implemented by infusing heparin into the arterial line at a rate of 13,000 USP units/hr using a syringe infusion pump model Sage 361 (Sage Instruments, Boston, MA). This infusion rate, which is higher than that performed in humans, was necessary to prevent clotting in the circuit since sheep have platelet counts in the range of 200,000 - 800,000/ μ l (Gajewski and Povar, 1971). The heparinized blood passed through the reactor, a venous thrombus trap, and back to the sheep. The blood flow rate in the extracorporeal circuit and plasma pump flow rate in the reactor were 150 and 55 ml/min, respectively. The rotation rate of the inner cylinder was 1,200 rpm. Blood samples were taken at the inlet and outlet of the reactor and assayed for heparin concentrations (WBRT assay) and other hematologic parameters. The pressure drops across the reactor inlet/outlet and across the microporous membrane were measured with two Tyco strain gauge pressure transducers (Tyco Co., Asheville, NC) to monitor any flow resistance.

The percent heparin effect removed by the reactor (also referred to as heparin conversion), %H, was calculated as:

$$\%H = \left[1 - \left(\frac{WBRT_{outlet} - WBRT_{baseline}}{WBRT_{inlet} - WBRT_{baseline}} \right) \right] \times 100$$

The priming volume (whole blood path) and cell free volume (reaction chamber) of the reactor were 45 ml and 70 ml, respectively. The reactor was loaded with approximately 27 ml of agarose immobilized heparinase with a specific activity of 18 IU/cc of gel.

Hematology

Blood samples were collected from the reactor outlet into the appropriate vacutainer tubes (Becton Dickinson, Rockville, MA) at various time points. The following parameters were measured: white cell and platelet counts, hematocrit, fibrinogen, total protein (albumin + IgG) and plasma free hemoglobin. The samples were analyzed manually for white cell counts, platelet counts, and hematocrit at the diagnostic laboratory of the M.I.T Division of Comparative Medicine. Fibrinogen and total protein were sent out for analysis at Quest Laboratories (Cambridge, MA). Cell counts and fibrinogen concentrations were normalized by the animal's baseline values and reported as percents. Plasma free hemoglobin, which is an indicator of hemolysis, was measured in the laboratory using a hemoglobin detection kit from Sigma Chemical Co.(St. Louis, MO).

Necropsy

The animals were euthanized using an overdose of sodium pentobarbitol, which was injected directly into the catheter. A complete necropsy with a careful gross examination of all organs and tissues was performed. Tissue samples from the brain, kidney, spleen, liver, heart, and lung were taken for histological evaluation at the diagnostic laboratory of the M.I.T. Division of Comparative Medicine.

5.3 Results and Discussion

Reactor Safety

The results of the reactor safety control study, which exposed the sheep to the VFPR without the agarose beads, are shown in **Figure 5.2a** and **5.2b**. The values reported are for the mean of 4 experiments. There was no observed transient initial decrease in white cell counts (**Fig. 5.2a**) and platelet counts were within 10 % of the initial values. Initial decreases in the white cell population are usually correlated with complement activation which may promote sequestration of the white cells by the lungs (Holmes, 1995). The concentrations of C3a and C5a (indicators of complement activation) were not measured for the *ex vivo* experiments due to lack of an available standardized ovine complement assay. However, the absence of the white cell count drop within the first 30 minutes of operation suggests minimal complement activation. Nevertheless, there is no substantial evidence of a negative clinical outcome in the form of increased morbidity or mortality among patients (Holmes, 1995).

Figure 5.2b shows the mean hematocrit (a measure of the volume percent of cells in plasma), which was also maintained within physiological levels (22-35 v/v %). The maintenance of the hematocrit during the extracorporeal circulation is a positive sign since it is known that sheep can alter their hematocrit significantly when they are under stress (Hecker, 1993). A significant decrease in hematocrit could also suggest internal bleeding within the animal or excessive red cell lysis (hemolysis). To further confirm the integrity of the red cells, plasma free hemoglobin (HbP) concentrations were measured before and after the extracorporeal procedure. The beginning and final (2 hour) plasma free hemoglobin concentrations were found to be 6 ± 0.6 and 7 ± 1.5 mg/dL, respectively. These low plasma free hemoglobin concentrations reflect a significant improvement in reactor design when compared to past hemolysis observations reported in the literature (Bernstein *et al.*, 1987; Freed, 1988). In these reports, previous immobilized heparinase devices based on fluidized agarose beads, were tested in sheep and plasma free hemoglobin concentrations of up to 90 mg/dL were found after one hour of operation. The data on the mean hematocrit together with the low levels of plasma free hemoglobin generated during the experiment with the control sheep suggest a very small degree of hemolysis. It should be mentioned that no decrease in heparin anticoagulant activity was observed during the control experiments.

The reactor safety data for 11 regional heparinization studies performed on each of four animals are presented in **Figures 5.3 - 5.6**. The safety data for the four animals were pooled and the results are shown in **Figure 5.7**. The white cell counts seemed to follow the reported trends that are associated with complement activation. However, in most cases the white cell count rebounded to approximately 80% of the initial values within one hour and throughout the end of extracorporeal circulation. In addition, the white cell counts were within normal values prior to the beginning of subsequent experiments. Platelet counts were normal throughout the experiments. The maintenance of a normal platelet count during the experiments is another significant improvement over a previous reactor which depleted platelets down to 50% of the initial value after one hour of operation without the dialyzer (Bernstein *et al.* 1987). By the end of the regional heparinization procedure with the VFPR, plasma free hemoglobin concentrations were below 15 mg/dL, on average. Therefore, separation of the blood cells from the agarose immobilized heparinase accomplished the objective of significantly minimizing cell destruction.

The results for the total protein and fibrinogen measurements are shown in **Table 5.1**. After one hour of extracorporeal circulation, there was no significant change in the total protein for the one control or the four treated sheep. The mean of the normalized fibrinogen concentrations for 3 regionally heparinized animals and 1 control animal decreased to $94 \pm 2\%$ and $92 \pm 3\%$ of initial baseline concentrations, respectively, after one hour of extracorporeal circulation through the

VFPR. The fact that fibrinogen levels decreased in both, enzyme exposed and control sheep, suggests that the deheparinization process within the VFPR did not significantly augment clot formation as judged by this assay.

Table 5.1. Total protein and fibrinogen values for experiments involving 1 control and 4 regionally heparinized sheep. Mean \pm S.E.M.

	Total Protein (g/dL)		Fibrinogen (% initial)	
	Control 1 sheep 4 experiments	Reg. Hep. 4 sheep 11 experiments.	Control 1 sheep 4 experiments.	Reg. Hep. 3 sheep 8 experiments
Before Circulation	6.5 \pm 0.2	6.1 \pm 0.1	100	100
1 Hour of Circulation	6.2 \pm 0.2	6.0 \pm 0.2	92 \pm 3	94 \pm 2

The VFPR did not experience any membrane clogging problems (as long as the membrane undulations were present) for transmembrane plasma flow rates as high as 60 ml/min when judged by monitoring the pressure drop across the membrane. **Figure 5.8** shows environmental scanning electron micrographs of a microporous polyester membrane that was recovered after a regional heparinization experiment and fixed in formalin. There were no adhered white cells or clots on the membrane surface. In addition, visual inspections of the reactors, at the end of each procedure, did not identify any macroscopic clots in the compartments of the device. To confirm the above findings, detailed hemostasis tests such as the pro-thrombin time (PT) and thrombin-antithrombin (TAT) assays need to be performed. The small fibrinogen concentration changes observed in the current sheep studies (8%) compare favorably to similar measurements that were taken in a deheparinization system using a poly-L-lysine adsorbent device which was tested in a bovine model (Von Segesser *et al.*, 1994). In those studies, fibrinogen levels were reduced by 21% at the end of one hour of operation using control (no adsorbent) and active devices.

The necropsy examinations, performed on all sheep, did not show any evidence of tissue damage, due to application of the VFPR. Tissue sections from the brain, kidney, spleen, liver, heart, and lung looked normal which is very encouraging given the large amount of heparin that was required to prevent clotting in the extracorporeal circuit. There were normal tissue healing responses associated with the placement of a catheter in the jugular vein.

Reactor Efficacy:

For a heparin filter to be clinically useful, heparin conversions in the range of 45-50% should be achieved. This target range implies reactor inlet clotting times of 230 - 250 seconds and reactor outlet clotting times of 170-180 seconds according to the definition for percent heparin effect removed presented in the Methods section. These calculated clotting times assume a baseline or normal clotting time of 110 seconds. The regional heparinization data for a representative set of experiments are shown in **Figures 5.9.a-c**. As observed in the figures, the reactor could maintain a heparin concentration difference across the inlet and outlet, therefore effecting regional heparinization. The mean percent heparin effect removed (%H) was calculated to be 42 ± 2 , 36 ± 4 , and 39 ± 4 %, for the profiles shown in **Figures 5.9.a** through **5.9.c**, respectively. The blood flow rate was 150 ml/min and the plasma flow rate was set to 55 ml/min. Although the experimental heparin conversions were not within the target range of 45-50%, the feasibility of safely achieving regional heparinization with this novel enzymatic device was demonstrated.

The reactor performance is explained as follows: since the average hematocrit for this particular animal was 27, the plasma flow through the reactor was $150 \times (1 - 0.27) = 110$ ml/min. If the reactive chamber were 100% efficient, 50% of the plasma leaving the reactor would be cleared of heparin. However, the modeling from Chapter 4 showed that for an enzyme loading of 20 ml gel (16 IU/cc gel) the predicted conversion in the reactive chamber would be 92.6 % for a transmembrane flow rate of 55 ml/min (**Table 4.3.b**). In addition, according to the model, 11% of the transmembrane flow bypasses the immobilized enzyme (49 ml/min of the transmembrane plasma flow effectively encounters the immobilized heparinase). By approximating the conversions in the reactor with the above values, the following conversion is expected:

$$\% \text{ Conversion} = 1 - \left[\frac{110 - 49 \times 0.926}{110} \right] \times 100 = 41\%.$$

This predicted conversion has a 5% error difference when compared to the mean conversion of 39% obtained from the 3 regional heparinization experiments shown in **Figures 5.9.a-c**. The predicted conversion is also very close to the model prediction of 40% for a VFPR operated with a transmembrane plasma flow rate of 60 ml/min and an inlet flow rate of 120 ml/min. This is probably so because the operating conditions are also very similar (flow split of 0.5 for both cases).

During preliminary regional heparinization studies in sheep, a drop in conversion, usually on the order of 40 % by the end of 2 hours, was observed. The activity of the beads were tested *in*

vitro with saline after the regional heparinization procedure in sheep. Approximately 64% of the enzymatic activity of the beads was recovered. **Figures 5.10 and 5.11** show environmental scanning electron micrograph of immobilized heparinase agarose beads exposed to the sheep plasma within the reactor and plain agarose beads in saline, respectively. There was a significant difference in surface morphology between the two samples probably due to protein deposition or micro clots. Specifically, there were globular patches throughout the surface of the beads.

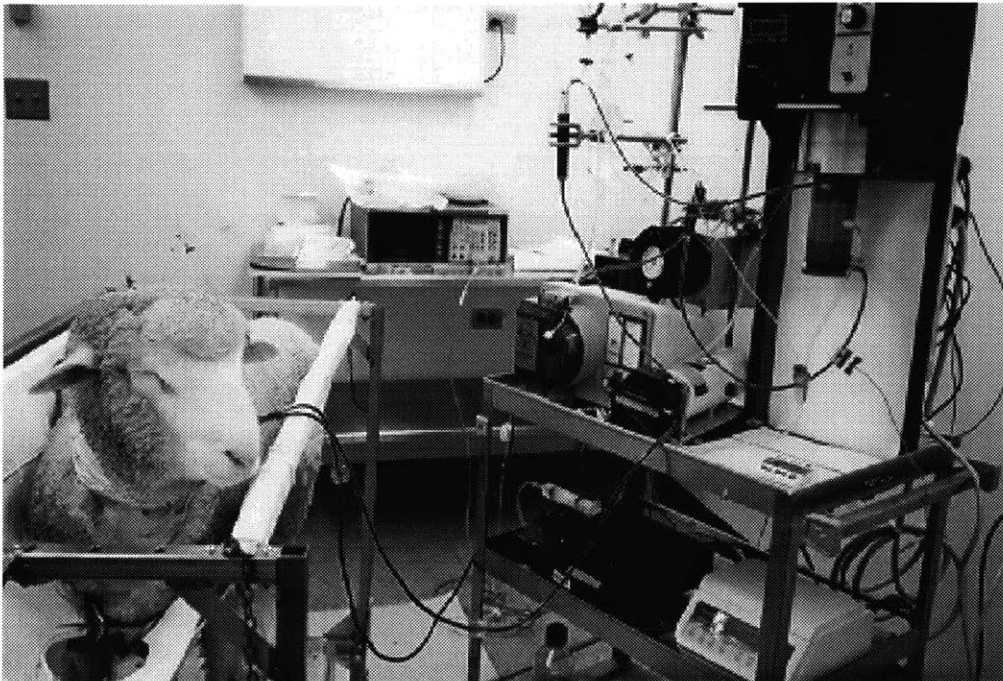
After taking the observed specific activity drop into consideration, the remaining enzymatic activity on the agarose beads should have been enough (in the absence of significant external mass transfer limitations) to maintain the desired heparin conversions in the circuit. This is true provided that the fluidization conditions within the reactor were not altered during the course of the experiment. As pointed out in Chapter 4, it is possible that fluid bypassing through the reactive compartment may be an issue for the current reactor configuration. It was also observed during the regional heparinization experiments that within 30 minutes of reactor operation a small concentration gradient of agarose immobilized heparinase was visible in the reactive chamber. The concentration of fluidized beads appeared higher at the bottom end of the chamber than at the top. Therefore the observed decrease in enzymatic activity could be attributed to a mechanical phenomenon (reactor induced) or to a physico-chemical process that takes place within the beads. Taking all the observations into account, it is plausible that the following situations may be occurring: 1) deposition of plasma proteins onto the agarose immobilized heparinase increases the specific density of the agarose beads, effectively increasing their settling velocity. Although the beads are fluidized within circumferential flow in the reactive chamber, the bypass flow predicted by the model in Chapter 4 is significantly increased since a larger amount of the beads migrate to the bottom half of the reactive chamber (mechanical phenomenon). 2) The high specific activity on the beads effectively create a heparin free zone within the inner pores of the beads. This zone may promote the formation of fibrin meshes (microclots) within the pores of the beads. These microclots block or inhibit the diffusion pathway of the heparin-antithrombin complex making it inaccessible to the enzyme (physico-chemical process). This case would significantly reduce the biological enzymatic activity of the immobilized enzyme, especially at the low heparin concentrations used in clinical applications.

This chapter has shown that the novel reactor design based on Taylor-Couette flow, simultaneous separation and reaction, and agarose fluidization within circumferential flow could safely maintain a heparin concentration difference within the extracorporeal circuit. With future design and optimization, the reactor could be used for regional heparinization in humans.

Recommendations and optimization strategies for future studies to improve reactor performance and safety are outlined in Chapter 6.

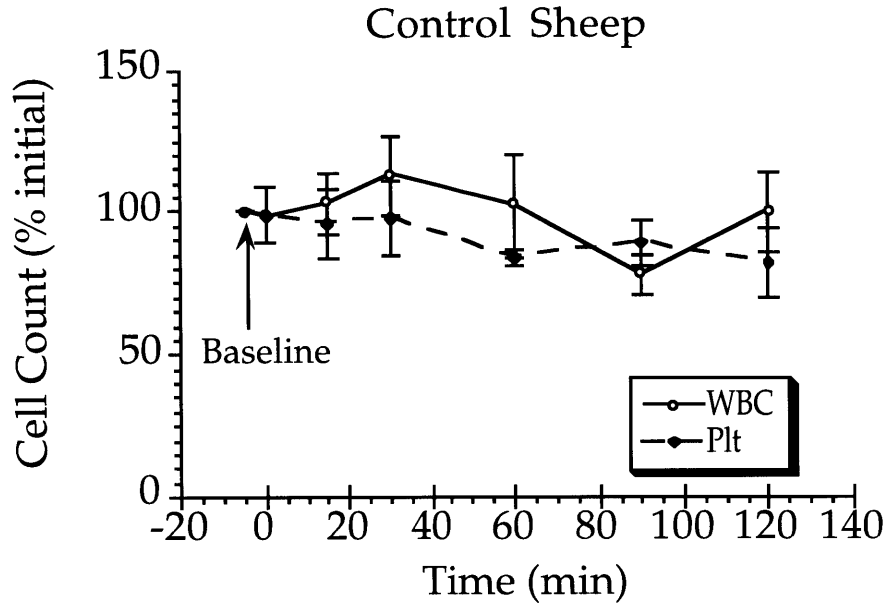


a.

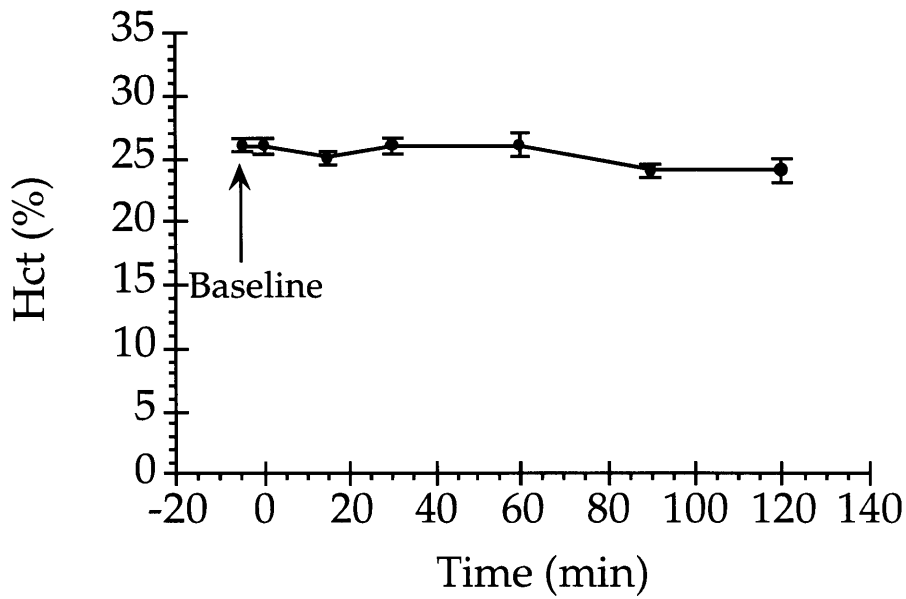


b.

Figure 5.1 a. A double lumen catheter was inserted into the left jugular vein of the sheep to gain vascular access. b. Experimental set up for the *ex vivo* studies in sheep. The animal was conscious during the procedure but restrained within a specially designed sling.

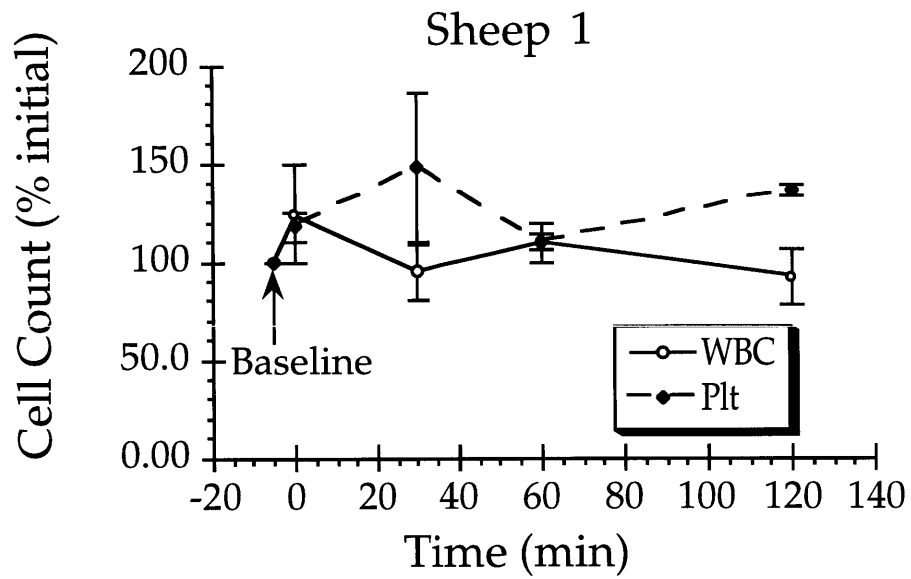


a.

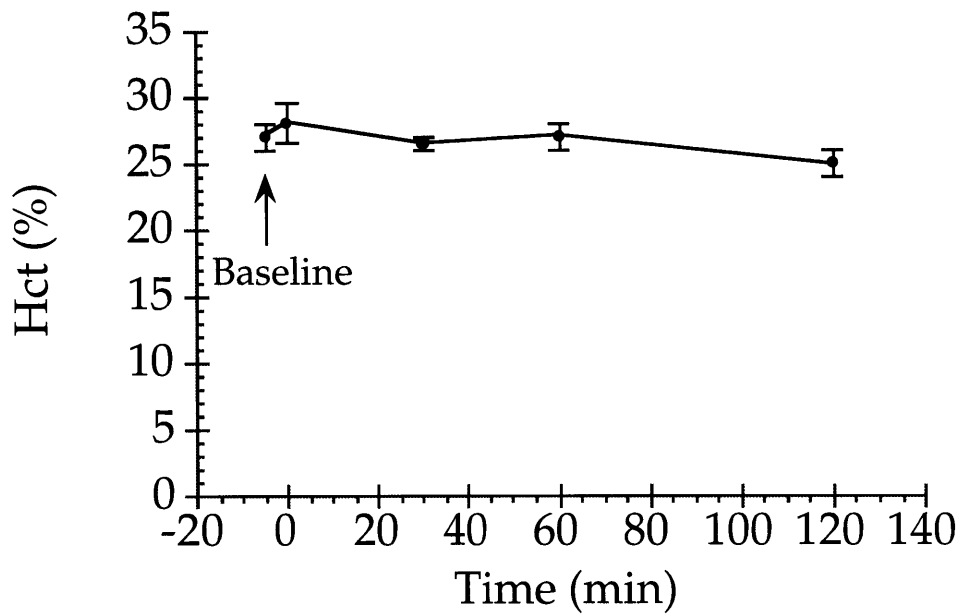


b.

Figure 5.2. Safety data for a control sheep. **a.** White cell and platelet count profiles were normalized with baseline values. **b.** Hematocrit. Mean \pm S.E.M 4 experiments.

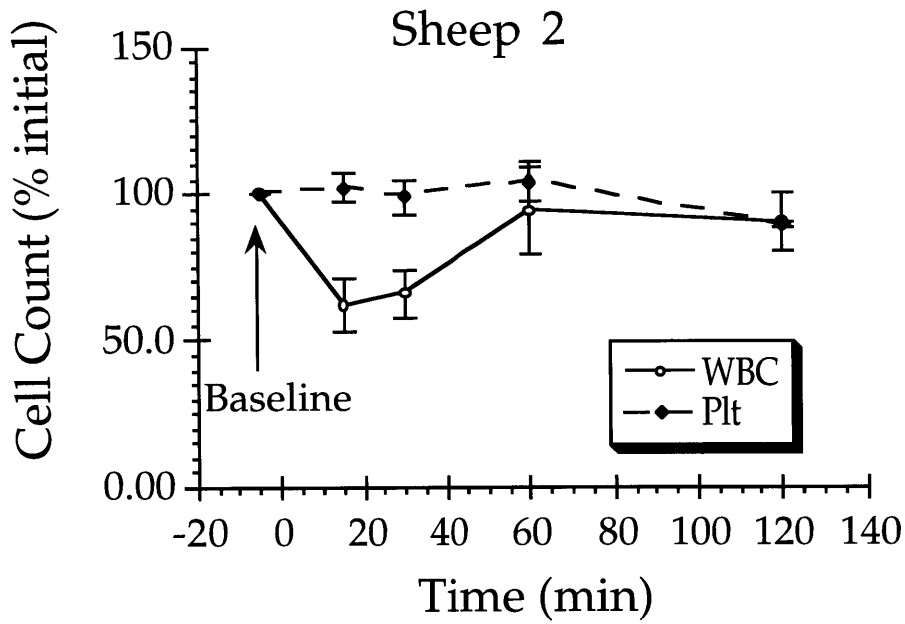


a.

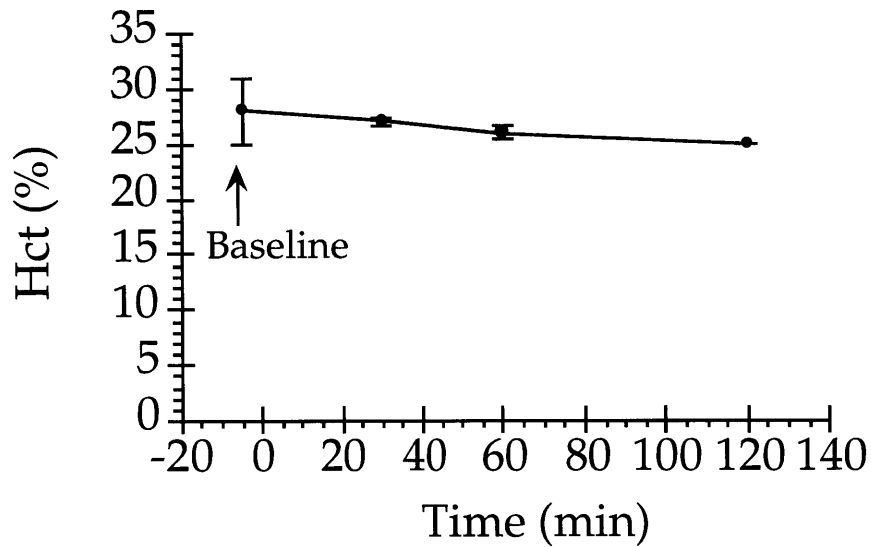


b.

Figure 5.3 Safety data for a regionally heparinized sheep. **a.** White cell and platelet count profiles were normalized with baseline values. **b.** Hematocrit. Mean \pm S.E.M of 2 experiments.

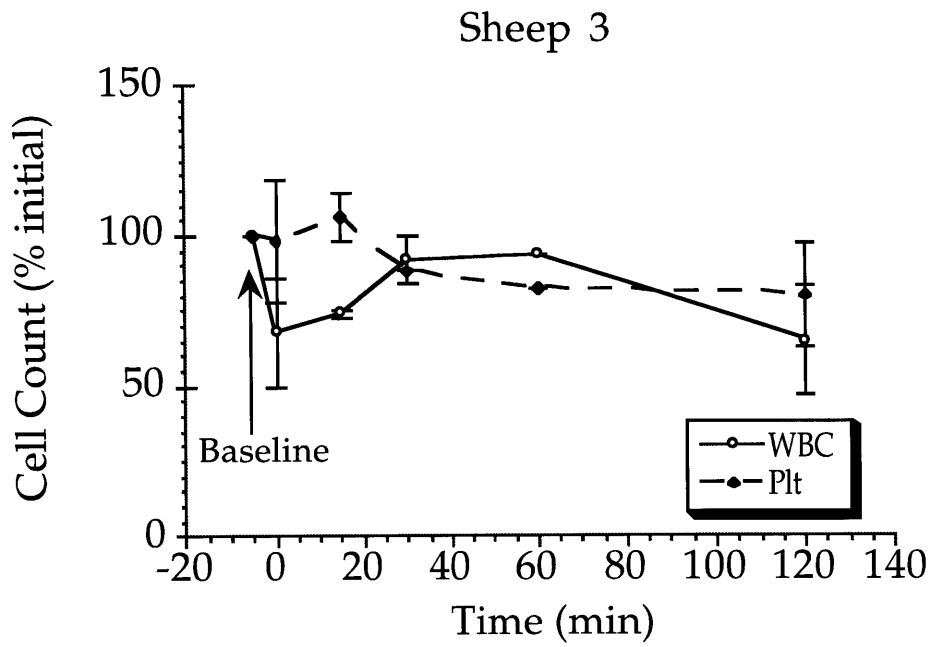


a.

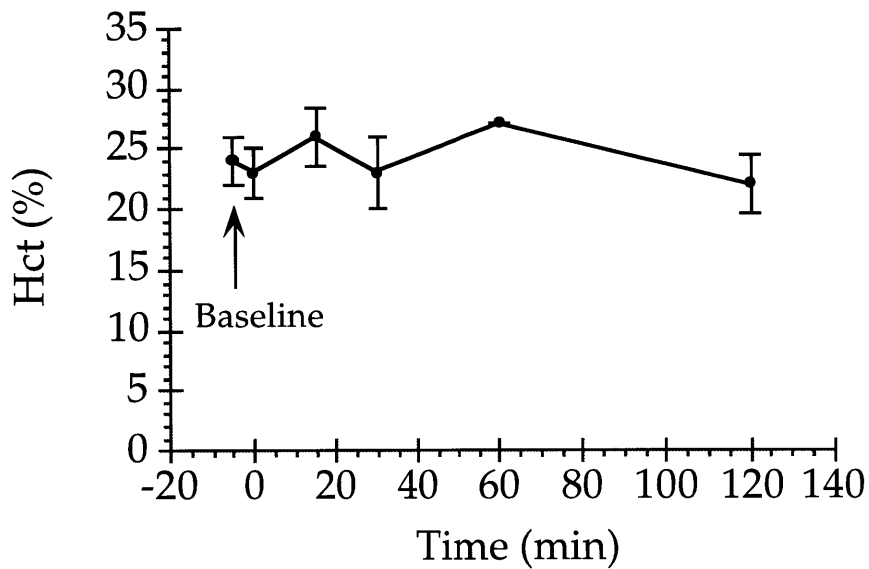


b.

Figure 5.4 Safety data for a regionally heparinized sheep. **a.** White cell and platelet count profiles were normalized with baseline values. **b.** Hematocrit. Mean \pm S.E.M of 4 experiments.

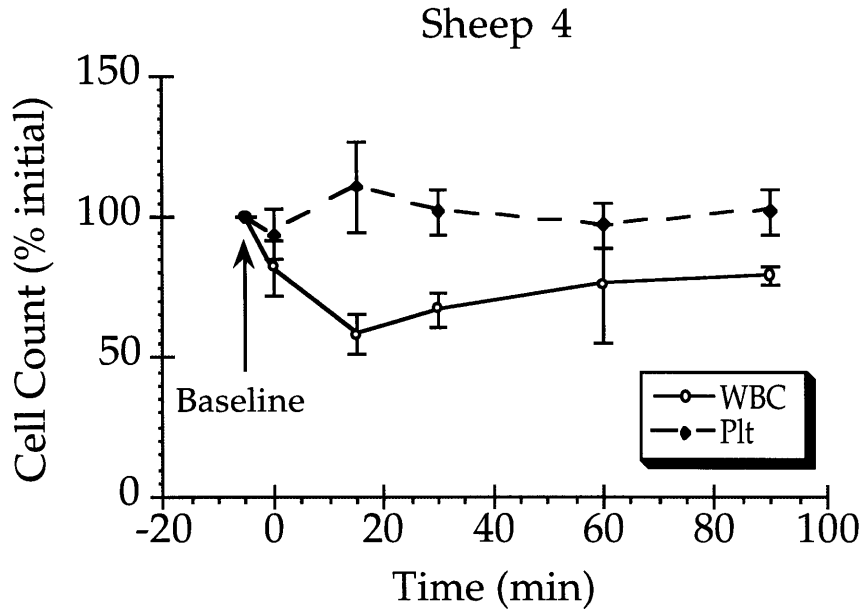


a.

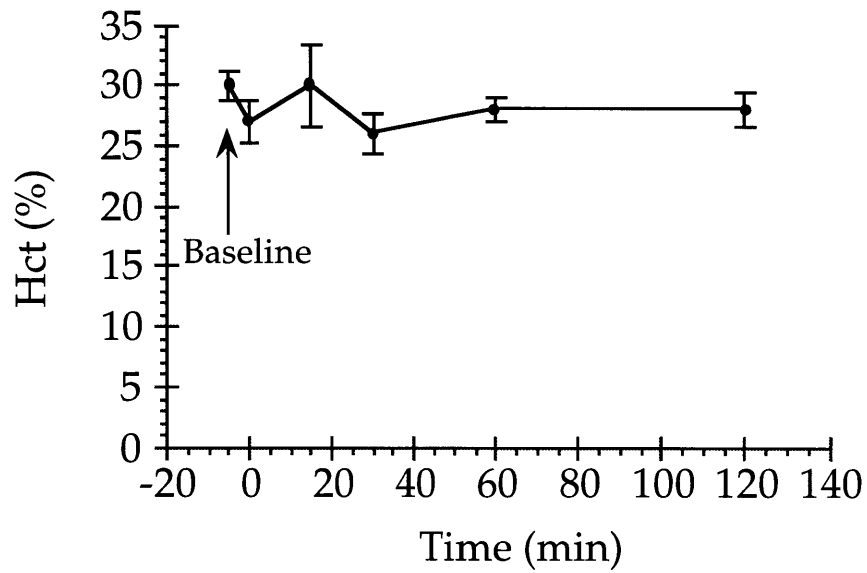


b.

Figure 5.5 Safety data for a regionally heparinized sheep. **a.** White cell and platelet count profiles were normalized with baseline values. **b.** Hematocrit. Mean \pm S.E.M of 2 experiments.



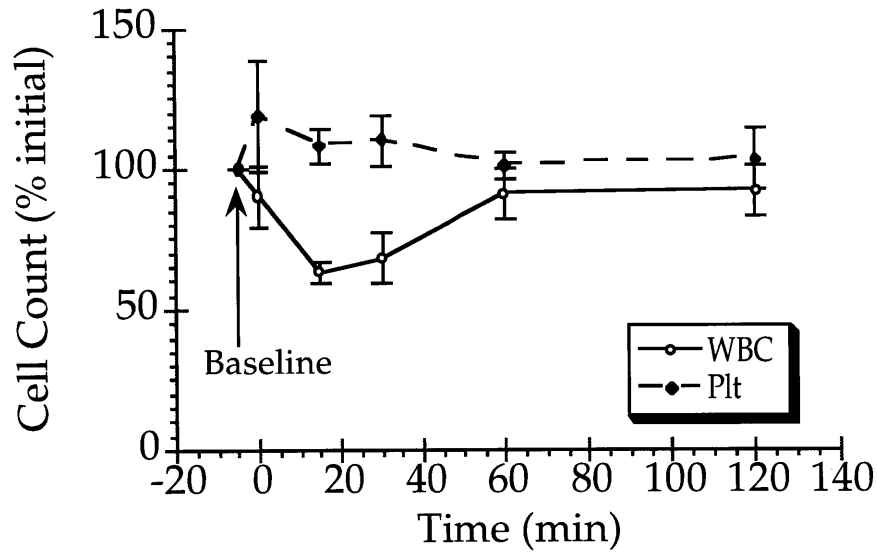
a.



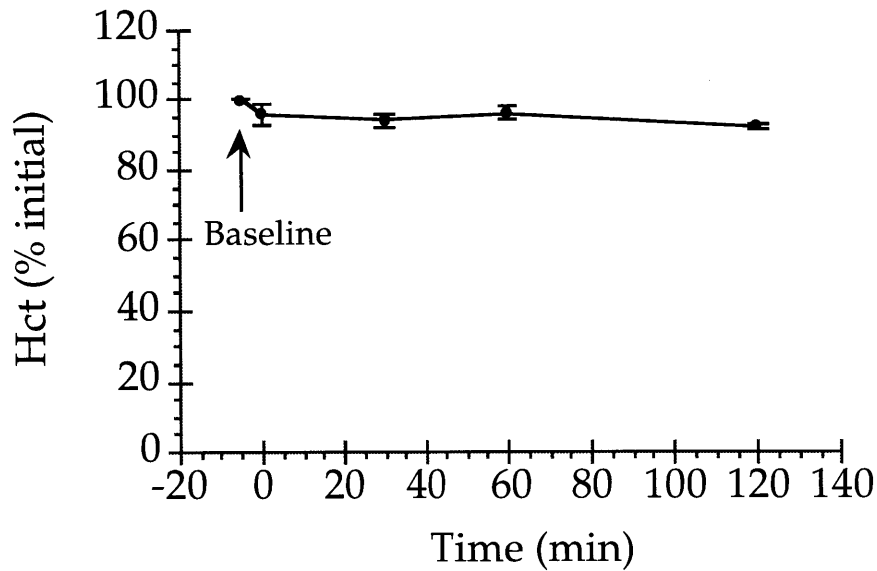
b.

Figure 5.6 Safety data for a regionally heparinized sheep. **a.** White cell and platelet count profiles were normalized with baseline values. **b.** Hematocrit. Mean \pm S.E.M of 3 experiments.

Grouped Safety Data for 4 Treated Sheep



a.



b.

Figure 5.7 Grouped safety data for a regionally heparinized sheep. **a.** White cell and platelet count profiles were normalized with baseline values. **b.** Hematocrits were also normalized with baseline values. There was an initial drop in white cell count followed by a rebound to within 20% of initial. The Mean \pm S.E.M of 11 experiments.

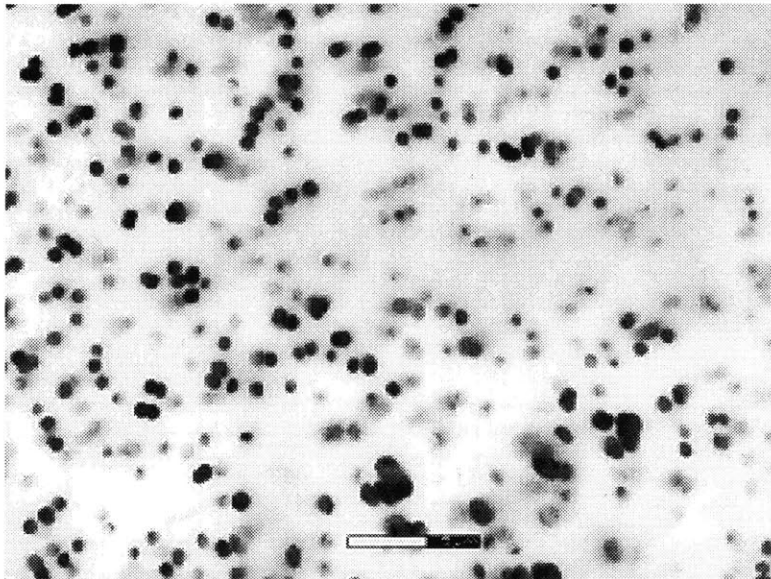
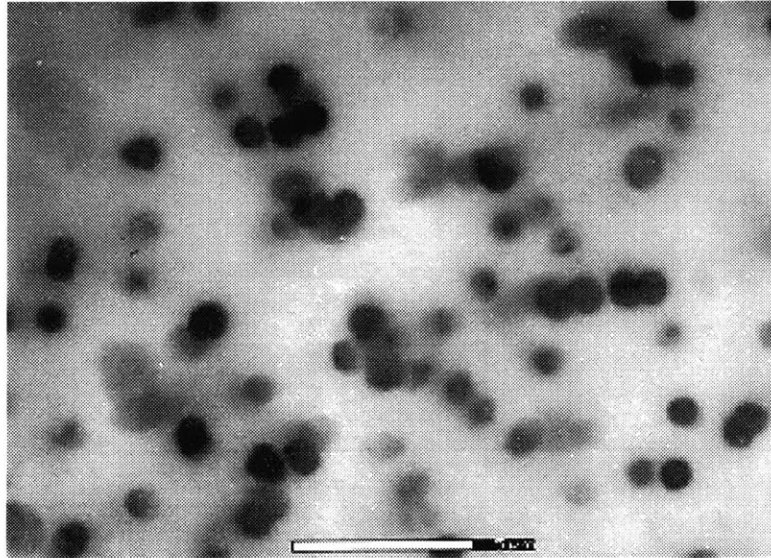
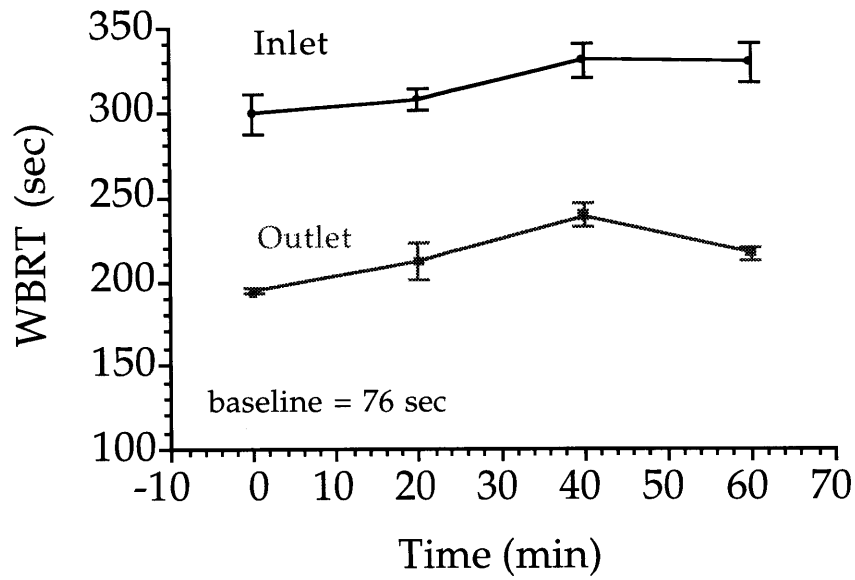
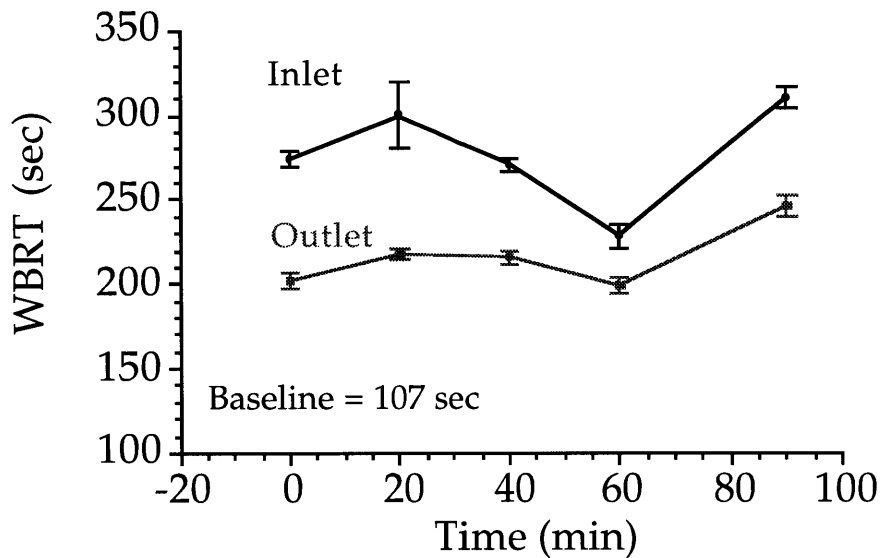


Figure 5.8. Environmental scanning electron micrographs of the polyester microporous membrane used to separate the cells from the agarose immobilized enzyme within the reactor. The dark holes are the etched pores of the membrane which were 1 μ m diameter. Sheep red cells range from 4-6 μ m in diameter. The bar represents 5 μ m.

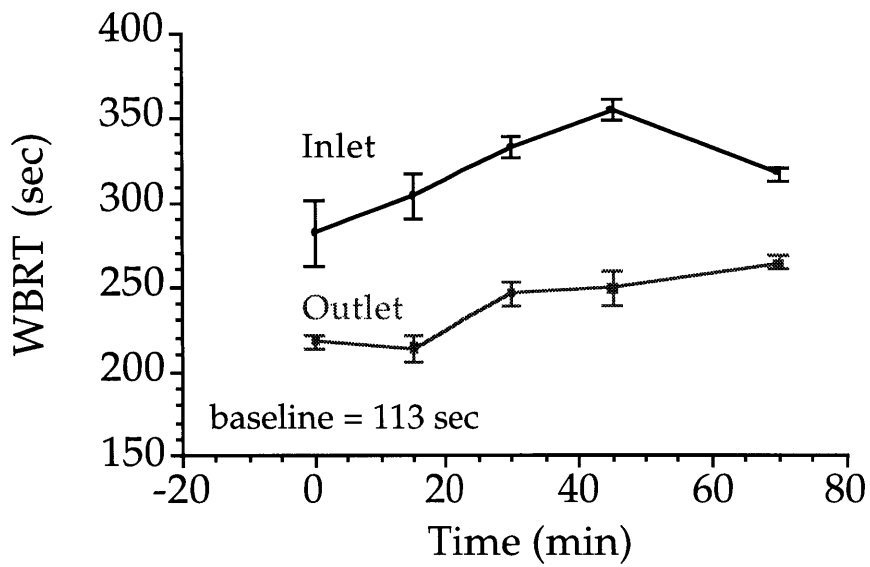


a.



b.

Figure 5.9. a-c. Regional heparinization of a sheep demonstrating the capacity of the VFPR to maintain lower clotting times at the outlet of the device. Reactor inlet flow rate was 150 ml/min at 33°C. Plasma pump flow rate was 55 ml/min. Mean \pm S.E.M of 4 measurements



C.

Figure 5.9. a-c. Regional heparinization of a sheep demonstrating the capacity of the VFPR to maintain lower clotting times at the outlet of the device. Reactor inlet flow rate was 150 ml/min at 33°C. Plasma pump flow rate was 55 ml/min. Mean \pm S.E.M of 4 measurements

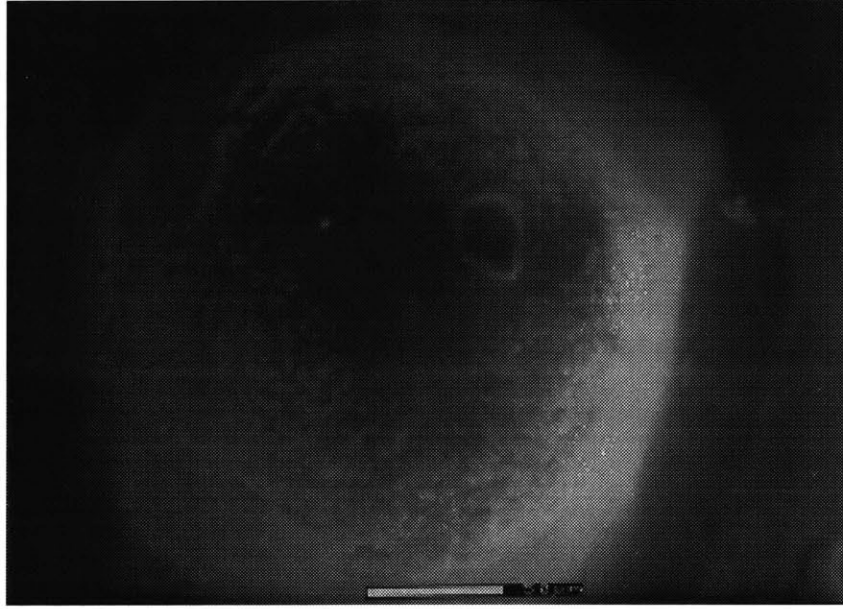


Figure 5.10. Environmental scanning electron micrograph of an agarose immobilized heparinase bead after a regional heparinization study in the VFPR. The surface of the bead is covered with what may be a proteinaceous material. The bar represents 50 μm .

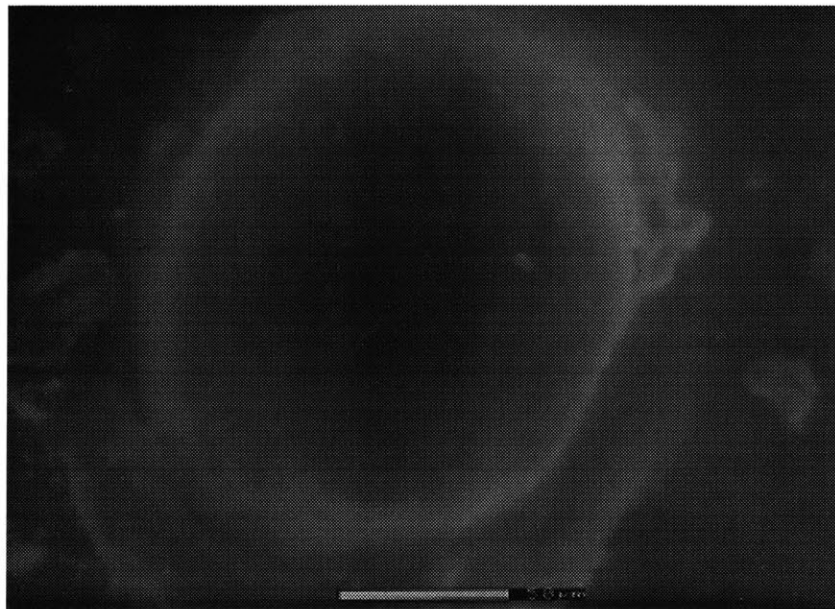


Figure 5.11. Environmental scanning electron micrograph of a control agarose immobilized heparinase bead which was exposed to saline. The bar represents 50 μm .

References

- Bernstein, H., Yang, V., Lund, d., Randhawa, M., Harmon, W., and Langer R. Extracorporeal enzymatic heparin removal: Use in a sheep dialysis model, *Kidney Int.* **32**: 452-463.
- Burhop, K.E., Johnson, R.J., Simpson, J. Chenoweth, D.E., and Borgia, J. 1991. Biocompatibility of hemodialysis membranes: evaluation in an ovine model. *J. Lab Clin Med.* **121(2)**: 276-293.
- Freed, L.E. An enzymatic fluidized bed reactor for blood deheparinization; Development and testing in lambs on extracorporeal circulation. Ph.D. thesis, M.I.T., 1988.
- Gajewski, J. and Povar, M. 1971. Blood coagulation values of sheep. *Am J. Vet Res* **32**: 405-409.
- Hecker, J.F. 1993. The sheep as an experimental animal. Academic Press, London.
- Holmes C.J. 1995. Hemodialyzer performance: biological indices. *Artif Organs* **19(11)**: 1126-1135.
- Von Segesser, L.K., Mihailevic, T., Tonz, M., Leskosek, B., Von Felten, A., and Turina, M. 1994. Coagulation patterns during deheparinization with immobilized polycation. *ASAIO J.* **40**: M565-M569.

Chapter 6

Conclusions and Recommendations for Future Work

Taylor-Couette flow was evaluated for potential use in an immobilized heparinase I medical reactor. Specifically, this thesis evaluated the use of immobilized heparinase I to achieve regional heparinization of a closed circuit. From the studies in Chapter 2, it was concluded that the fluidization of small porous agarose particles (under 200 μm diameter) in whole blood resulted in significant blood damage in the form of hemolysis and cell count depletion. Therefore, fluidization of small particles would require a totally new approach to maintain the flow rate flexibility, safety, and the maximum use of the immobilized heparinase demanded by clinicians. The lesson learned from the studies with agarose immobilized heparinase, fluidized in whole blood, paved the way to design a reactor that would separate the blood cells from the agarose beads. Nevertheless, these are the first studies to evaluate the use of agarose immobilized species fluidized within Taylor vortices for a medical application and the results have been accepted for publication in a peer reviewed journal.

The concept of the vortex flow plasmapheretic reactor (VFPR) was a direct consequence of the conclusions formulated in Chapter 2. The basis for the VFPR design assumed that if the agarose beads were kept separate from the blood cells while maintaining adequate fluidization, an effective and safe reactor may result. The challenge was to obtain high plasma clearances within the device without causing premature clotting or membrane clogging. The studies in Chapter 3 confirmed that separation of the cells from the agarose resulted in good hemocompatibility and efficacy. Moreover, fluidization of the agarose beads via circumferential flow was observed within the reactive chamber. The observed fluidization was independent of the axial flow rate through the reactor which is an important operating parameter in hospitals. The new type of fluidization, observed and reported for the first time during the course of this research, was the result of undulatory motions of the microporous membrane. The periodic membrane undulations are attributed to both, fluid dynamics caused by rotation of the inner cylinder and the membrane material.

In Chapter 4, residence time distribution studies were performed with the VFPR to characterize the type of mixing within the device in order to predict heparin conversion. The complex nature of the device necessitated a multi-compartment model to adequately describe the experimental residence time distribution curve. The convolution integral was a useful mathematical tool that enabled integration of the model compartments and the prediction of heparin conversions.

The model revealed the existence of a bypass zone within the reactive chamber of the VFPR which could account for the lower observed conversions.

Finally, in Chapter 5, the device was tested *ex vivo* in sheep to determine the safety and efficacy of regional heparinization, a potential treatment modality to make heparin anticoagulation safer for the patient suffering from acute renal failure. Steady state conversions in the range of 36-42% were obtained for up to one hour of operation at a blood flow rate of 150 ml/min. These conversions are close to the initial objective which is in the range of 45-50%. These results, although not within the specified range of 45-50%, demonstrated the feasibility of regional heparinization of a closed circuit with a reactor using Taylor-Couette flow. The safety profile of the device was also evaluated by monitoring changes in cell counts, total protein, fibrinogen, and the release of free hemoglobin into the plasma. The white cell count profiles suggest some degree of complement activation but this was shown to be due to the presence of agarose beads and not the reactor materials. In addition, the white cell count rebounded to within 25% of the initial values. In general, by all of the latter criteria, the device demonstrated good “biocompatibility”. These studies lay the foundation for a small scale animal preclinical trial in order to test the device in humans.

Recommendations for Future Work:

The following issues should be addressed before the VFPR can be used on humans:

Efficacy:

The mechanism for decrease in conversion has to be addressed as the device should function for up to 5 hours if necessary. The modeling studies from Chapter 4 predicted a bypass that is a function of the transmembrane flow and the permeability of the membrane. Therefore, a membrane with the proper mechanical strength and permeability (smaller pore size) should be identified in collaboration with the manufacturer (Whatman Inc.). In addition, according to the model, another way to enhance reaction efficacy and reduce flow bypass would be the concentration of the beads within the reactive chamber (smaller reactive chamber volume). This line of research should also address the bead concentration gradient that was observed in some of the experiments.

Safety:

A very important consideration when designing a medical device is the safety of the patient. Based on the experiments, the immediate danger to the patients would be accidental rupture of the microporous membrane which would release the beads into the extracorporeal circuit. To prevent

bead release into the blood stream and to also address the conversion issue mentioned above, modifications to the VFPR design are proposed and illustrated in **Figure 6.1**.

To facilitate human clinical trials with the VFPR, more sheep studies should be done to confirm the safety and efficacy data presented in Chapter 5. The sheep studies should include a reactor prototype manufactured at an F.D.A. approved facility. This strategy is encouraged because the hospital internal review board and the F.D.A. will consider device fabrication methods as part of their criteria for approval when the data is reviewed.

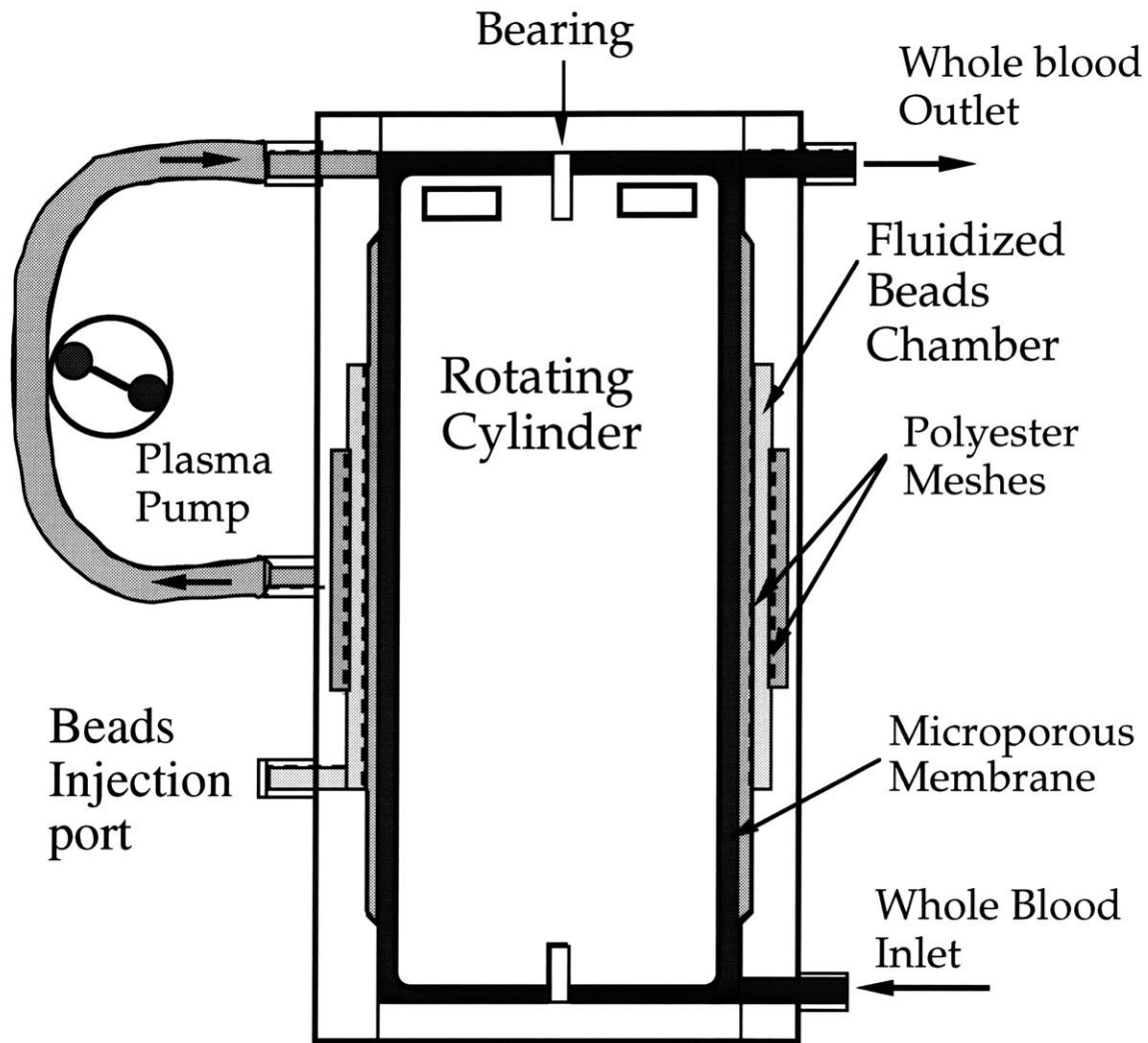


Figure 6.1. The modifications to the VFPR consist of adding a polyester mesh behind the microporous membrane, effectively “sandwiching” the beads within two polyester meshes. This design would allow independence of the bead chamber and its dimensions from the microporous membrane dimensions required to maintain high flux without causing clogging problems. In this configuration, the reactive chamber can be optimized for good fluidization conditions to minimize flow bypass and bead concentration gradients that may occur during operation of the reactor in blood.

Appendix

Immobilization of Heparinase I

Pure heparinase I preparations with specific activities of up to 92 IU/mg were used for immobilization studies. The trials to covalently bind heparinase I to porous membrane supports resulted in membranes with very low enzymatic activities (**Tables A.1** and **A.2**). Therefore, agarose beads were selected to be the polymeric support since they worked well in the past and could serve as a good model system. The chemistry used to covalently bind heparinase to the agarose was cyanogen bromide (CNBr) activation. Despite literature reports of labile bonds between the protein and the support, this method resulted on an average protein binding of greater than 90% and activity retention of 30-40 % on average. The resulting immobilized heparinase activity ranged from 8-16 IU/cc of packed wet gel.

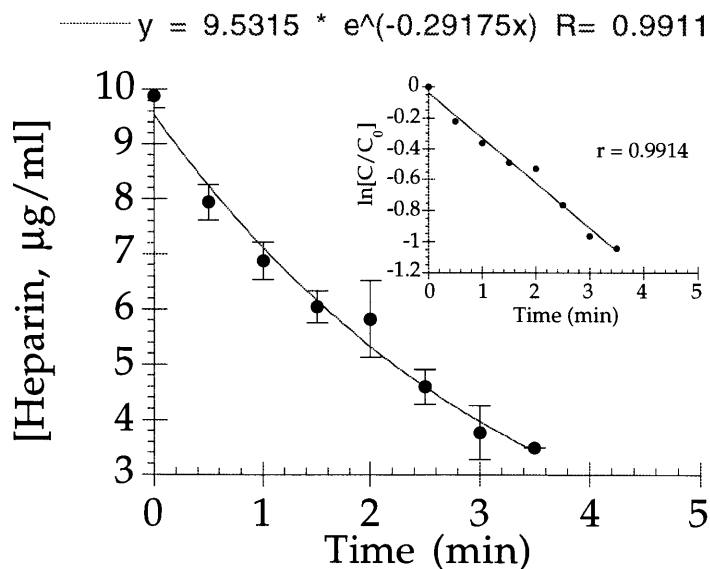
Table A.1. Efficiencies of immobilization for different chemistries and for different solid supports.

	specific activity	% Bound	% Retained	% Yield
Immunodyne ABC	0.0138	85.0	0.90	0.76
ultrabind	0.0025	67.7	0.20	0.13
nitrocellulose	0.0101	100.0	0.57	0.57

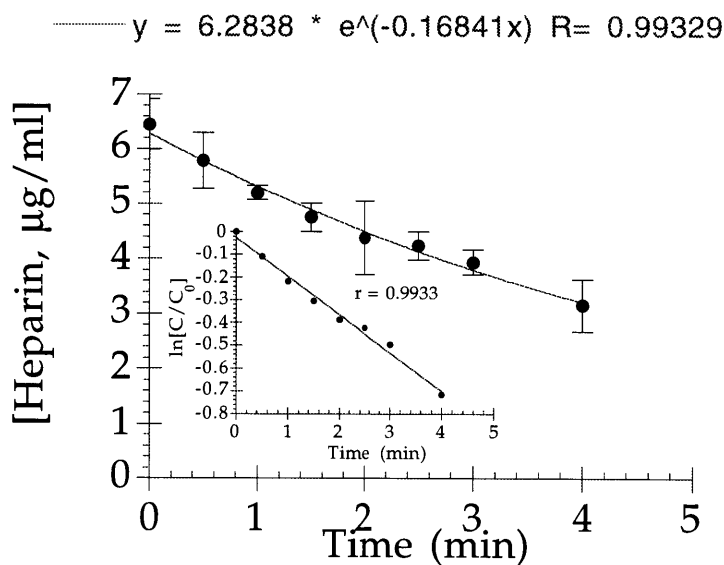
Table A.2. Results of membrane experiments with heparinase I. The specific activity of the original enzyme solution ranged from 2.5-5 IU/ml. The membranes were charged with 0.5 ml solution/cm² membrane.

Membrane	Activation chemistry	> 80% protein bound	membrane activity
immunodyne	proprietary to Millipore	+	-
ultrabind	proprietary to Gelman Sciences	+	-
nitrocellulose	CNBr	+	-
regen. cellulose	tresyl chloride	+	-
regen. cellulose	CNBr	+	-
hydroxyl-nylon	CNBr	+	-
amine-nylon	EDC	+	-
azlactone	proprietary to 3M	±	-
-polyethylene			

This activity is a 4 - 8 fold improvement over the maximum enzymatic activities used previously. There was no detectable leaching of enzymatic activity. Cumulative protein loss as measured by a protein assay for a period of one week at 4°C was under 2%.



a.



b.

Figure A.1. Experimental data used for the calculation of k_{het} in Chapter 4. The specific activity of the agarose immobilized heparinase was 16 IU/cc gel. $T = 37^{\circ}\text{C}$. The data was obtained *in vitro* with well mixed batch reactors. Heparin concentrations were measured with the Azure II assay described in the Materials and Methods section of Chapter 3. **a.** Batch removal of heparin from buffered saline with $V_p/V_{liq} = 0.02$ (0.2 ml gel in 10 ml buffer). The apparent $k_{het} = 14.6 \text{ min}^{-1} * \text{ml saline/ml gel}$. Mean \pm S.D. of 4 experiments. **b.** Batch removal of heparin from buffered saline with $V_p/V_{liq} = 0.01$ (0.1 ml gel in 10 ml buffer). The apparent $k_{het} = 16.8 \text{ min}^{-1} * \text{ml saline/ml gel}$. Mean \pm S.D. of 3 experiments.